DLR-IB-FT-BS-2017-248

Reduction of the rotor blade root bending moment and increase of the rotational-speed strength of a 5 MW IPC wind turbine based on a stochastic disturbance observer

Interner Bericht

Autor: Taha Fouda

DLR Deutsches Zentrum für Luft- und Raumfahrt

DLR Institutsbericht

DLR-IB-FT-BS-2017-248

Reduction of the rotor blade root bending moment and increase of the rotational-speed strength of a 5 MW IPC wind turbine based on a stochastic disturbance observer

Taha Fouda

Institut für Flugsystemtechnik

Braunschweig

56 Seiten
28 Abbildungen
5 Tabellen
21 Referenzen

Deutsches Zentrum für Luft- und Raumfahrt e.V.
in der Helmholtz Gemeinschaft
Institut für Flugsystemtechnik
Lilienthalplatz 7, 38108 Braunschweig

Stufe der Zugänglichkeit: II, intern unbeschränkt und extern beschränkt zugänglich
Availability/Distribution: Internally unlimited and externally limited distribution

Braunschweig, 16. März 2018

Unterschriften:

Institutsdirektor:	Prof. Dr.-Ing. Stefan Levedag
Abteilungsleiter:	Dr.-Ing. Christoph Keßler
Betreuer:	Dr.-Ing. Arndt Hoffmann
Verfasser:	BSc. Taha Fouda

Verfasser:

Taha Fouda

Titel:

Reduction of the rotor blade root bending moment and increase of the rotational-speed strength of a 5 MW IPC wind turbine based on a stochastic disturbance observer

Deutsches Zentrums für Luft- und Raumfahrt e.V. (DLR)

Institut für Flugsystemtechnik, Abteilung Hubschrauber

Institutsbericht

Acknowledgement

After I have finished this thesis, I would like to thank my supervisor Dr.-Ing. Arndt Hoffmann for his great help and advices. He had the idea behind this work. Recently, he investigated it and applied it for the aircraft wing. He guided me through all the steps from the beginning till the end.

I would also like to thank my family for their sincere encouragement throughout my studies.

Finally, I would like to thank all the colleagues working at DLR institute of flight systems specially M.Sc. Felix Weiß for his support in different technical issues.

Contents

List of Abbreviations

AeroDyn	Aerodynamics
ADAMS	Automatic Dynamic Analysis of Mechanical Systems
DAC	Disturbance Accommodation Control
DLL	Dynamic - Link – Library
DLR	Deutsches Zentrum für Luft- und Raumfahrt
DOF	Degree of Freedom
DOWEC	Dutch Offshore Wind Energy Converter project
Dry	Dryden spectrum
DUWECS	Delft University Wind Energy Converter Simulation Program
E	Expected value
CAE	Computer-Aided Engineering
ElastoDyn	Elasto Dynamics
FAST	Fatigue, Aerodynamics, Structures, and Turbulence
HAWT	Horizontal Axis Wind Turbine
IPC	Individual Pitch Control
LQG	linear Quadratic Gaussian
LQR	Linear Quadratic Regulator
MIMO	Multi Input Multi Output
NREL	National Renewable Energy Laboratory
OP	Operating point
PSD	Power Spectrum Density
RECOFF	Recommendations for Design of Offshore Wind Turbines project
ServoDyn	Servo Dynamics
VAR	Variance
WindPACT	Wind Partnerships for Advanced Component Technology project
WT	Wind Turbine

List of Symbols

$\underline{\underline{A}}$	State matrix	[...]
$\underline{\underline{B}}$	input matrix	[...]
$\underline{\underline{C}}$	output matrix	[...]
$\underline{\underline{D}}$	input-transmission matrix	[...]
D_i	Damage	[1]
$\underline{\underline{\underline{DspC}}}$	displacement output matrix	[...]
d	damping factor of the inverted notch	[1]
$\underline{\underline{E}}$	wind input disturbance matrix	[...]
$\underline{e_k}$	Posteriori estimate error	[...]
e_k^-	Priori estimate error	[...]
$\underline{\underline{F}}$	wind input disturbance transmission	[...]
f	nonlinear forcing function	-
$f_X(x)$	the probability density function	-
$\underline{\underline{G}}$	stiffness matrix	[...]
I	Turbulence intensity	[1]
J	cost function	[1]
$\underline{\underline{\underline{K_k}}}$	Kalman gain	[...]
$\underline{\underline{K}}^*$	observer gain	[...]
$\underline{\underline{K}}_{LQR}$	Feedback gain	[...]
$\underline{\underline{L}}$	control input matrix	[...]
L_u	length scale	[m]
$\underline{\underline{M}}$	mass matrix	[...]
m	number of the system	[1]
N	feedforward gain	[...]
N_i	Number of load cycles	[...]
n	number of the system states	[1]
$\underline{\underline{P}}_K$	error covariance matrix	[...]
P_i	Probability of x_i	-
p	number of the system outputs	[1]
$\underline{\underline{Q}}_{LQR}$	State weighting matrix for LQR	[...]
$\underline{\underline{Q}}_{var}$	Process noise covariance matrix	[...]

$\underline{q}$	Displacement DOF	[...]
$\underline{\dot{q}}$	Velocity DOF	[...]
$\underline{\ddot{q}}$	Acceleration DOF	[...]
$\underline{\underline{R}}_{LQR}$	Control effort weighting matrix for LQR	[...]
$\underline{\underline{R}}_{var}$	Measurement error covariance matrix	[...]
$\underline{\underline{R}}^*$	closed loop gain	[...]
s	Laplace variable	[1/s]
t	Time	[s]
T	time constant	[s]
$\underline{u}$	the vector of control inputs	[...]
V	wind speed	[m/s]
V_m	steady mean wind speed	[m/s]
$\underline{\underline{VelC}}$	velocity output matrix	[...]
v	atmospheric turbulence	[...]
$\underline{v_k}$	measurement noise	[...]
$\underline{w_k}$	system uncertainties	[...]
$\underline{x}$	the vector of system states	[...]
$\underline{x_d}$	the vector of disturbance states	[...]
$\underline{\hat{x}}$	Posteriori estimated state	[...]
$\underline{\hat{x}_k^-}$	Prior state estimate	[...]
$\underline{y}$	the vector of system outputs	[...]
$\underline{\hat{y}}$	Estimated output	[...]
$\underline{z}$	the vector of wind input "disturbances"	[...]
Ω	Rotational speed	rpm
θ	Pitch angel	°
σ	standard deviation	[...]
μ	Expected value or Mean	[...]
σ^2	Variance	[...]
σ_i	Stress	N/m

List of Figures

List of Table

Abstract

The control- and operation-system of a wind turbine must primarily ensure the fully automatic operation of wind turbines in a constantly changing environment (gusts, turbulence). In addition, economic efficiency charges the control-system to ensure that the highest possible efficiency is achieved, and the mechanical loads caused by disturbances are minimized. The reduction of loads in wind turbines becomes more important.

According to the "internal model principle", the control quality or the potential for disturbance rejection is increased; the more information there is available on the character of the disturbance (turbulence). This principle is directly taken up by the observer-based Disturbance Accommodation Control (DAC).

The ability of an observer to estimate non-measurable states from a set of measurements using a model of the plant suggests the idea of extending the model of the plant by a model of the disturbance. The states of the disturbance can thus also be reconstructed, and an easy-to-determine feedforward control can be implemented to counteract the disturbance. In this thesis DAC has to adjusted to suppress stochastic disturbances in wind turbines (NREL 5 MW).

1 Introduction

Wind energy is one of the most growing renewable energy technologies in the world. The total worldwide installed capacity increased from 8 MW at 1980 till 18039 MW at 2000. In 2016 the installed capacity reached 500 GW. At the same year, the total worldwide electricity generated by wind energy was 900 TWh which means more than 4% of the global electricity demand. It is expected that the worldwide installed capacity will reach 800 GW by the end of 2020 [1]. To cover the demand, the size and the rotor diameter increased over the last decades as you can see in figure 1.1. On the other hand, the increment in the size and the rotor diameter develops new challenges that need to be faced. One of those challenges is the increase in the blade mass and therefore the weight. Another one is the reduction in the natural frequencies.

These loads can be reduced by implementing a control system that must primarily ensure the fully automatic operation of wind turbines in a constantly changing environment (gusts, turbulence). In addition, economic efficiency charges the control-system to ensure that the highest possible efficiency is achieved.

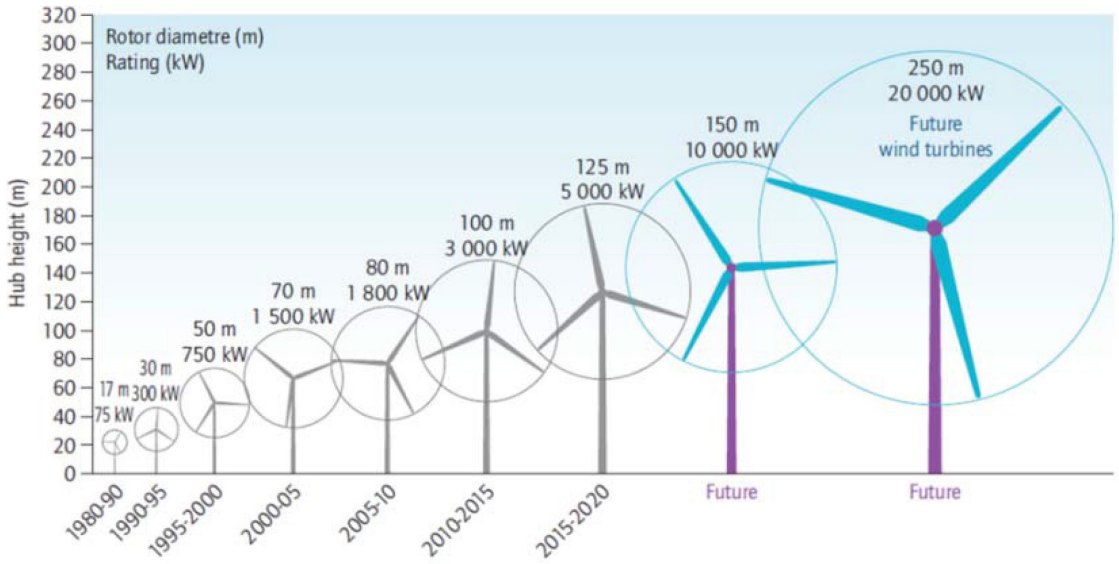

Figure 1.1: Trend towards increasingly larger wind turbines [2]

According to the "internal model principle", the control quality or the potential for disturbance rejection is increased; the more information about the disturbance is known. This principle is directly taken up by the observer-based Disturbance Accommodation Control. Disturbance Accommodation Control (DAC) is a new branch of modern control

theory that address the problems of dynamic modelling of uncertain disturbances which act on systems and designing feedback/feedforward controllers which achieve and maintain system performance specifications in the face of the disturbances [3]. It was developed by Johnson (1976) [3]. The theory was extended to wind turbine control by Balas (1998) [4]. He was the first who used it for the rejection of deterministic disturbances on the wind turbine [4]. He further elaborated and investigated the method in [5].

The turbulence is a stochastic disturbance that cannot be easily measured, However the disturbance states can be estimated. The ability of an observer to estimate non-measurable states from a set of measurements using a model of the plant suggests the idea of extending the model of the plant by a model of the disturbance. The states of the disturbance can thus also be reconstructed, and an easy-to-determine a feedforward controller that can be implemented to close the control loop, cf. [3]. This method was adapted for stochastic disturbances on a motor glider [6] and will be adjusted to suppress stochastic disturbances in wind turbines (NREL 5 MW reference turbine) in this thesis.

The thesis is organized as follows: Chapter two discusses the modelling of wind turbine for controller design, the definition of NREL 5 MW baseline turbine and the development of a linear representation of the nonlinear wind turbine using the aeroelastic FAST tool. Chapter three illustrates the modelling of wind disturbance based on the Dryden wind turbulence model. Chapter four explains the state estimation based on the Discrete Kalman Filter and the design of the controller based on the disturbance accommodation control theory. In chapter five, the controller structure is implemented in a linear and nonlinear simulation environment. Chapter six shows a comparative study with a given classical load controller. Finally, Chapter seven contains a summary of this thesis.

2 Modelling of wind turbines for controller design

A mathematical model of wind turbine gives the ability to understand the behavior of the wind turbine over its region of operation. A horizontal axis onshore wind turbine model can consist of a rotor model, a drive train model, a electrical generator model and a tower model.

Nowadays, all described models can be implemented in various analytical tools such as FAST, SymDyn and DUWECS. All these tools can Linearize and simulate. The aero-elastic simulation tool FAST has been used in this study for modelling of NREL 5 MW Baseline turbine. The baseline turbine is modelled nonlinear in FAST but can be linearized for analysis or controller design purposes. The definition of NREL 5 MW Baseline turbine will be discussed in the following section.

2.1 NREL 5 MW baseline wind turbine

This study is based on NREL 5 MW baseline onshore Individual Pitch Control (IPC) wind turbine as a reference turbine. NREL 5 MW baseline wind turbine has been developed by New and Renewable Energy Laboratory (NREL) to act as a reference model used for wind energy related studies and by wind turbine researches, however it has not been built. It has been designed based on the largest wind turbine prototypes in the world at that time; Multibrid M5000 and the REpower 5MW -each had a 5-MW rating. Because of unavailable detailed information about these machines at that time, available properties from other models used in WindPACT, RECOFF, and DOWEC projects have been gathered with Multibird M5000 and REpower 5 MW properties to extract the best available and most representative specifications [8].

NREL 5MW baseline turbine is a three-bladed upwind turbine with a variable-speed, active-pitch control system. Table 2.1 shows the baseline properties.

Rated Power	5 MW
Rotor Orientation, Configuration	Upwind, 3 Blades
Control	Variable Speed, Individual Pitch
Drivetrain	High Speed, Multiple-Stage Gearbox
Rotor, Hub Diameter	126 m, 3 m

Hub Height	90 m
Cut-In, Rated, Cut-Out Wind Speed	3 m/s, 11.4 m/s, 25 m/s
Cut-In, Rated Rotor Speed	6.9 rpm, 12.1 rpm
Rated Tip Speed	80 m/s
Rotor Mass	110,000 kg
Nacelle Mass	240,000 kg
Tower Mass	347,460 kg

Table 2.1: NREL 5MW baseline wind Turbine properties [8]

The relationships of the generator speed, rotor power, generator power, rotor thrust, and rotor torque are represented as a function of wind speed in figure 2.1.

Figure 2.1 is divided into four different regions. Region 1½ is the startup region where the wind speed is a little bit higher than the cut in speed. In this region, the generator speed is set to the lower limits which is defined to be in between 670 rpm and 30% above this value (or 871 rpm). Region 2 is a maximum power tracking control region where the generator torque is proportional to the square of the generator speed to maintain a constant (optimal) tip speed ratio. Region 2½ is a linear transition between region 2 and region 3 with a torque slope corresponding to the slope of an induction machine. The generator-slip percentage in this region is taken to be 10%, according to the value used in the DOWEC study. In region 3, the wind speed is above the rated speed. The generator speed is kept constant in this region so that the generator torque is inversely proportional to the generator speed [8].

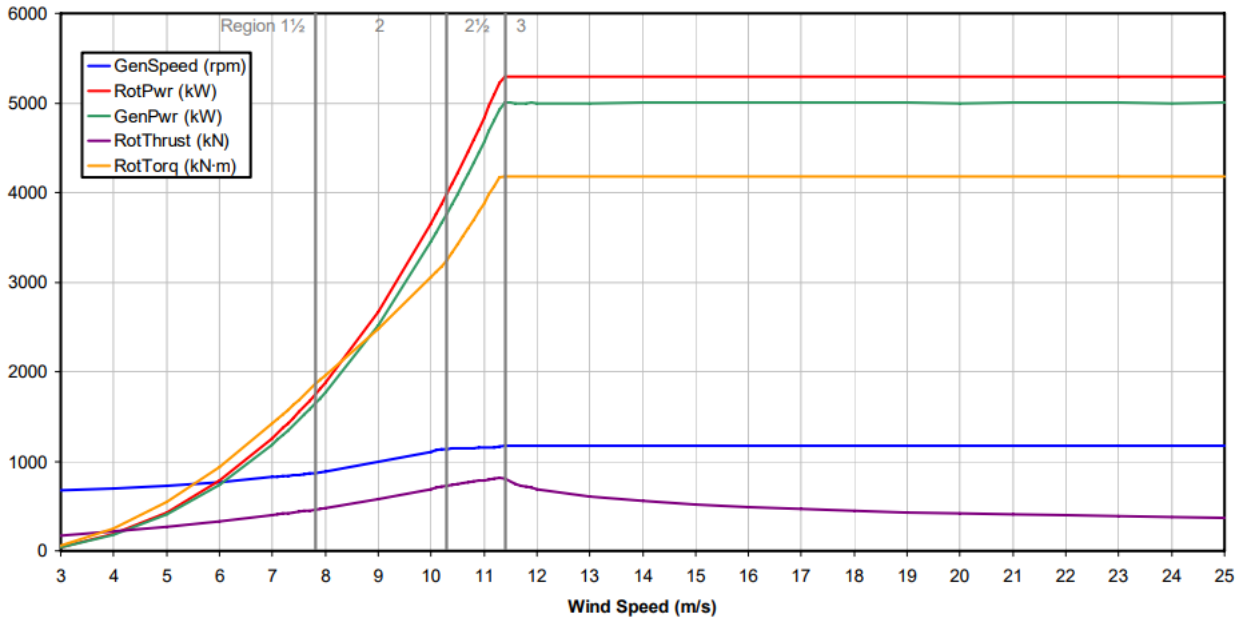

Figure 2.1: wind speed relationships of 5 MW baseline turbine [8]

2.2 FAST

FAST (Fatigue, Aerodynamics, Structures, and Turbulence) is an aeroelastic Computer-Aided Engineering (CAE) tool for onshore and offshore horizontal axes wind turbines developed by New and Renewable Energy Laboratory (NREL) to simulate the nonlinear coupled dynamic response of wind turbines in the time domain. Wind turbines with two or three blades, up wind or downwind rotor, pitch or stall regulation, rigid or teetering hub, and lattice or tabular tower can be analyzed using FAST [9].

The FAST Code is the result of combination of three distinct codes; the FAST2 Code for two-bladed HAWTs; the FAST3 Code for three-bladed HAWTs; and the AeroDyn subroutines for HAWTs with additional modification. The FAST Code have been modified since 2003 till now and additional features have been added. The ability of FAST to develop a linearized state space model used for control design was added in 2003. An interface between FAST and MATLAB Simulink has also been developed in 2004 which allows the user to implement a advanced turbine controls in Simulink environment. In 2005, FAST got Germanischer Lloyd certificate [9].

Three-bladed horizontal axes wind turbine with 24 degree of freedoms (DOFs) and two-bladed HAWT with 22 DOFs can be modelled using FAST. The three-bladed HAWT DOFs counts for 6 DOF for the platform translational (surge, sway, and heave) and rotational

(roll, pitch, and yaw) motions, 4 DOF for the tower flexibility; two are longitudinal modes, and two are lateral modes, 1 DOF for the Yaw motion of the nacelle, 2 DOF for the variations in generator speed and the drivetrain flexibility, 9 DOF for the blade flexibility; 3 for the first flapwise bending mode of each blade, 3 for the second flapwise bending modes of each blade and 3 for the edgewise motion of each blade. 1 DOF for the rotor-furl, and 1 DOF for the tail-furl. The two- bladed HAWT has the same DOFs as for the three-bladed but with the addition of 1 DOF for the blade teetering and only 6 DOF for the blade flexibility; 2 for the first flapwise bending mode of each blade, 2 for the second flapwise bending modes of each blade and 2 for the edgewise motion of each blade [9]. Here in this thesis, 10 DOFs are chosen to be modelled as shown in table 2.2.

There are two different modes of operation supported by FAST, Simulation mode and Linearization mode. The simulation mode is used for the load analyses where the linearization mode is used to develop a linear model from the aeroelastic nonlinear wind turbine model.

2.3 Linearization process using FAST

The nonlinear description of the wind turbine can be linearized by FAST through two main steps, determination of an operating point and derivation about the selected operating point.

2.3.1 Determination of an Operating point (OP)

A trim point or an operating point is the point at which the system is in steady state where the system's state derivatives equal zero. Selecting this point is one of the most important steps in the linearization process as the linear representation of the nonlinear system is only valid for small perturbations from an operating point. It can be steady state operating point for operating turbine as in our case or static-equilibrium operating point for idling turbine. It is defined by selecting the system DOFs that need to be modelled and setting the initial conditions for control inputs and wind inputs.

Trim conditions are defined as:

- 18 m/s steady horizontal wind speed.
- 5 MW rated power.
- Region III

- 12,1 rpm as initial rotor speed.

The result pitch angel is $\theta_{trim} = 14.92°$

The selected DOFs of the linear model are listed in table 2.2.

System DOFs: -

x_1	1st tower fore-aft bending mode
x_2	Variable speed generator
x_3	1st flapwise bending-mode of blade 1
x_4	1st flapwise bending-mode of blade 2
x_5	1st flapwise bending-mode of blade 3
x_6	First time derivative of 1st tower fore-aft bending mode
x_7	First time derivative of Variable speed generator
x_8	First time derivative of 1st flapwise bending-mode of blade 1
x_9	First time derivative of 1st flapwise bending-mode of blade 2
x_{10}	First time derivative of 1st flapwise bending-mode of blade 3

Table 2.2: Linearized model DOFs

System inputs: -

u_1	Blade 1 pitch command
u_2	Blade 2pitch command
u_3	Blade 3 pitch command

Table 2.3: Control inputs

3.3.2 linearization

Suppose that the system nonlinear differential equation can be written in the following form

$$\dot{\underline{x}} = \frac{d\underline{x}}{dt} = f(\underline{x}, \underline{u}) \quad , \qquad \underline{y} = g(\underline{x}, \underline{u}) \tag{2-1}$$

where $\underline{x}$ is the vector of the system states, $\underline{u}$ is the vector of the control inputs, and $\underline{y}$ is the vector of the system outputs.

By applying the Taylor expansion on the nonlinear equation (2-1) and neglecting the higher order terms, we get

$$\underline{\dot{x}} = f(\underline{x},\underline{u}) \approx f(\underline{x}|_{op},\underline{u}|_{op}) + \frac{\partial \underline{f}}{\partial \underline{x}}|_{op}\,\delta\underline{x} + \frac{\partial \underline{y}}{\partial \underline{u}}|_{op}\,\delta\underline{u} \tag{2-2}$$

$$\underline{y} = g(\underline{x},\underline{u}) \approx g(\underline{x}|_{op},\underline{u}|_{op}) + \frac{\partial \underline{g}}{\partial \underline{x}}|_{op}\,\delta\underline{x} + \frac{\partial g}{\partial u}|_{op}\,\delta\underline{u} \tag{2-3}$$

At steady state conditions

$$\underline{f}(\underline{x}|op,\underline{u}|op) = 0, \qquad \underline{g}(\underline{x}|op,\underline{u}|op) = 0$$

The description of the trim point is as following

$$\delta\underline{\dot{x}} \approx \frac{\partial \underline{f}}{\partial \underline{x}}|_{op}\,\delta\underline{x} + \frac{\partial \underline{y}}{\partial \underline{u}}|_{op}\,\delta\underline{u} \tag{2-4}$$

$$\delta\underline{y} \approx \frac{\partial \underline{g}}{\partial \underline{x}}\,\delta\underline{x} + \frac{\partial g}{\partial \underline{u}}\,|_{op}\delta\underline{u} \tag{2-5}$$

These two equations can be written in other two forms as

$$\delta\underline{\dot{x}} = \underline{\underline{A}}\delta\underline{x} + \underline{\underline{B}}\,\delta\underline{u} \tag{2-6}$$

$$\delta\underline{y} = \underline{\underline{C}}\,\delta\underline{x} + \underline{\underline{D}}\,\delta\underline{u} \tag{2-7}$$

The matrices $\underline{\underline{A}}$, $\underline{\underline{B}}$, $\underline{\underline{C}}$, $\underline{\underline{D}}$ in the last two equations are defined as

$$\underline{\underline{A}} = \frac{\partial \underline{f}}{\partial \underline{x}}|_{op}, \quad \underline{\underline{B}} = \frac{\partial \underline{y}}{\partial \underline{u}}|_{op}, \; \underline{\underline{C}} = \frac{\partial \underline{g}}{\partial \underline{x}}|_{op}, \; \underline{\underline{D}} = \frac{\partial \underline{g}}{\partial \underline{u}}|_{op}\,.$$

where $\underline{\underline{A}}$ is the state matrix, $\underline{\underline{B}}$ is the input matrix, $\underline{\underline{C}}$ is the output matrix and $\underline{\underline{D}}$is the input-transmission matrix.

FAST applies the same principle for the following nonlinear equation of motion to get the linear representation from the nonlinear wind turbine model.

$$\underline{\underline{M}}(\underline{q},\underline{u},t)\underline{\ddot{q}} + f\left(\underline{q},\underline{\dot{q}},\underline{u},\underline{z},t\right) = 0 \tag{2-8}$$

where $\underline{\underline{M}}$ is the mass matrix. $\underline{f}$ is the vector of the nonlinear forcing function, $\underline{q}$, $\underline{\dot{q}}$, $\underline{\ddot{q}}$ are the vectors of the displacements, velocities and accelerations DOFs. $\underline{\mathrm{u}}$ is the vector of control inputs, $\underline{z}$ is the vector of the wind disturbances input and t is the time [9].

The operating points are defined as

$$\underline{q} = \underline{q}|_{op} + \delta\underline{q}\,, \quad \dot{\underline{q}} = \dot{\underline{q}}|_{op} + \delta\dot{\underline{q}}, \quad \ddot{\underline{q}} = \ddot{\underline{q}}|_{op} + \delta\ddot{\underline{q}}, \quad \underline{u} = \underline{u}|_{op} + \delta\underline{u},$$
$$\underline{z} = \underline{z}|_{op} + \delta\underline{z}$$

by substituting these expressions into the equation of motion and applying Taylor expansion as it's mentioned before, we get the following linear equation

$$\dot{\underline{x}} = \underline{\underline{A}}\,\underline{x} + \underline{\underline{B}}\,\underline{u} + \underline{\underline{E}}\,\underline{z} \tag{2-9}$$
$$\underline{y} = \underline{\underline{C}}\,\underline{x} + \underline{\underline{D}}\,\underline{u} + \underline{\underline{F}}\,\underline{z} \tag{2-10}$$

The matrices $\underline{\underline{A}}$, $\underline{\underline{B}}$, $\underline{\underline{C}}$, $\underline{\underline{D}}$ into equations (2-9) and (2-10) are defined as

$$\underline{\underline{A}} = \begin{bmatrix} 0 & I \\ -\underline{\underline{M}}^{-1}\underline{\underline{G}} & -\underline{\underline{M}}^{-1}\underline{\underline{C}} \end{bmatrix}, \quad \underline{\underline{B}} = \begin{bmatrix} 0 \\ \underline{\underline{M}}^{-1}\underline{L} \end{bmatrix}, \quad \underline{\underline{E}} = \begin{bmatrix} 0 \\ \underline{\underline{M}}^{-1}\underline{\underline{F_d}} \end{bmatrix}, \quad \underline{\underline{C}} = \begin{bmatrix} \underline{\underline{DspC}} & \underline{\underline{VelC}} \end{bmatrix},$$
$$\underline{L} = \left[\frac{\partial \underline{\underline{M}}}{\partial \underline{u}}\ddot{\underline{q}} + \frac{\partial \underline{f}}{\partial \underline{u}}\right]|_{op}\,.$$

where

$\underline{\underline{M}}$: mass matrix; $\underline{\underline{M}} = M|_{op}$,

$\underline{\underline{C}}$: damping / gyroscopic matrix; $\underline{\underline{C}} = \frac{\partial f}{\partial \dot{q}}|_{op}$,

$\underline{\underline{G}}$: stiffness matrix; $\underline{\underline{G}} = \left[\frac{\partial \underline{f}}{\partial \underline{u}}\ddot{\underline{q}} + \frac{\partial \underline{f}}{\partial \underline{u}}\right]|_{op}$,

$\underline{\underline{E}}$: wind input disturbance matrix,

$\underline{\underline{F}}$: wind input disturbance transmission matrix,

$\underline{\underline{DspC}}$: the displacement output matrix wind input disturbance transmission matrix,

$\underline{\underline{VelC}}$: the velocity output matrix.

Figure 2.2 shows the state space representation of the Linearized model.

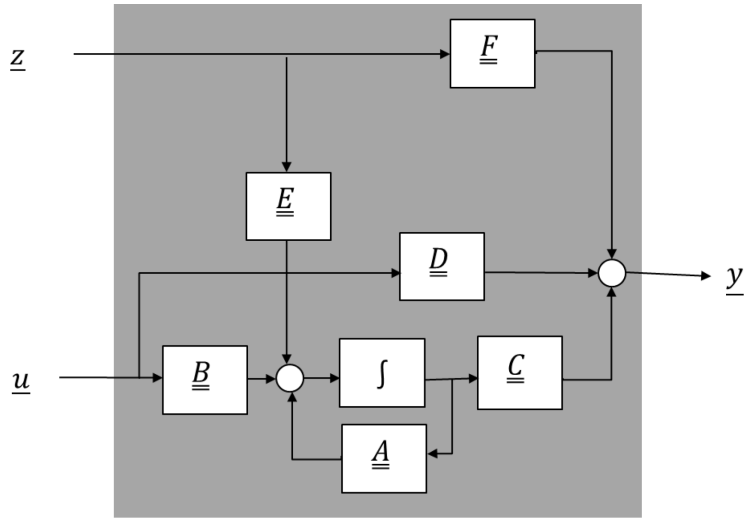

Figure2.2: FAST linearized state space model

As the wind turbine rotor is spinning by 12.1 rpm, the operating point is periodic that leads to periodicity in the state space matrices $\underline{\underline{A}}, \underline{\underline{B}}, \underline{\underline{C}}, \mathrm{D}, \underline{\underline{E}}$ and $\underline{\underline{F}}$. To overcome this problem, the linearization process has been done 36 times, every 10-degree azimuth angle position and the linearized output model is taken as an average over the number of linearization processes per one revolution.

3 Modelling of Wind Disturbance

According to Disturbance Accommodation Control (DAC) theory, the first requirement in order to accommodate the disturbance is to modell it. Here in this chapter, we will discuss how to model the wind disturbance based on Dryden wind turbulence model.

The wind speed V can be divided in two components,

$$V = V_m + v \tag{3-1}$$

Where V_m represents the steady mean wind speed and v represents the atmospheric turbulence that covers the fluctuations of the wind speed. As the wind speed is experienced by a rotating wind turbine, the rotational sampling effect should be taken into consideration. Figure 3.1 shows the block diagram of the effective wind model where the rotational sampling effect is added to the turbulence model [7]. Each part of this model will be discussed in the following subsections.

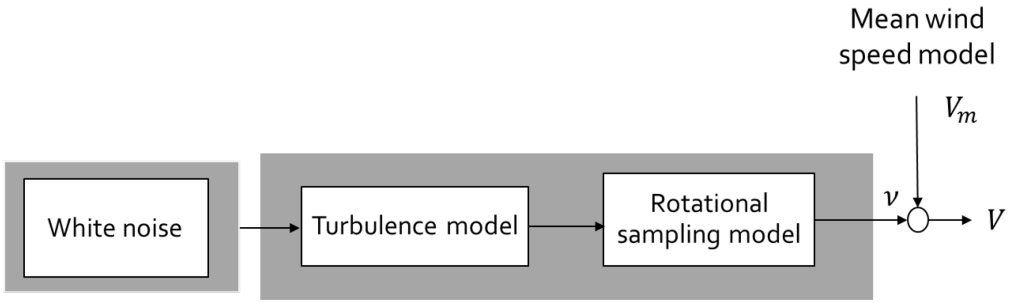

Figure 3.1: Effective wind model [7]

3.1 Mean wind speed

Mean wind speed describes the low frequency variations and is defined as the wind speed averaged over a specific time interval at a specific height. It is used to for the assessment of the expected energy yield. It is often modelled as a Weibull's distribution.

3.2 Turbulence

The high frequency random variations of the flow towards the wind turbine over a period typically 10 min is referred to Turbulence [10]. These variations can be caused by the friction of the flow with the earth surface or the thermal effects in the planetary boundary layer near the earth surface. The turbulence can't be avoided but it's effect can be reduced by implementing a good control system that can react to it.

3.2.1 Turbulence model

Turbulence is often considered as a stochastic process which is hard to be modelled in deterministic equations. Often, it is sufficient to modell just the characteristics via a Power Spectral Density (PSD).

The Dryden wind Turbulence model is of that kind and will be used here. because of its simpler form and its easy access to the time simulation, it's often used in the aerospace industry. The random functions associated with Dryden spectra can be generated by passing Gaussian white noise through appropriate form filter as shown in figure 3.2 [6]. The model consists of the power spectral density for the horizontal turbulence velocity u.

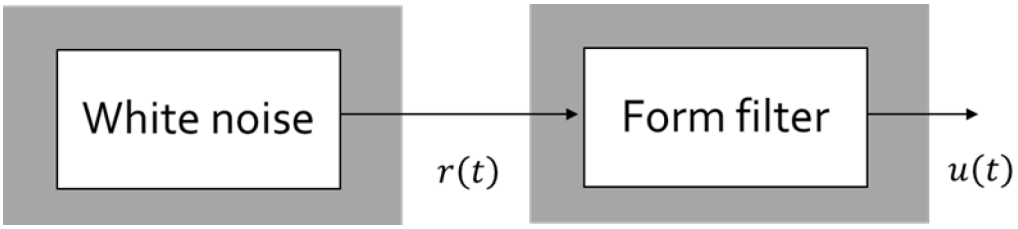

Figure 3.2: Dryden wind turbulence model [6]

The transfer function of the form filter generating a random signal having Dryden spectra from a white noise can be obtained by spectral factorization. it is given as the following equation for the horizontal turbulence.

$$\hat{F}_{u_w} = \frac{\underline{u}(s)}{\underline{r}(s)} = \sqrt{2{\sigma_u}^2 T_u} \cdot \frac{1}{1 + sT_u} \tag{3-2}$$

where

$$T_u = \frac{L_u}{V} = \frac{1}{\omega_u}$$

where L_u is the length scale, σ is the standard deviation and it is a measure of the turbulence intensity, T is the time constant, V is the steady mean wind speed, u is the index for the horizontal turbulence. L_u is modelled as described in [11] where $V = V_m =$ 18 m/s

Turbulence intensity I describes the level of the random variation from the mean wind speed as shown in figure 3.3. It is defined as the ratio of the standard deviation of wind speed variations to the mean wind speed V_m in a certain averaging time, usually defined over 10 min or 1 h.

$$I = \frac{\sigma}{V_m}$$

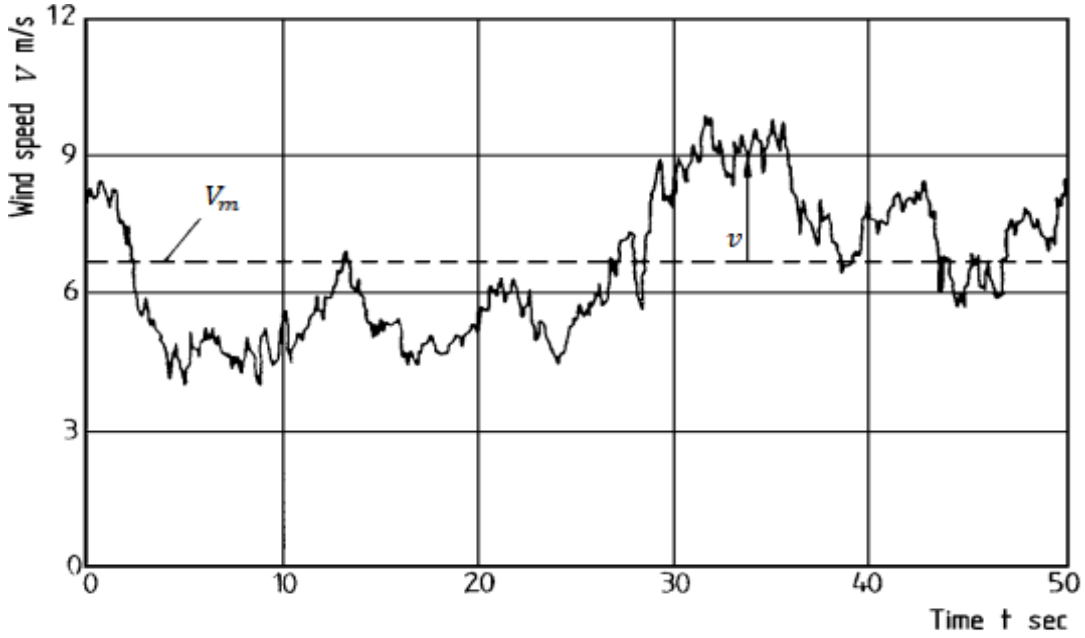

Figure 3.3: Measured time history of wind speed [12]

This equation can be represented in a state space form as

$$\underline{\dot{x}}_{Dry} = \underline{\underline{A}}_{Dry}\underline{x}_{Dry} + \underline{\underline{B}}_{Dry}\,\underline{r} \tag{3-4}$$

$$\underline{z} = \underline{\underline{C}}_{Dry}\underline{x}_{Dry} \tag{3-5}$$

where $\underline{\underline{A}}_{Dry} = \left[-\frac{V}{L_u}\right]$ $\underline{\underline{B}}_{Dry} = \left[\sigma\sqrt{2\frac{V}{L_u}}\right]$ $\underline{\underline{C}}_{Dry} = [1]$

Figure 3.4 shows the state space representation of Dryden model.

For a three-bladed wind turbine

$$\underline{\underline{A}}_{Dry} = \begin{bmatrix} \frac{-1}{T_u} & 0 & 0 \\ 0 & \frac{-1}{T_u} & 0 \\ 0 & 0 & \frac{-1}{T_u} \end{bmatrix}, \quad \underline{\underline{B}}_{Dry} = \begin{bmatrix} \sigma_u\sqrt{2\frac{V_k}{L_u}} & 0 & 0 \\ 0 & \sigma_u\sqrt{2\frac{V_k}{L_u}} & 0 \\ 0 & 0 & \sigma_u\sqrt{2\frac{V_k}{L_u}} \end{bmatrix}, \quad \underline{\underline{C}}_{Dry} = \begin{bmatrix} 1 & 0 & 0 \\ 0 & 1 & 0 \\ 0 & 0 & 1 \end{bmatrix}$$

To be sure that the turbulence acting on each blade is uncorrelated and the speed of the three white noise generators are different.

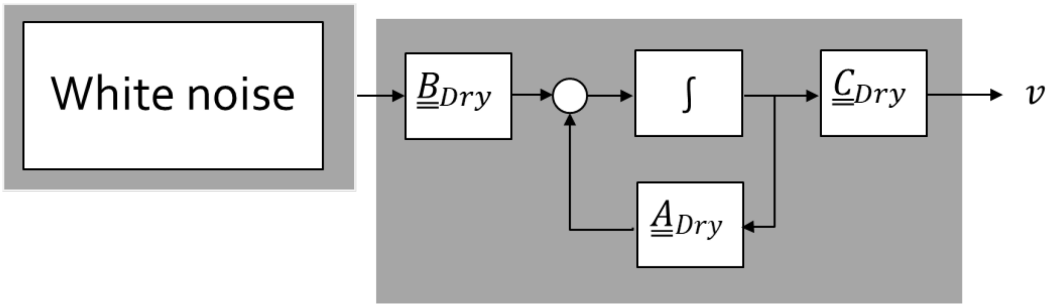

Figure 3.4: State space representation of Dryden model

3.3 Rotational Sampling Effect

The rotational sampling effect adds the effect of the rotating blades to the turbulence as shown in figure 3.5 where the PSD shows peaks at the rotational frequency f_{1b} and at higher harmonics ($f_{2b} = 2f_{1b}, f_{3b} = 3f_{1b}$).

For well understanding this effect, we need to discuss the following two cases. The first case, when the size of the eddy is much bigger than the rotor swept area. In this case there is no consideration for the rotational sampling effect and the observed wind speed will be the same for a rotating blade as for a fixed position. The second case, when the size of the eddy is smaller than the rotor swept area as we assume in our study. In this case, the turbine rotor samples the eddy periodically with each rotation until the eddy passes the rotor [13]. The sampling rate is dependent on the rotational speed and the loads acting on the blades in this case will be dependent on where the blade is.

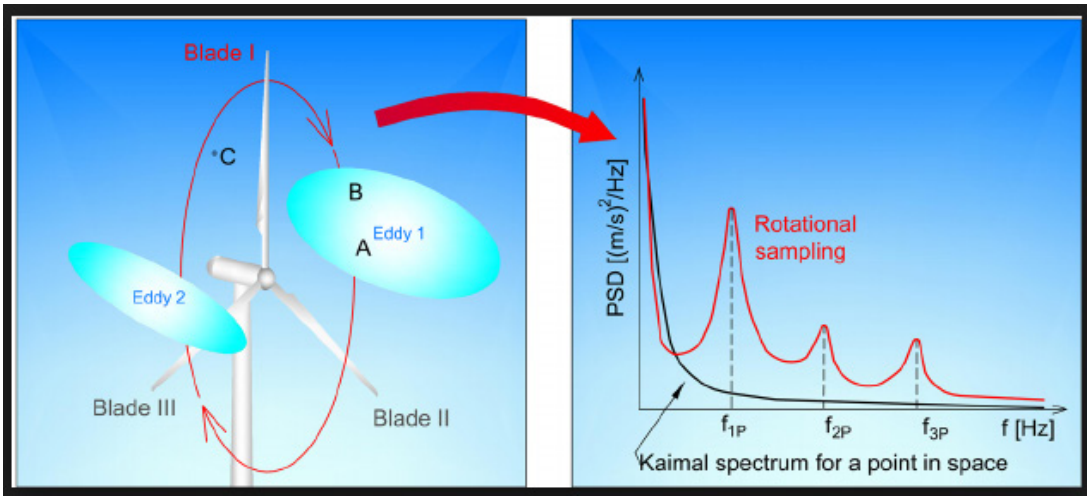

Figure 3.5: Schematic representation of the power spectral density (PSD) of rotational sampling [14]

This effect can be described by the meaning of the inverse notch filter. The inverse notch filter is a narrow band pass filter and it has an infinite impulse response. It rejects all frequencies expect of a stop frequency band centered on a center frequency, which is the wind turbine rotational frequency in our case. figure 3.6 shows the frequency response of the inverted notch filter. The state space representation of the three inverted notch filters for the three blades is:

$$\dot{\underline{x}}_{wind} = \underline{\underline{A}}_{Wind}\underline{x}_{wind} + \underline{\underline{B}}_{Wind}\,\underline{u}_{wind} \tag{4-6}$$

$$\underline{y}_{wind} = \underline{\underline{C}}_{Wind}\underline{x}_{wind} + \underline{\underline{D}}_{Wind}\underline{u}_{wind} \tag{4-7}$$

The matrices $\underline{\underline{A}}_{Wind}$, $\underline{\underline{B}}_{Wind}$, $\underline{\underline{C}}_{Wind}$, $\underline{\underline{D}}_{Wind}$ are represented as

$$\underline{\underline{A}}_{Wind} = \begin{bmatrix} 0 & 1 & 0 & 0 & 0 & 0 \\ -\Omega^2 & -2d\Omega^2 & 0 & 0 & 0 & 0 \\ 0 & 0 & 0 & 1 & 0 & 0 \\ 0 & 0 & -\Omega^2 & -2d\Omega^2 & 0 & 0 \\ 0 & 0 & 0 & 0 & 0 & 1 \\ 0 & 0 & 0 & 0 & -\Omega^2 & -2d\Omega^2 \end{bmatrix}, \underline{\underline{B}}_{Wind} = \begin{bmatrix} 0 & 0 & 0 \\ 1 & 0 & 0 \\ 0 & 0 & 0 \\ 0 & 1 & 0 \\ 0 & 0 & 0 \\ 0 & 0 & 1 \end{bmatrix}$$

$$\underline{\underline{C}}_{Wind} = \begin{bmatrix} 0 & 2\Omega & 0 & 0 & 0 & 0 \\ 0 & 0 & 0 & 2\Omega & 0 & 0 \\ 0 & 0 & 0 & 0 & 0 & 2\Omega \end{bmatrix}, \qquad \underline{\underline{D}}_{Wind} = \begin{bmatrix} 1 & 0 & 0 \\ 0 & 1 & 0 \\ 0 & 0 & 1 \end{bmatrix}$$

where d represents the damping factor and Ω the rotational speed.

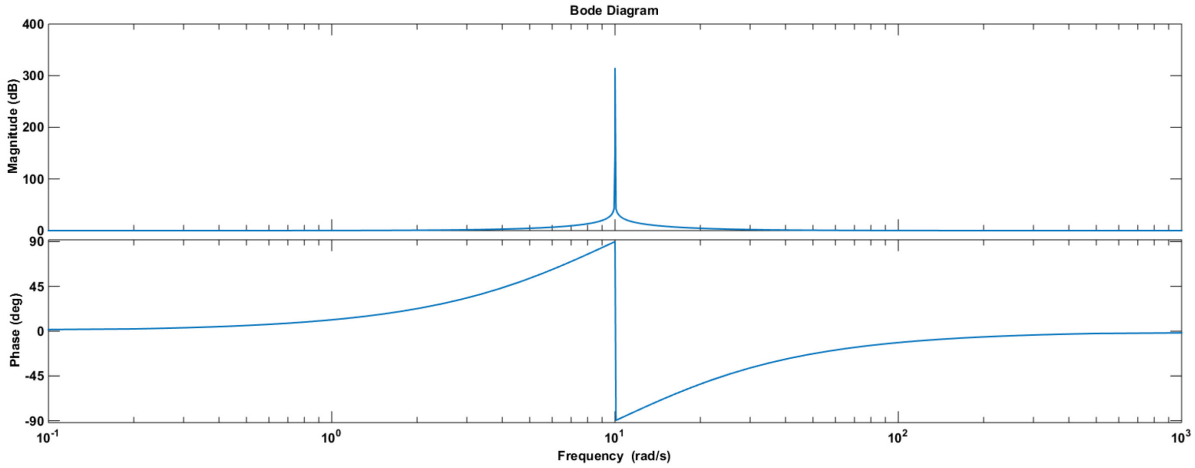

Figure 3.6: Inverted notch filter response.

4 Derivation of a controller structure based on a stochastic disturbance observer

4.1 Setting up design criteria

The high frequency variations in wind speed (turbulence) are the primary reasons for the fatigue of the different wind turbine components. Designing a control system to mitigate the loads caused by the turbulence will directly translate into a reduction in the fatigue damage. This directly leads to increase in the life time of the wind turbine as it will be illustrated in chapter 6.

Another impact of the turbulence on wind turbine is the fluctuations in the rotational speed. In order to increase the rotational speed strength, the turbulence effect should be reduced. Chapter 5 shows how much the reduction in the standard deviation of the rotational speed before and after applying the controller.

Briefly, the specific criteria for designing the control system are: -

1- Decreasing the fatigue damage.

2- Increasing the rotational speed strength.

4.2 State Estimation using Kalman Filter

The ability of an observer to estimate unmeasurable states from a set of measurements with the help of a model of the control path suggests the idea of extending the model of the control path by a model of the disturbance and reconstructing the states of the disturbance as well. State estimation is the process of determining an estimate of the internal system states depending on a set of measurements of system inputs and outputs. The estimated states are a combination of the wind turbine estimated states and the augmented wind disturbance estimated states. In this thesis, the Discrete Kalman Filter will be used as an observer for the estimation process. It is an optimal recursive data processing algorithm that gives the optimal estimates of the system states for a linear system with additive Gaussian white noise in the process and the measurements which is correct in our case [15]. Kalman filter is optimal by minimizing the mean squared error between the estimated state and the real state. The recursive operation mode of the Kalman filter comes from its ability to depend only the previous estimate to get the current estimate rather than depending on the history of all previous estimates. Figure 4.1 shows how is the Kalman filter estimates the system states with the help of the measurement of system's output.

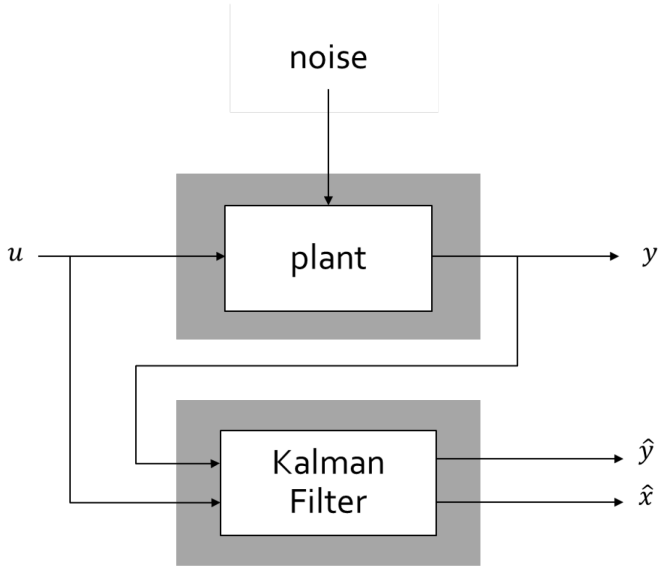

Figure 4.1: State estimation based on Kalman filter [16]

For nonlinear systems, different Kalman filters such as the extended Kalman filter and the unscented Kalman filter can be used. Nowadays, Kalman filter is used in many different applications such as tracking systems, navigation and many computer vision applications.

Before starting the discussion about the operation of the Kalman filter algorithm, we need to understand the definitions of what's called mean or expected value, variance and standard deviation.

Expected value or Mean (μ):-

For a random variable X, Expected value of X is

$$E[X] = \sum_{i}^{n} P_i x_i \tag{4-1}$$

where $x_1, x_2 \ldots\ldots\ldots x_n$ are the possible realization of X and $P_1, P_2 \ldots\ldots\ldots P_n$ are the corresponding probabilities. If X is a continuous random variable, the Expected value will be

$$E[X] = \int_{-\infty}^{\infty} x f_X(x)\, dx \tag{4-2}$$

where $f_X(x)$ is the probability density function.

Variance: -

$$VAR(X) = E\left[\left(X - E(X)\right)^2\right] \tag{4-3}$$
$$= E[X^2] - \mu^2$$

It is a measure of the spread of X around mean.

Standard deviation: -

It is the square root of variance.

$$\sigma(X) = \sqrt{VAR(X)} \tag{4-4}$$

4.2.1 The Discrete Kalman Filter derivation

For the derivation of the Discrete Kalman filter, suppose that the linear system is represented in a state space representation as following:

$$\underline{x}_{k+1} = \underline{\underline{A}}\underline{x}_k + \underline{\underline{B}}\underline{u}_{k+1} + \underline{w}_k \tag{4-5}$$

$$\underline{y}_k = \underline{\underline{C}}\underline{x}_k + \underline{\underline{D}}\underline{u}_k + \underline{v}_k \tag{4-6}$$

Where

$\underline{x}_k$: $(n \text{ x } 1)$ system state at time t_k

$\underline{y}_k$: $(p \text{ x } 1)$ measured output at time t_k

$\underline{u}_k$: $(m \text{ x } 1)$ control input at time t_k

$\underline{\underline{A}}$: $(n \text{ x } n)$ state matrix

$\underline{\underline{B}}$: $(n \text{ x } m)$ input matrix

$\underline{\underline{C}}$: $(p \text{ x } n)$ output matrix

$\underline{\underline{D}}$: $(p \text{ x } m)$ state matrix

$\underline{w}_k$: $(n \text{ x } 1)$ process noise

$\underline{v}_k$: $(p \text{ x } 1)$ measurement noise

n: number of the system states

p: number of the system outputs

m:number of the system

It is assumed that the process noise $\underline{w}_k$ and the measurement noise $\underline{v}_k$ are normally gaussian distributed and uncorrelated.

The covariance matrices for $\underline{w}_k$ and $\underline{v}_k$are given by

$$E\left[\underline{w}_k \underline{w}_i{}^T\right] = \underline{\underline{Q}}_{var}$$
$$E\left[\underline{v}_k \underline{v}_i{}^T\right] = \underline{\underline{R}}_{var}$$

Assume that the prior (or a priori) error in estimation is $\underline{e}_k^-$ where

$$\underline{e}_k^- = \underline{x}_k - \underline{\hat{x}}_k^- \tag{4-7}$$

where $\underline{\hat{x}}_k^-$ is the prior estimate.

A Priori means the estimation is done before the measurement and a posteriori means the estimation is done after the measurement.

The associated error covariance matrix $\underline{\underline{P}}_k^-$ is

$$\underline{\underline{P}}_k^- = E\left[\underline{e}_k^- \underline{e}_k^{-T}\right] = E\left[\left(\underline{x}_k - \underline{\hat{x}}_k^-\right)\left(\underline{x}_k - \underline{\hat{x}}_k^-\right)^T\right] \tag{4-8}$$

where $\underline{\hat{x}}_k^-$ is the prior state estimate.

With the new noisy measurement $\underline{y}_k$, the predicted state $\underline{\hat{x}}_k$ is corrected by a feedback of the difference between the measured output vector and the estimated output vector $\left(\underline{y}_k - \underline{\underline{C}}\,\underline{\hat{x}}_k^-\right)$ via a weighting factor $\underline{\underline{K}}_k$ as shown in the following equation

$$\underline{\hat{x}}_k = \underline{\hat{x}}_k^- + \underline{\underline{K}}_k\left(\underline{y}_k - \underline{\underline{C}}\,\underline{\hat{x}}_k^-\right) \tag{4-9}$$

This weighting factor is called Kalman gain and it will be determined later.

The updated error in the estimate or posteriori estimate error is

$$\underline{e}_k = \underline{x}_k - \underline{\hat{x}}_k \tag{4-10}$$

and the corresponding updated error covariance matrix is

$$\underline{\underline{P}}_k = E\left[\underline{e}_k\, \underline{e}_k^T\right] = E\left[\left(\underline{x}_k - \underline{\hat{x}}_k\right)\left(\underline{x}_k - \underline{\hat{x}}_k\right)^T\right]. \tag{4-11}$$

by substituting equation (4-9) into equation (4-11), we get

$$\begin{gathered} P_k = E\left[\underline{e}_k\, \underline{e}_k^T\right] = \\ E\left[\left(\underline{x}_k - \left[\underline{\hat{x}}_k^- + \underline{\underline{K}}_k(\underline{y}_k - \underline{\underline{C}}\,\underline{\hat{x}}_k^-)\right]\right)\left(\underline{x}_k - \left[\underline{\hat{x}}_k^- + \underline{\underline{K}}_k(\underline{y}_k - \underline{\underline{C}}\,\underline{\hat{x}}_k^-)\right]\right)^T\right] \end{gathered} \tag{4-12}$$

If equation (4-5) is substituted into equation (4-12), the updated error covariance matrix can be written as

$$\begin{aligned} \underline{\underline{P}}_k = E[&\left(\underline{x}_k - \left[\underline{\hat{x}}_k^- + \underline{\underline{K}}_k(\underline{\underline{C}}\,x_k + \underline{\underline{D}}\,\underline{u}_k + \underline{v}_k - \underline{\underline{C}}\,\underline{\hat{x}}_k^-)\right]\right) \\ &\left(\underline{x}_k - \left[\underline{\hat{x}}_k^- + \underline{\underline{K}}_k(\underline{\underline{C}}\,x_k + \underline{\underline{D}}\,\underline{u}_k + \underline{v}_k - \underline{\underline{C}}\,\underline{\hat{x}}_k^-)\right]\right)^T] \end{aligned} \tag{4-13}$$

$$\begin{aligned} \underline{\underline{P}}_k = E\{&\left(\underline{x}_k - \underline{\hat{x}}_k^-\right) - \underline{\underline{K}}_k(\underline{\underline{C}}\,x_k + \underline{\underline{D}}\,\underline{u}_k + \underline{v}_k - \underline{\underline{C}}\,\underline{\hat{x}}_k^-)]\big] \\ &\left[\left(\underline{x}_k - \underline{\hat{x}}_k^-\right) - \underline{\underline{K}}_k(\underline{\underline{C}}\,x_k + \underline{\underline{D}}\,\underline{u}_k + \underline{v}_k - \underline{\underline{C}}\,\underline{\hat{x}}_k^-)\right]^T\} \end{aligned} \tag{4-14}$$

performing this expectation, we get

$$\underline{\underline{P}}_k = \underline{\underline{P}}_k^- - \underline{\underline{K}}_k\underline{\underline{C}}\,\underline{\underline{P}}_k^- - \underline{\underline{P}}_k^-\,\underline{\underline{C}}^T\underline{\underline{K}}_k^T + \underline{\underline{K}}_k\left(\underline{\underline{C}}\,\underline{\underline{P}}_k^-\,\underline{\underline{C}}^T + \underline{\underline{R}}_{var}\right)\underline{\underline{K}}_k^T\ . \tag{4-15}$$

Now, the Kalman gain $\underline{\underline{K}}_k$ needs to be determined such that $\underline{\underline{P}}_k$ is minimized. This can be done using the straightforward differential calculus approach [17]. This approach can be

applied by differentiating the trace of $\underline{\underline{P}}_k$ which represents the sum of the mean square errors in the estimate with respect to $\underline{\underline{K}}_k$ and setting this derivative equal to zero

$$\frac{d(trace\ \underline{\underline{P}}_k)}{d\underline{\underline{K}}_k} = -2\left(\underline{\underline{C}}\,\underline{\underline{P}}_k^-\right)^T + 2\,\underline{\underline{K}}_k\left(\underline{\underline{C}}\,\underline{\underline{P}}_k^-\,\underline{\underline{C}}^T + \underline{\underline{R}}_{var}\right)\underline{\underline{K}}_k{}^T \tag{4-16}$$

$$-2\left(\underline{\underline{C}}\,\underline{\underline{P}}_k^-\right)^T + 2\,\underline{\underline{K}}_k\left(\underline{\underline{C}}\,\underline{\underline{P}}_k^-\,\underline{\underline{C}}^T + \underline{\underline{R}}_{var}\right)\underline{\underline{K}}_k{}^T = 0 \tag{4-17}$$

$$\underline{\underline{K}}_k = \underline{\underline{P}}_k^-\,\underline{\underline{C}}^T\left(\underline{\underline{C}}\,\underline{\underline{P}}_k^-\,\underline{\underline{C}}^T + \underline{\underline{R}}_{var}\right)^{-1} \tag{4-18}$$

Substituting the Kalman gain $\underline{\underline{K}}_k$ into equation (4-15), we get

$$\underline{\underline{P}}_k = \underline{\underline{P}}_k^- - \underline{\underline{P}}_k^-\,\underline{\underline{C}}^T\left(\underline{\underline{C}}\,\underline{\underline{P}}_k^-\,\underline{\underline{C}}^T + \underline{\underline{R}}_{var}\right)^{-1}\underline{\underline{C}}\,\underline{\underline{P}}_k^- \tag{4-19}$$

or

$$\underline{\underline{P}}_k = \underline{\underline{P}}_k^- - \underline{\underline{K}}_k\,\underline{\underline{C}}\,\underline{\underline{P}}_k^- \tag{4-20}$$

$$\underline{\underline{P}}_k = \left(I - \underline{\underline{K}}_k\,\underline{\underline{C}}\right)\underline{\underline{P}}_k^- \tag{4-21}$$

The next estimation can be obtained using equation (4-4) with ignoring w_k because it has zero mean and it is not correlated with any of the previous values

$$\underline{\hat{x}}_{k*1}^- = \underline{\underline{A}}\,\underline{\hat{x}}_k + \underline{\underline{B}}\,\underline{u}_{k+1}\ . \tag{4-22}$$

The associated error is

$$\begin{aligned} \underline{e}_{k*1}^- &= x_{k+1} - \underline{\hat{x}}_{k*1}^- \\ \underline{e}_{k*1}^- &= \underline{\underline{A}}\,\underline{x}_k + \underline{\underline{B}}\,\underline{u}_{k+1} + \underline{\underline{D}}\,\underline{u}_{k+1} + \underline{w}_k - \underline{\underline{A}}\,\underline{\hat{x}}_k - \underline{\underline{B}}\,\underline{u}_{k+1} - \underline{\underline{D}}\,\underline{u}_{k+1} \\ \underline{e}_{k*1}^- &= \underline{\underline{A}}\,\underline{e}_k + \underline{w}_k \end{aligned} \tag{4-23}$$

and the associated error covariance matrix in this case is

$$\underline{\underline{P}}_{k*1}^- = E\left[\underline{e}_{k*1}^-\,\underline{e}_{k*1}^{-\,T}\right]$$

$$\underline{\underline{P}}_{k*1}^- = E\left[\left(\underline{\underline{A}}\,\underline{e}_k + \underline{w}_k\right)\left(\underline{\underline{A}}\,\underline{e}_k + \underline{w}_k\right)^T\right] \tag{4-24}$$

$$\underline{\underline{P}}_{k*1}^- = \underline{\underline{A}}\,\underline{\underline{P}}_k\underline{\underline{A}}^T + \underline{\underline{Q}}_{var}\ .$$

Figure 4.2 shows the operation of the Kalman filter algorithm

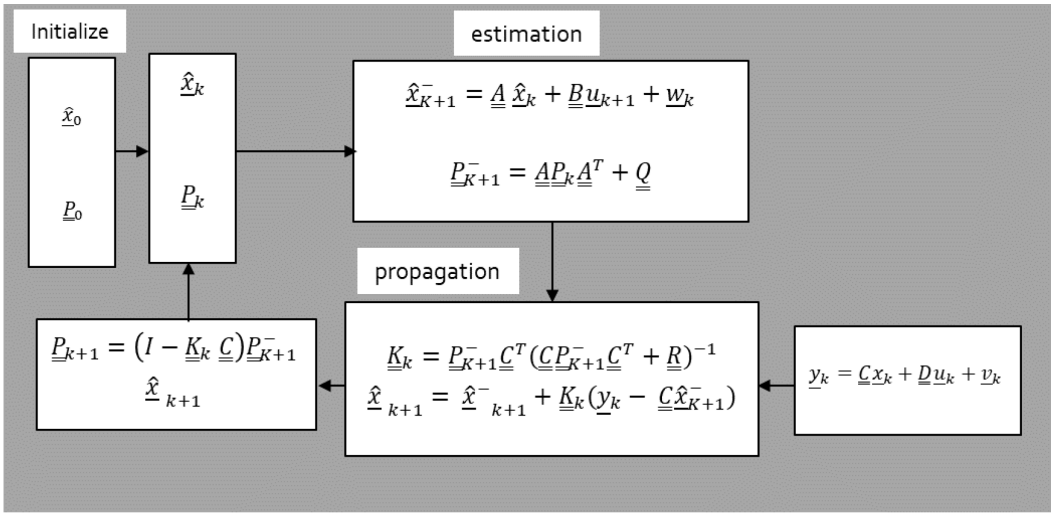

Figure 4.2: Kalman filter algorithm

4.2.2 Disturbance Observation

The model required for a disturbance observation using the Discrete Kalman filter consists of the combination of the linearized wind turbine model and the disturbance model as shown in figure 4.3. where $\underline{w}_k$ and $\underline{w}_{k_{Dry}}$ represent the process noise and the turbulence noise respectively. WT is an index for Wind Turbine and Dis is an index for Disturbance.

$$\begin{bmatrix} \dot{\underline{x}}_{WT} \\ \dot{\underline{x}}_{Dis} \end{bmatrix} = \begin{bmatrix} \underline{\underline{A}} & \underline{\underline{E}}\,\underline{\underline{C}}_{Dis} \\ 0 & \underline{\underline{A}}_{Dis} \end{bmatrix} \begin{bmatrix} \underline{x}_{WT} \\ \underline{x}_{Dis} \end{bmatrix} + \begin{bmatrix} \underline{\underline{B}} \\ 0 \end{bmatrix} \underline{u} + \begin{bmatrix} 0 \\ \underline{\underline{B}}_{Dis} \end{bmatrix} \underline{r} + \begin{bmatrix} \underline{w}_k \\ \underline{w}_{k_{Dis}} \end{bmatrix} \tag{4-25}$$

$$\underline{y}_{WT} = [\underline{\underline{C}} \quad \underline{\underline{F}}\,\underline{\underline{C}}_{Dis}] \begin{bmatrix} \underline{x}_{WT} \\ \underline{x}_{Dis} \end{bmatrix} + \underline{\underline{D}}\,\underline{u} + \underline{v}_k \tag{4-26}$$

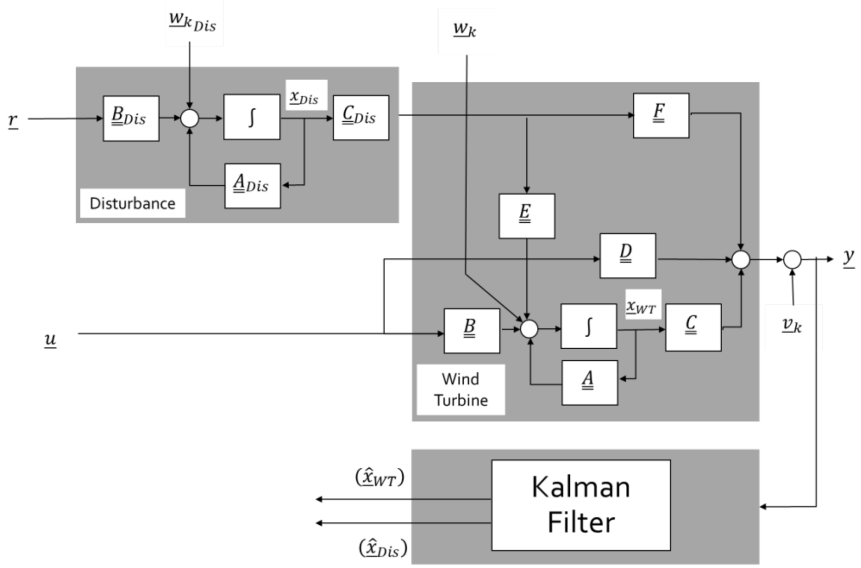

Figure 4.3: The required model for state estimation using Kalman filter

4.2.3 Kalman Filter Tuning

The tuning of the Kalman filter is done via determination of the process noise covariance matrix $\underline{\underline{Q}}_{var}$ and the measurement noise covariance matrix $\underline{\underline{R}}_{var}$.

For the tuning process, often just the main diagonal elements $\underline{\underline{Q}}_{var}$ and $\underline{\underline{R}}_{var}$ are engaged where the other elements are neglected.

The measurement noise covariance matrix is determined through the error in the measurement. This error can be obtained from the sensors datasheet. The approximated measured noise is modelled by the following values

$\underline{\underline{R}}_{var}(1,1) = 6{,}25 * 10^{-6}$

$\underline{\underline{R}}_{var}(2,2) = 0{,}0001$

$\underline{\underline{R}}_{var}(3,3) = 0{,}0001$

$\underline{\underline{R}}_{var}(4,4) = 0{,}0001$

$\underline{\underline{R}}_{var}(5,5) = 0{,}0001$

$\underline{\underline{R}}_{var}(6,6) = 0{,}0001$

$\underline{\underline{R}}_{var}(7,7) = 0{,}0001$

$\underline{\underline{R}}_{var}(8,8) = 0{,}0001$

$\underline{\underline{R}}_{var}(9,9) = 0{,}0001$

$\underline{\underline{R}}_{var}(10,10) = 0{,}0001$

The process noise covariance matrix is not so easy to be determined because there is no specific way to get it. Often this noise is selected via trial and error. One of these trials, which has been used here uses the model uncertainties caused by the preciosity of the un models. This can be shown in figure 4.4 where a66, a77, a88, a99 and a 1010 represents the average model uncertainties over the azimuth for $\underline{\underline{A}}(6,6)$, $\underline{\underline{A}}(7,7)$, $\underline{\underline{A}}(8,8)$, $\underline{\underline{A}}(9,9)$, $\underline{\underline{A}}(10,10)$ respectively.

These are the values of the diagonal elements of the process noise covariance matrix where the first ten elements are for the wind turbine states and the other 9 elements are for the disturbance states.

$\underline{\underline{Q}}_{var}(1,1) = 6 * 10^{-9}$

$\underline{\underline{Q}}_{var}(6,6) = 6 * 10^{-9}$

$\underline{\underline{Q}}_{var}(2,2) = 3 * 10^{-8}$

$\underline{\underline{Q}}_{var}(7,7) = 3 * 10^{-8}$

$\underline{\underline{Q}}_{var}(3,3) = 9 * 10^{-6}$

$\underline{\underline{Q}}_{var}(8,8) = 9 * 10^{-6}$

$\underline{\underline{Q}}_{var}(4,4) = 9 * 10^{-6}$

$\underline{\underline{Q}}_{var}(5,5) = 9 * 10^{-6}$

$\underline{\underline{Q}}_{var}(9,9) = 9 * 10^{-6}$

$\underline{\underline{Q}}_{var}(10,10) = 3 * 10^{-7}$

$\underline{\underline{Q}}_{var}(11,11) = 3 * 10^{-7}$

$\underline{\underline{Q}}_{var}(12,12) = 3 * 10^{-7}$

$\underline{\underline{Q}}_{var}(13,13) = 3 * 10^{-7}$

$\underline{\underline{Q}}_{var}(13,13) = 3 * 10^{-7}$

$\underline{\underline{Q}}_{var}(14,14) = 3 * 10^{-7}$

$\underline{\underline{Q}}_{var}(14,14) = 3 * 10^{-7}$

$\underline{\underline{Q}}_{var}(15,15) = 3 * 10^{-7}$

$\underline{\underline{Q}}_{var}(16,16) = 3 * 10^{-7}$

$\underline{\underline{Q}}_{var}(17,17)$ =0.0006666

$\underline{\underline{Q}}_{var}(18,18)$ =0.00066667

$\underline{\underline{Q}}_{var}(19,19)$ =0.00066667

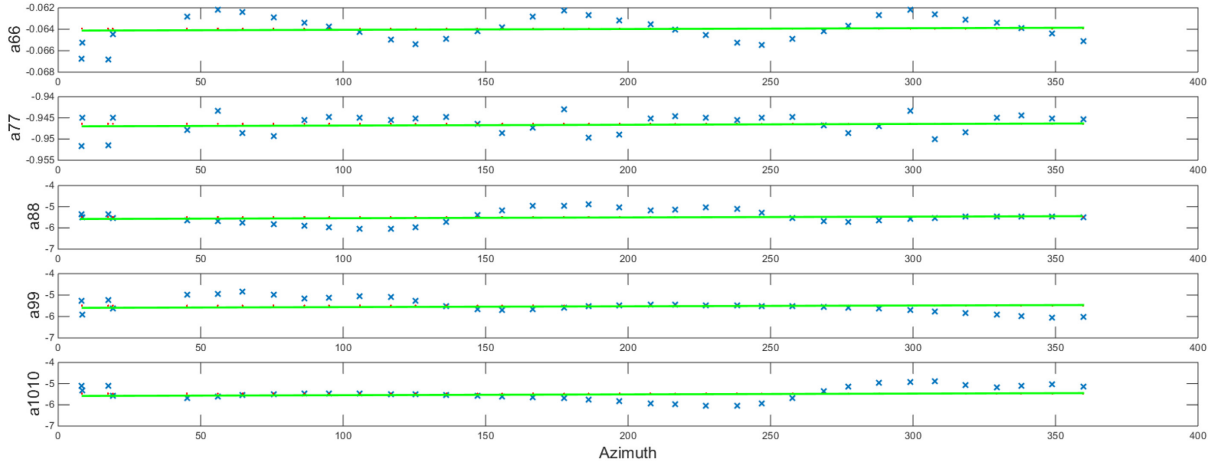

Figure 4.4: Determination of the process noise covariance matrix

4.3 Controller structure based on stochastic Disturbance accommodation control

As it is discussed before, the second requirement in the disturbance accommodation control theory is to design a feedback/feedforward controller in order to stabilize the system and accommodate the disturbance. In our case, the Linear Quadratic Regulator (LQR) will be used as a full state feedback controller for tuning the wind turbine plant and a feedforward controller to accommodate the wind disturbances.

4.3.1 linear quadratic regulator

The linear quadratic regulator design is as an important design technique for linear systems since the sixties. There are two main objectives of LQR design, the first objective is to find a full state feedback controller to stabilize the wind turbine based on the turbine estimated states, which have been obtained from the Kalman filter, as we discussed in the previous section, where the second objective is to minimize the cost function J that has been given in equation (4-27). This combination of an optimal estimator and an optimal regulator is called linear Quadratic Gaussian (LQG).

Due to the separation principle, the estimation process via an observer e.g. Kalman Filter can be done separately to the controller tuning.

According to Kalman, a linear time - invariant system is optimal if the following quadratic cost function is minimized

$$J = \int_0^\infty (\underline{x}^T \underline{\underline{Q}}_{LQR}\, \underline{x} + \underline{u}^T \underline{\underline{R}}_{LQR}\, \underline{u}) dt \ . \qquad (4\text{-}27)$$

where $\underline{\underline{Q}}_{LQR}$ and $\underline{\underline{R}}_{LQR}$ are constant weighting matrices and must meet the following conditions:

- $\underline{\underline{R}}_{LQR}$ must be positive definite (regular and symmetrical)
- $\underline{\underline{Q}}_{LQR}$ must be positive semidefinite (all principal determinants ≥ 0)

Therefore, no negative cost components will occur. By appropriate selection of the weighting matrices, it can be a more meaningful compromise between the system states and the control effort [18].

The solution of the above variational problem (minimization of the cost function under the constraint of the state equations) leads to Hamiltonian canonical equations, which are solved by linear approach. From this, the cost function is minimized for the control law

$$\underline{u} = -\underline{\underline{K}}_{LQR}\ \underline{x} \tag{4-29}$$

The $\underline{\underline{K}}_{LQR}$ is defined as

$$\underline{\underline{K}}_{LQR} = \underline{\underline{R}}_{LQR}{}^{-1}\underline{\underline{B}}^{T}\underline{\underline{P}} \tag{4-30}$$

where $\underline{\underline{P}}$ is an (nxn) matrix and equal to the solution of the following non-linear Riccati differential equation

$$\dot{\underline{\underline{P}}} = \underline{\underline{P}}\,\underline{\underline{A}} + \underline{\underline{A}}^{T}\underline{\underline{P}} - \underline{\underline{P}}\,\underline{\underline{B}}\,\bar{\bar{R}}^{-1}\underline{\underline{B}}^{T}\underline{\underline{P}} + \underline{\underline{Q}}_{LQR} = 0\ . \tag{4-31}$$

If the process is fully controllable and $\underline{\underline{A}}, \underline{\underline{B}}, \underline{\underline{C}}, \underline{\underline{Q}}_{LQR}$ and $\underline{\underline{R}}_{LQR}$ are constants, $\underline{\underline{P}}$ is a constant, real, symmetric, positive-definite nxn matrix [18].

The advantages of this approach are: -

- It provides an optimal controller structure including its parameters.
- It always leads to a stable control system.
- Relatively fast calculation algorithms are available to solve the nonlinear algebraic Riccati equation for $\underline{\underline{P}}$.
- It is also optimal in the sense of minimizing the variance of the state variables in stochastic disorders.

But it has the following disadvantages: -

- The structure of the quality function and the selection of the weighting matrices are formally restricted.
- The cost function converges only when $\underline{x}$ and $\underline{u}$ are close to zero for $t \to \infty$.
- It is only applicable to a complete state vector feedback, so the state variables must be measured or estimated, the controller structure is specified fixed.

4.3.1.1 LQR Tuning

LQR Tuning means choosing values for the weighting matrices $\underline{\underline{Q}}_{LQR}$ and $\underline{\underline{R}}_{LQR}$ to penalize the state variables and the control effort. In case of choosing a large value for $\underline{\underline{R}}_{LQR}$, the control effort will be highly penalized. Similarly, for $\underline{\underline{Q}}_{LQR}$, if the $\underline{\underline{Q}}_{LQR}$ value is large, this means that the system is stabilized with less changes in the states. The values of the main diagonal elements in the $\underline{\underline{Q}}_{LQR}$ are calculated according to this rule of thumb

$$\underline{x}^T \underline{\underline{Q}}_{LQR} \underline{x} = q_{11}\underline{x}_1^2 + \cdots + q_{1010}\underline{x}_{1010}^2 \quad (4\text{-}31)$$

where q_{11} is inversely proportional to maximum allowed value of $\underline{x}_1$(similar withq_{22}). Those are the calculated values of the main diagonal elements of $\underline{\underline{Q}}_{LQR}$ and $\underline{\underline{R}}_{LQR}$.

$\underline{\underline{R}}_{LQR}(1,1) = 1$

$\underline{\underline{R}}_{LQR}(2,2) = 1$

$\underline{\underline{R}}_{LQR}(3,3) = 1$

$\underline{\underline{Q}}_{LQR}(1,1) = 1$

$\underline{\underline{Q}}_{LQR}(2,2) = 0{,}1$

$\underline{\underline{Q}}_{LQR}(3,3) = 10$

$\underline{\underline{Q}}_{LQR}(4,4) = 10$

$\underline{\underline{Q}}_{LQR}(5,5) = 10$

$\underline{\underline{Q}}_{LQR}(6,6) = 1$

$\underline{\underline{Q}}_{LQR}(7,7) = 0{,}1$

$\underline{\underline{Q}}_{LQR}(8,8) = 10$

$\underline{\underline{Q}}_{LQR}(9,9) = 10$

$\underline{\underline{Q}}_{LQR}(10,10) = 10$

4.3.2 Feedforward Control

In this subsection, we will discuss how a feedforward controller can be used to accommodate the wind disturbances.

If the disturbance can be modelled as

$$\dot{\underline{x}_d} = \underline{\underline{A}}_d \underline{x}_d \tag{4-32}$$

$$\underline{z} = \underline{\underline{C}}_d \underline{x}_d \tag{4-33}$$

The disturbance model can be combined with the model of wind turbine and giving the following state space model

$$\dot{\underline{x}} = \underline{\underline{A}}\underline{x} + \underline{\underline{B}}\,\underline{u} + \underline{\underline{E}}\underline{\underline{C}}_d \underline{x}_d \tag{4-34}$$

$$\underline{y} = \underline{\underline{C}}\,\underline{x} + \underline{\underline{D}}\,\underline{u} + \underline{\underline{F}}\underline{\underline{C}}_d \underline{x}_d \ . \tag{4-35}$$

This can be written in matrix form as

$$\begin{bmatrix} \dot{\underline{x}} \\ \dot{\underline{x}}_d \end{bmatrix} = \begin{bmatrix} \underline{\underline{A}} & \underline{\underline{E}}\underline{\underline{C}}_d \\ 0 & \underline{\underline{A}}_d \end{bmatrix} \begin{bmatrix} \underline{x} \\ \underline{x}_d \end{bmatrix} + \begin{bmatrix} \underline{\underline{B}} \\ 0 \end{bmatrix} \underline{u} \tag{4-36}$$

$$\underline{y} = \begin{bmatrix} \underline{\underline{C}} & \underline{\underline{F}}\underline{\underline{C}}_d \end{bmatrix} \begin{bmatrix} \underline{x} \\ \underline{x}_d \end{bmatrix} \tag{4-37}$$

Or in a short form as

$$\dot{\underline{x}}^* = \underline{\underline{A}}^*\,\underline{x}^* + \underline{\underline{B}}^*\,\underline{u} \tag{4-38}$$

$$\underline{y} = \underline{\underline{C}}^*\,\underline{x}^* \tag{4-39}$$

Where

$$\underline{\underline{A}}^* = \begin{bmatrix} \underline{\underline{A}} & \underline{\underline{E}}\underline{\underline{C}}_d \\ 0 & \underline{\underline{A}}_d \end{bmatrix}, \qquad \underline{\underline{B}}^* = \begin{bmatrix} \underline{\underline{B}} \\ 0 \end{bmatrix}, \qquad \underline{\underline{C}}^* = \begin{bmatrix} \underline{\underline{C}} & \underline{\underline{F}}\underline{\underline{C}}_d \end{bmatrix}$$

The previous state equations (4-38) and (4-39) combines the turbine states and the wind disturbance states. Those states can be estimated using the Luenberger full state observer as shown in figure 4.5.

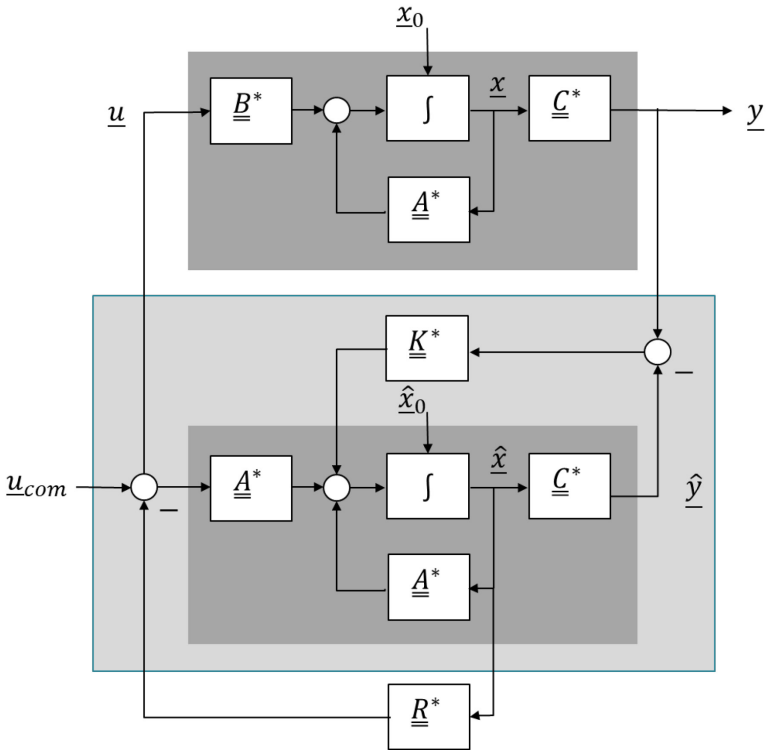

Figure 4.5: State estimation and state feedback based on Luenberger full state observer

The control input $\underline{u}$ can be written as

$$\underline{u} = -\underline{\underline{R}}^* \hat{\underline{x}}^* + \underline{u}_{com} \tag{4-40}$$

where $\underline{\underline{R}}^*$ is the closed loop gain; $\underline{\underline{R}}^* = [\underline{\underline{K}}_{LQR} \quad \underline{\underline{N}}]$, $\underline{\underline{K}}_{LQR}$ is the feedback gain, $\underline{\underline{N}}$ is the feedforward gain.

The observed state equation can be written as

$$\dot{\hat{\underline{x}}}^* = \underline{\underline{A}}^* \hat{\underline{x}}^* + \underline{\underline{B}}^* \underline{u} + \underline{\underline{K}}^* \underline{\underline{C}}^* \left(\underline{x}^* - \hat{\underline{x}}^*\right) \tag{4-41}$$

where $\underline{\underline{K}}^*$ is the observer gain; $\underline{\underline{K}}^* = [\underline{\underline{K}}_x \quad \underline{\underline{K}}_{xd}]^T$.

Equation (4-42) expresses the error in estimation which is the difference between the real state and the estimated state.

$$\underline{e}^* = \underline{x}^* - \underline{\hat{x}}^* = \begin{bmatrix} \underline{e}^* x \\ \underline{e}^* xd \end{bmatrix} = \begin{bmatrix} \underline{x} \\ \underline{x}_d \end{bmatrix} - \begin{bmatrix} \underline{\hat{x}} \\ \underline{\hat{x}}_d \end{bmatrix} \tag{4-42}$$

The first-time derivative in the estimation error is

$$\underline{\dot{e}}^* = \begin{bmatrix} \underline{\dot{e}}_x \\ \underline{\dot{e}}_{xd} \end{bmatrix} = \dot{x}^* - \underline{\hat{\dot{x}}}^* = \left[\underline{\underline{A}}^* - \underline{\underline{K}}^* \underline{\underline{C}}^*\right] \begin{bmatrix} \underline{e}_x \\ \underline{e}_{xd} \end{bmatrix} \tag{5-43}$$

The state equation of the total system can be obtained by substituting the control input u into the state equation (4-38). it can be written as

$$\begin{bmatrix} \underline{\dot{x}}^* \\ \underline{\dot{e}}^* \end{bmatrix} = \begin{bmatrix} \underline{\underline{A}}^* - \underline{\underline{B}}^* \underline{\underline{R}}^* & \underline{\underline{B}}^* \underline{\underline{R}}^* \\ 0 & \underline{\underline{A}}^* - \underline{\underline{K}}^* \underline{\underline{C}}^* \end{bmatrix} \begin{bmatrix} \underline{x}^* \\ \underline{e}^* \end{bmatrix} + \begin{bmatrix} \underline{\underline{B}}^* \\ 0 \end{bmatrix} \underline{u}_{com} \tag{4-44}$$

If A^*,$\underline{\underline{B}}^*$,$C^*$,$K^*$,$R^*$ are replaced into equation (4-44) by their definitions, the total system state equation will be written in the following detailed form

$$\begin{bmatrix} \underline{\dot{x}} \\ \underline{\dot{x}}_d \\ \underline{\dot{e}}_x \\ \underline{\dot{e}}_{xd} \end{bmatrix} = \begin{bmatrix} \underline{\underline{A}} - \underline{\underline{B}} \underline{\underline{K}}_{LQR} & \underline{\underline{E}}\, \underline{\underline{C}}_d - \underline{\underline{B}} \underline{\underline{N}} & \underline{\underline{B}} \underline{\underline{K}}_{LQR} & \underline{\underline{B}} \underline{\underline{N}} \\ 0 & \underline{\underline{A}}_d & 0 & 0 \\ 0 & 0 & \underline{\underline{A}} - \underline{\underline{K}}_x \underline{\underline{C}} & \underline{\underline{E}} \underline{\underline{C}}_d - \underline{\underline{K}}_x \underline{\underline{F}} \underline{\underline{C}}_d \\ 0 & 0 & -\underline{\underline{K}}_{xd} \underline{\underline{C}} & \underline{\underline{A}}_d - \underline{\underline{K}}_{xd} \underline{\underline{F}} \underline{\underline{C}}_d \end{bmatrix} \begin{bmatrix} \underline{x} \\ \underline{x}_d \\ \underline{e}_x \\ \underline{e}_{xd} \end{bmatrix} + \begin{bmatrix} \underline{\underline{B}} \\ 0 \\ 0 \\ 0 \end{bmatrix} \underline{u}_{com} \,. \tag{4-45}$$

From the previous equation, it is shown that the disturbance states $\underline{x}_d$ influences the first-time derivative of the system state $\underline{\dot{x}}$ through the term $\underline{\underline{E}} \underline{\underline{C}}_d - \underline{\underline{B}} \underline{\underline{N}}$.
This influence can be neglected if

$$\underline{\underline{N}} = \underline{\underline{B}}^{-1} \underline{\underline{E}} \underline{\underline{C}}_d \,. \tag{4-46}$$

In case of matrix $\underline{\underline{B}}$ is not invertible, an optimal disturbance variable response is possible in the sense of the smallest error squared using the pseudo inverse $\underline{\underline{B}}^* = (\underline{\underline{B}}^T \underline{\underline{B}})^{-1} \underline{\underline{B}}^T$.
It can be seen from equation (4-44) that the error in the estimation of the disturbance e_{xd} has an effect on the state vector of the control loop via matrix $\underline{\underline{E}} \underline{\underline{C}}_d - \underline{\underline{K}}_x \underline{\underline{F}} \underline{\underline{C}}_d$. A 100% compensation of this error is only possible for the theoretical case of an infinitely rapid estimation error dynamics. Due to the stochastic character of the turbulence but the variance in the estimation error $\sigma^2 = E\left(\underline{x}_i - \underline{\hat{x}}_i\right)$ can be minimized by using an optimal estimator such as Kalman filter as we discussed before.

5. Results

All the results shown in this chapter are done with the linear model at the trim point mentioned in chapter 2. The linearization has also been done for the following trim points and the results are shown in the appendix.

Trim point A: -

- 15 m/s steady horizontal wind speeds.
- 90 m as Reference height for horizontal wind speed.
- 10.45 degree as initial blade pitch angel for each blade.
- 12.1 rpm as initial rotor speed.

Trim point B: -

- 25 m/s steady horizontal wind speeds.
- 90 m as Reference height for horizontal wind speed.
- 23.47 degree as initial blade pitch angel for each blade.
- 12.1 rpm as initial rotor speed.

The system states after the combination between the wind turbine model and the disturbance model are the wind turbine states that were mentioned in chapter 2 with the addition of the following disturbance states: -

- Turbulence state for blade 1
- Turbulence state for blade 2
- Turbulence state for blade 3
- eddy slicing state 1 for blade 1
- eddy slicing state 2 for blade 1
- eddy slicing state 1 for blade 2
- eddy slicing state 2 for blade 2
- eddy slicing state 1 for blade 3
- eddy slicing state 2 for blade 3

where the measured outputs are: -

- Angular generator speed
- Blade 1 edgewise moment

- Blade 2 edgewise moment
- Blade 3 edgewise moment
- Blade 1 flapwise moment
- Blade 2 flapwise moment
- Blade 3 flapwise moment
- Tower side-to-side moment
- Tower fore-aft moment
- Tower torsional moment

The system stability has been checked and it shows that the system is unstable because of unstable pole. The reason behind this instability issue is a numerical problem with FAST caused from the generator azimuth state after applying Multi Blade Coordinate transformation (MBC). This unstable response can be shown in the first plot at figure 5.6. with applying the LQR as a full state feedback controller, the system becomes stable as shown in the third plot in the same figure. In case of neglecting this state, the wind turbine becomes stable as shown in the output response in figure 5.1 and 5.2.

The implementation of the linearized wind turbine model, Kalman filter and the controller structure is shown in MATLAB Simulink. The validations of the Discrete Kalman Filter and the feedback/feedforward controller are done first for the linear models then for the nonlinear model.

The advantage of the interface between FAST and Simulink with MATLAB gives the ability to use the FAST-nonlinear equations of motion through the FAST S-Function that has been incorporated in a Simulink model as shown in figure 6.4. This allows the validation of the results in the nonlinear simulation environment.

5.1 Validation of the Linear Model

Figure 5.1 and 5.2 show a good correspond between the linear model and the FAST-nonlinear model for the flapwise moment and the tower fore-aft.

The first 10 secs in those figures show the open loop response for the linear and nonlinear models without command pitch input. The next 50 secs show the open loop response for both models with pitch command input of one-degree pitch angle.

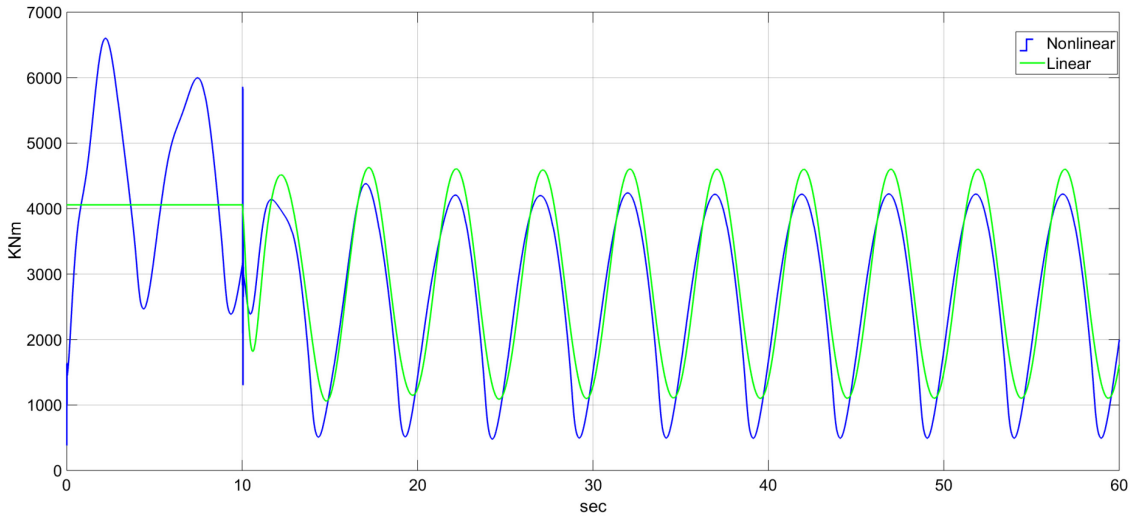

Figure 5.1: Validation of the linear model for the flapwise moment

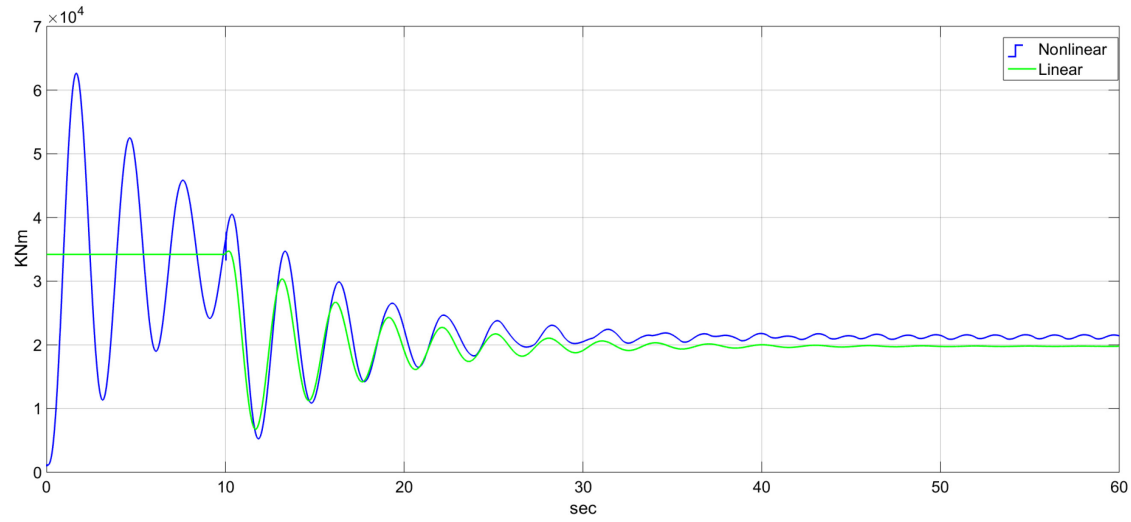

Figure 5.2: Validation of the linear model for the tower fore-aft moment

5.2 Validation of the Discrete Kalman Filter with the linear model

The Discrete Kalman Filter has been implemented in MATLAB Simulink and connected to the linearized model in combination with the disturbance model. The simulation has been run, the results shows a good and fast estimation for the wind turbine states as shown in figure 5.3 for the generator speed DoF and 1st flapwise bending mode DoF.

The prefect gaussian distribution with zero mean shows a correct implementation of the filter. The good quality of the estimation is shown by the low value of the standard deviation of the error.

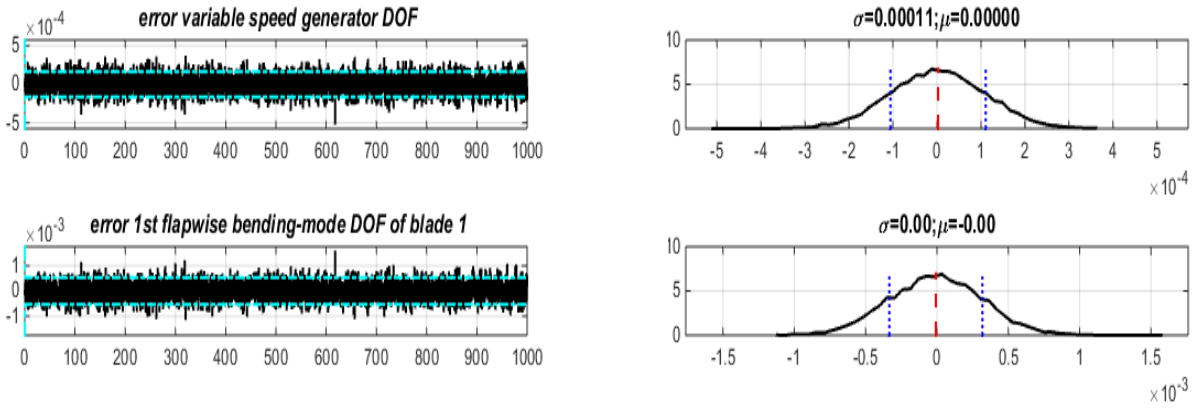

Figure 5.3: State estimation for generator speed DoF and 1st flapwise bending mode DoF based on Discrete Kalman Filter

The standard deviation of the error in estimation calculated from time series and plotted as a red dashed line in figure 5.3 shows a very fast and stable performance of the Kalman filter. It has a value of 0,00011 for the variable speed generator DOF where its value the first flapwise bending-mode DOF is zero. The cyan line shown in the same figure shows the standard deviation of the error in estimation calculated from the Kalman filter as shown in equation (4-10). it is shown that it has a smaller value less than 0,001 KNm for the first flapewise bending-mode DOF and less than 0,0005 rpm for the variable speed generator DOF. Results for other states and outputs are shown in figure A.1 and A.2 in the appendix.

The simulation also shows a good estimation of the disturbance states where the standard deviations of the errors between the real states and the estimated states are very small as shown in figure 5.4 for the turbulence states.

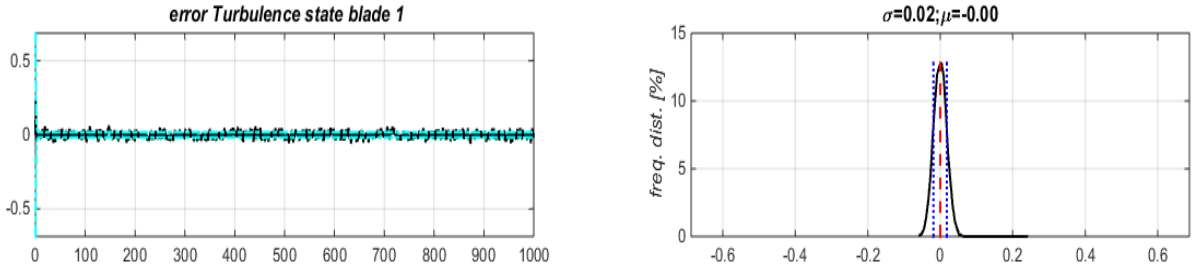

Figure 5.4: Turbulence state estimation for blade 1

5.3 Validation of the Discrete Kalman Filter with the nonlinear model

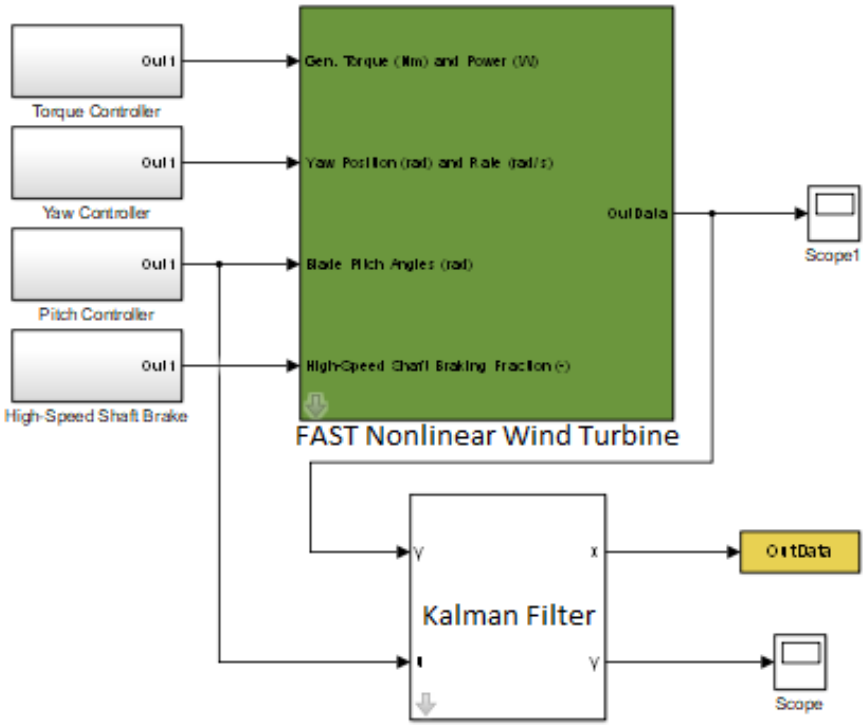

Figure 5.5: State estimation for FAST nonlinear wind turbine

The operation of the Kalman filter has been also validated with the nonlinear wind turbine supported by FAST as a S-Function in Simulink as shown in figure 5.5. Kalman Filter shows a good and fast estimation for the nonlinear wind turbine outputs as shown in Figure 5.6 for the flapwise moment.

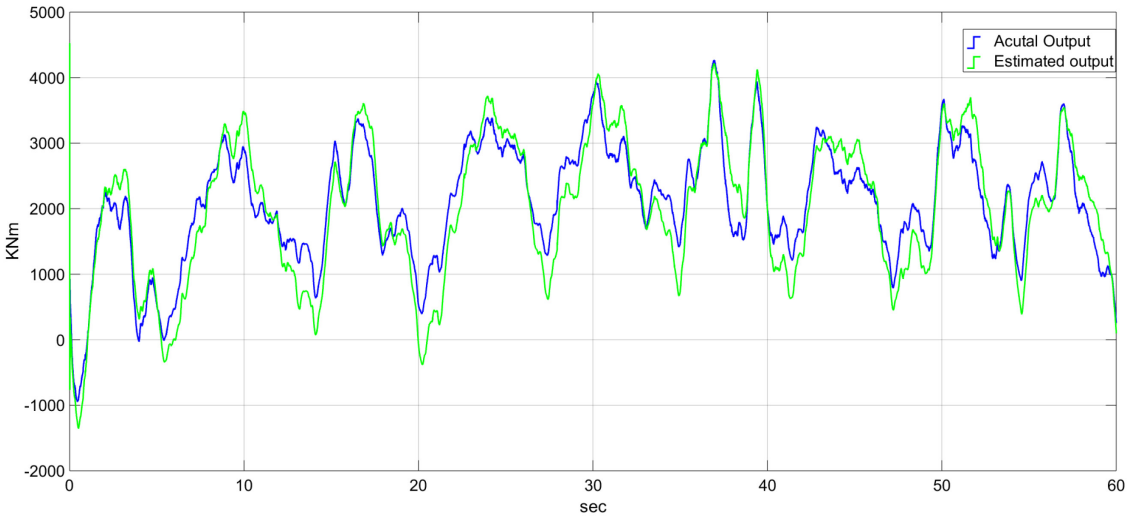

figure 5.6: Kalman filter state estimation for the flapwise moment in turbulent atmosphere.

5.4 The Controller Performance

The stochastic disturbance accommodation controller that is described in the previous chapter is implemented in this subsection. The controller structure consists of the feedback and the feedforward controller as shown in figure 5.7 where $\underline{\underline{K}}_{LQR}$ represents the feedback gain and $\underline{\underline{K}}_{FF}$ represents the feedforward gain.

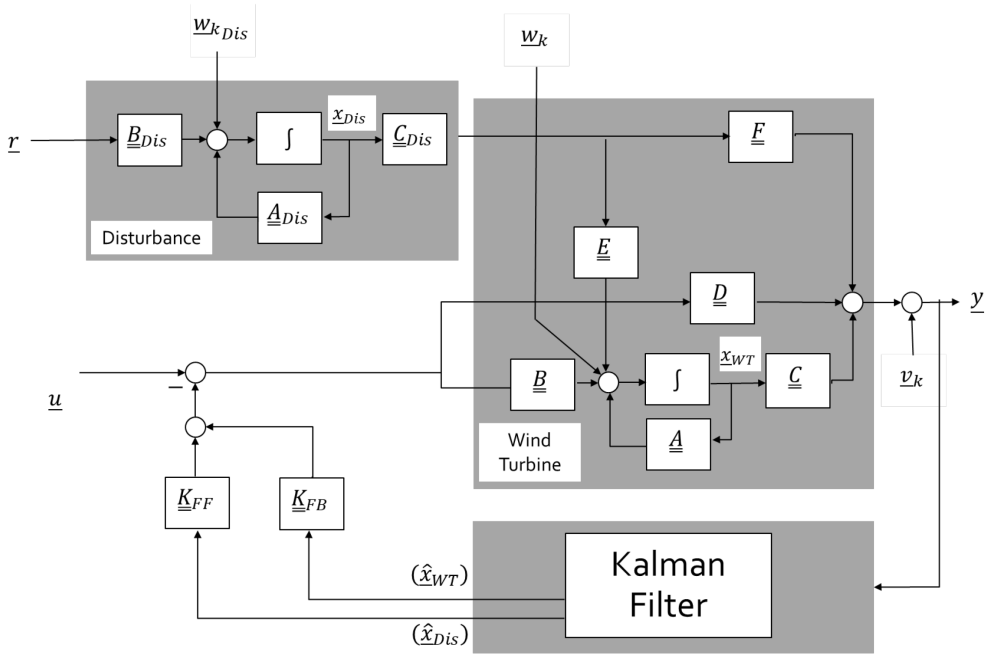

Figure 5.7: Controller structure in the linear simulation environment

The Controller shows a good behavior in the disturbance accommodation and wind turbine stabilization. Table 5.1 shows a comparison between uncontrolled turbine, feedforward controlled turbine and feedforward/feedback controlled turbine for the generator speed, blade flapwise moment and tower fore-aft moment where the standard deviation has a lower value for the feedforward/feedback controlled turbine and a higher value for the uncontrolled turbine. Other comparison for all the measured outputs including the blade torsion moment for each blade and the system stats are shown in figure A.9 the appendix.

	Uncontrolled turbine	Feedforward control	Feedforward/Feedback control
Generator speed	34.45 rpm	15.62 rpm	15.62 rpm
blade Flapwise	6272.9 KNm	5442.65 KNm	240.63 KNm

moment			
Tower fore-aft moment	2503.39 KNm	647.23 KNm	633.66 KNm

Table 5.1: A comparison between the uncontrolled turbine, feedforward controlled turbine and feedforward/feedback controlled turbine

It is noticed that the standard deviation has the same value with the feedforward/feedback control and the feedforward control alone for the generator speed but the difference between the two controllers in this case is shown in figure 5.9 where the generator speed has a higher value near the rated speed with the feedforward/feedback control that its value for the feedforward alone.

Figure 5.8 shows the controller behavior on the flap moment where the disturbance accommodation is achieved by the feedforward controller and the reduction in the flap moment is achieved by the LQR. The instability caused by unstable pole in the output response shown in the first two graphs in the same figure and not shown in the third graph clarifies that the Kalman Filter and the feedforward gain have no influence on the system eigenvalues, only the feedback via $\underline{\underline{K}}_{LQR}$ has an influence on the eigen values.

Figure 5.9 and figure 5.10 show also the controller behavior on the generator speed and the tower fore-aft moment respectively.

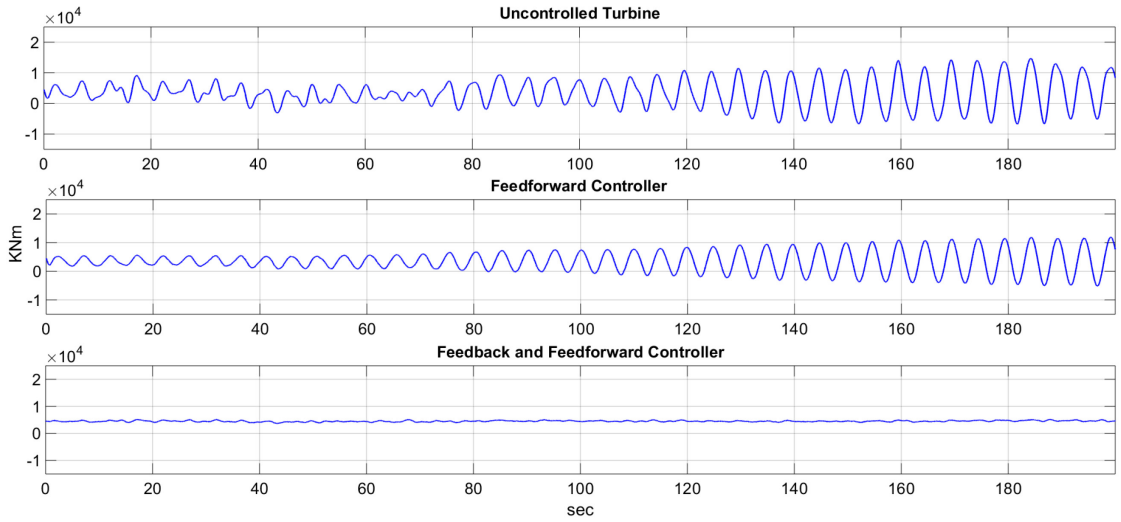

Figure 5.8: Comparison of the uncontrolled turbine against the feedforward controlled turbine and the feedforward/feedback controlled turbine for The flap moment

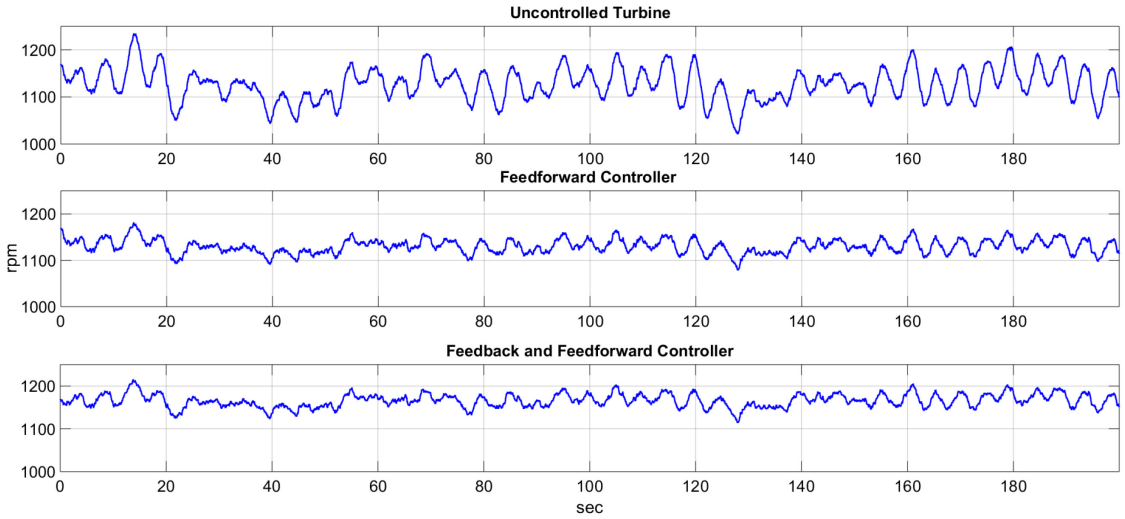

Figure 5.9: Comparison of the uncontrolled turbine against the feedforward controlled turbine and the feedforward/feedback controlled turbine for the generator speed

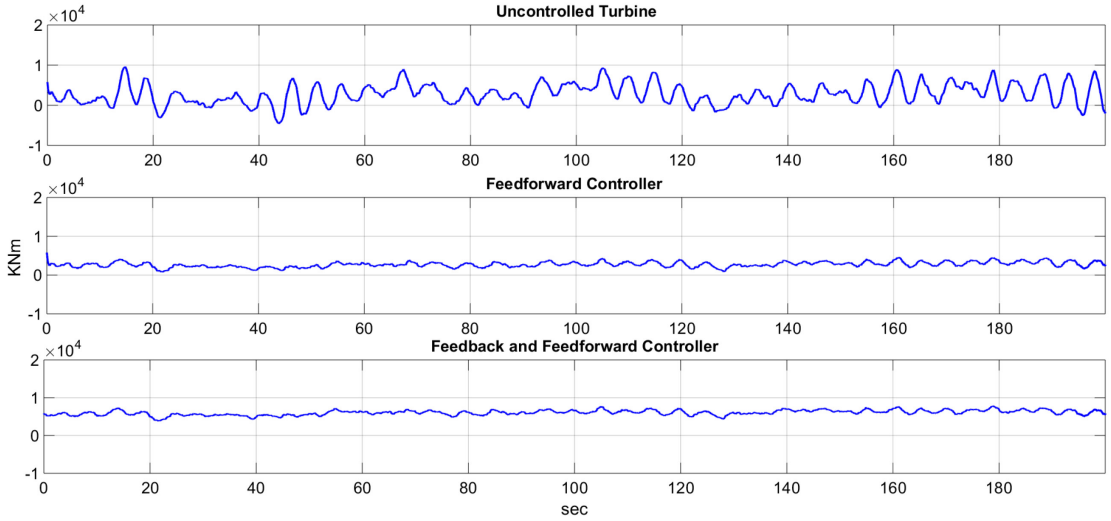

Figure 5.10: Comparison of the uncontrolled turbine against the feedforward controlled turbine and the feedforward/feedback controlled turbine The tower fore-aft moment

6. Comparative studies with a given "classical load controller"

The results of this study have to compared with the results of a classical load controller study [20]. The blade fatigue damage, the tower fatigue damage, and the rotational speed-strength are used as comparison criteria. The fatigue damage for the blade and the tower is calculated using rainflow counting that allows the application of Palmgren-Miner linear damage hypothesis or what's called Miner's rule. Miner's rule is one of the most widely models used to calculate the damage caused by cyclic loads. It had been proposed by A. Palmgren in 1924. It states that if a body that can stand certain amount of damage D experiences to damages D_i where $i = 1,2,3, \dots N$ from N loads, then it might be expected that the failure can occur if

$$\sum_{i=1}^{N} D_i = D \tag{6-1}$$

or

$$\sum_{i=1}^{N} \frac{D_i}{D} = 1 \tag{6-2}$$

This linear cumulative damage concept can be used in fatigue settings by considering the body is subjected to n_1 cycles at cyclic stress σ_1, n_2 cycles at cyclic stress $\sigma_2, \dots, n_n$ cycles at cyclic stress σ_n. the number of cycles to failure can be calculated from the $S - N$ curve for the body martialas shown in figure 6.1.

It can be clearly shown that the fractional fatigue damage at stress σ_i can be calculated as n_i/N_i and the fatigue failure occurs when the summtion of the fractional damages reaches the critical damage

$$\frac{n_1}{N_1} + \frac{n_2}{N_2} + \frac{n_3}{N_3} + \cdots = \sum_{i=1}^{N} \frac{n_i}{N_i} = 1 \tag{6-3}$$

Mathematically, the Miner´s rule is given by,

$$\sum_{i=1}^{N} \frac{n_i}{N_i} = 1 \tag{6-3}$$

In order to apply rainflow counting algorithm, the time series need to be first processed into peak-valley series to extrapolate the data from extrema, i.e., maxima and minima of a time series. Then this count is weighted and added using the Miner rule for damage accumulation.

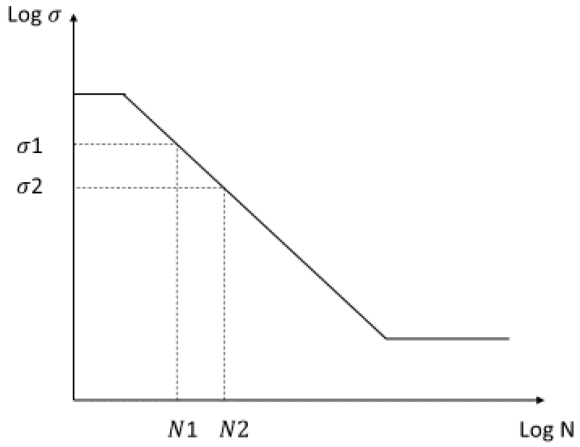

Figure 6.1: S-N material curve example

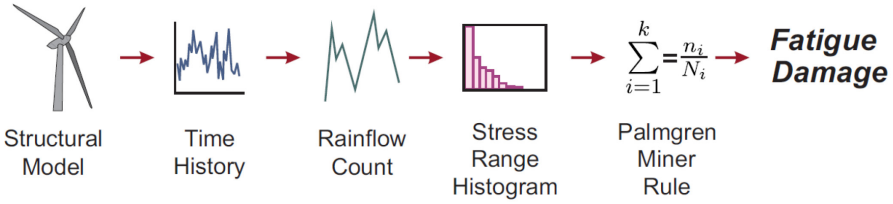

Figure 6.2: Rainflow counting damage estimation procedure [22]

The comparison shows a good behavior for the modern controller over the classical controller. The fatigue damage for the blade is reduced by a factor of 2.2 with appllying the feedforward controller alone and by a factor of 200 with the feedforward/feedback controller. The fatigue damage for the tower doesn't reduce so much with the feedforward controller but it reduced by a factor of 100 with the feedback/feedforward controller. Table 6.1 shows the comparison between the modern controller and the classical controller where the **where the standard deviation of the rotational speed is used as comparison criteria. The values in the table represent the division of the standard deviation before applying the controller to the standard deviation after applying the controller at 15 m/s and 25 m/s wind speeds.**

	Modern Control	**Classical control**
15 m/s	0,53	0,55
25 m/s	0,35	0,97

Table 6.1: A comparison between the modern controller and the classical controller where the standard deviation of the rotational speed is used as comparison criteria at 15 m/s and 25 m/s wind

7. Conclusion

In this thesis an observer based Disturbance Accomodation Controller was designed, implemented and tested with the linear and nonlinear models . The controller was benchmarked with a dreived set of critera for the well known NREL 5 MW wind turbine. The ability of an observer to estimate non-measurable states from a set of measurements using a model of the plant suggests the idea of extending the model of the plant by a model of the disturbance. The Discrete Kalman Filter has been used as an observer. The results show a good and fast estimation of the filter for the disturbance states. A feedforward/feedback controller has been used for counteracting the disturbance and stabilizing the wind turbine. The disturbance effect is reduced via a feedforward controller where the wind turbine is stabilized via a feedback controller. The LQR is used as a full state fedback controller. The results show that the better the estimation of the disturbance states, the better the disturbance rejection.

A comparative study has been done between this study; Modern load controller and a classical load controller. The modern controller shows a better performance than the classical controller.

8. References

[1] Sawyer, S., Teske, S., Dyrholm, M.: Global Wind Energy Outlook, Global Wind Energy Council ,2016

[2] N.N.: Technology Roadmap Wind Energy, 2013 Edition, International Energy Agency, 2013

[3] Johnsons, C.D.: Accommodating of external disturbances in linear regulator and servomecha-nism problems, IEEE Transaction on automatic control, Vol. AC-16, No. 6, 1972

[4] Balas, M., et. Al.: Disturbance Tracking Control Theory with Application of horizontal axis wind turbines, Proc. 17th ASME Wind Energy Symposium, Reno, Nv, 1998

[5] Wright, A.: Modern control design for flexible wind turbines, NREL/TP-500-35816, July 2004

[6] Hoffmann, A.: Regelungstechnische Beiträge zur Böenlastabminderung bei Flugzeugen, Dissertation, Technische Universität Berlin, 2016

[7] Bianchi, F., et. al.: Wind Turbine Control Systems, ISBN-10 978-1-84628-492-2, Springer Ver-lag, London, 2007

[8] Jonkman, J., Butterfield, S., Musial, W., and Scott, G. "Definition of a 5-MW Reference Wind Turbine for Offshore System Development," National Renewable Energy Laboratory: NREL/TP-500-38060, 2009

[9] Buhl, M.L., Jr., Jonkman, J.M., Wright, A.D., Wilson, R.E., Walker, S.N.; Heh, P.: FAST User's Guide. NREL/EL-500-29798. Golden, CO: NREL, 2005

[10] Burton,T., Sharpe,D., Jenkins,N., Bossanyi.E.: Wind Energy Handbook, ISBN 0-471-48997-2, John Wiley & Sons, Ltd , West Sussex, England, 2001

[11] Dryden, H.L.: A review of the statistical theory of turbulence. Turbulence-classical paper on statistical theory, New York: Interscience Publishers, Inc., 1961 (Nachdruck aus Quart. Appl. Math. I, S7-42, 1943).

[12] DEWI DeutschesWindenergie Institut: Offshore Potentialstudie für das Land Niedersachsen, Wilhelmshaven, 2000

[13] Halfpenny. A.: Dynamic Analysis of Both on and Oftshore Wind Turbines in the

Frequency Domain, Faculty of Engineering, University of London, 1998

[14] Bhattacharya, S., Arany, L., macdonald, J., Hogan, S.: Simplified critical mudline bending moment spectra of offshore wind turbine support structures, Wiley Online Library, 2014.

[15] Peter S. Maybeck.: Stochastic models, Estimation, and Control, ISBN 0-12-480701-1(v.1), Academic press, INC, New York, 1979

[16] Peter S. Maybeck.: The Kalman Filter: An Introduction to Concepts in Autonomous Robot Vehciles, I.J. Cox, G. T.Wilfong (eds), Springer-Verlag,1990

[17] Brown, R.,Hwang.,P.: Introduction to random signals and applied Kalman filtering: with MATLAB exercises —4th ed, ISBN 978-0-470-60969-9, John Wiley & Sons, Inc.

[18] Lunze, J.: Regelungstechnik 2, Mehrgrößensysteme, Digitale Regelung , 3. Auflage, Springer, ISBN 3-540-22177-8, Berlin

[19] Murry, R.: Lecture notes, CDS 110b, Control and Dynamical Systems, California Institute of Technology, 2006

[20] Voß,A.: Regelungstechnische Reduktion des Rotorblattwurzelbiegemoments und Erhöhung der Drehzahlfestigkeit einer 5 MW IPC-Windenergieanlage, DLR, Institut für Flugsystemtechnik, Braunschweig

[21] Barradas-Berglind, J.: Fatigue-Damage Estimation and Control for Wind Turbines, ISBN (online): 978-87-7112-398-2, Faculty of Engineering and Science, Aalborg University, Denmark, 2015

A Appendix

A.1 The Discrete Kalman Filter Performance

Figure A-1 shows the performance of the Discrete Kalman filter in the estimation of the wind turbine states and the disturbance states. The standard deviation for the error between the actual state and the estimated state is calculated through a MATLAB script and it's written upon each plot in the same figure.

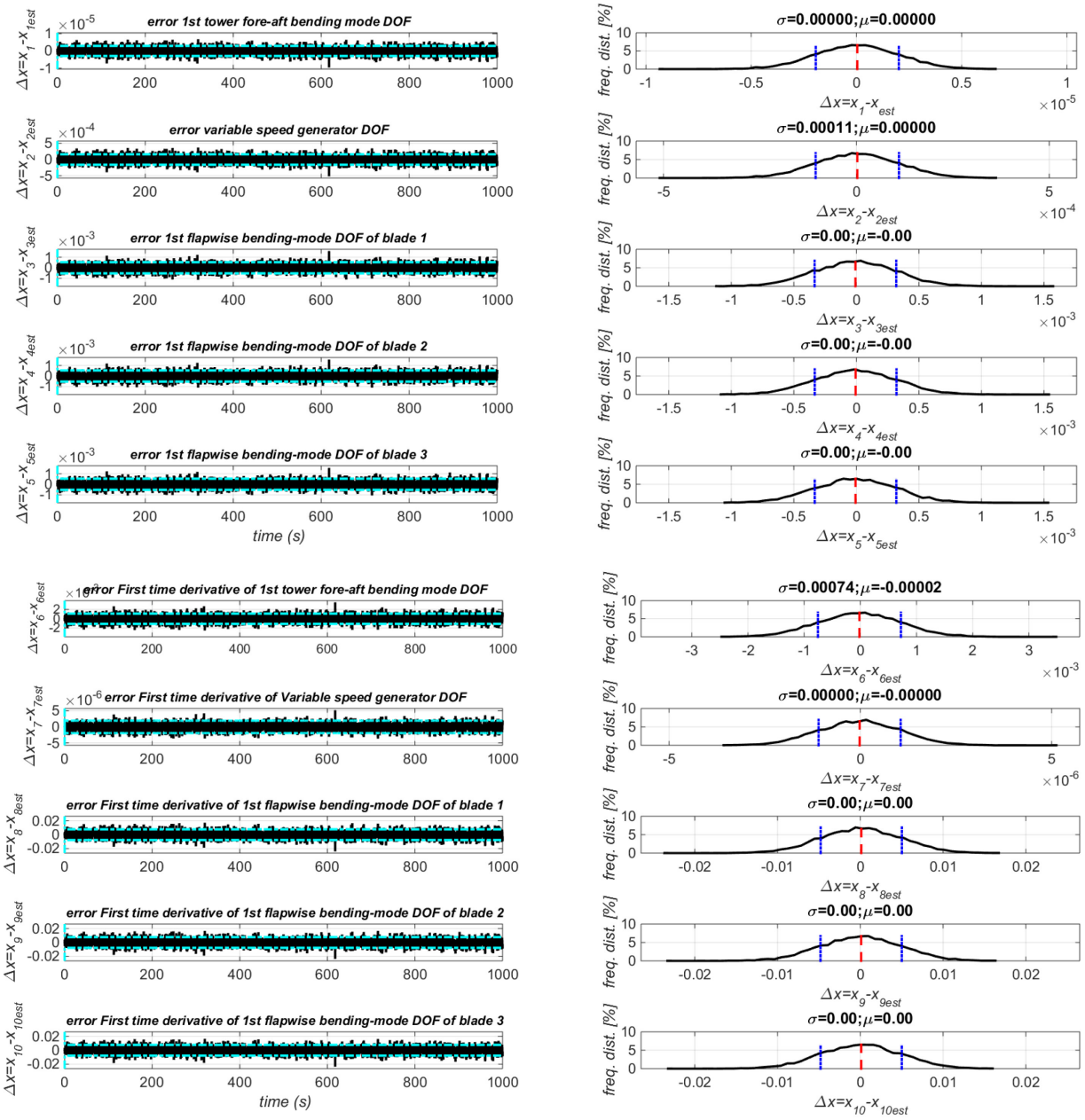

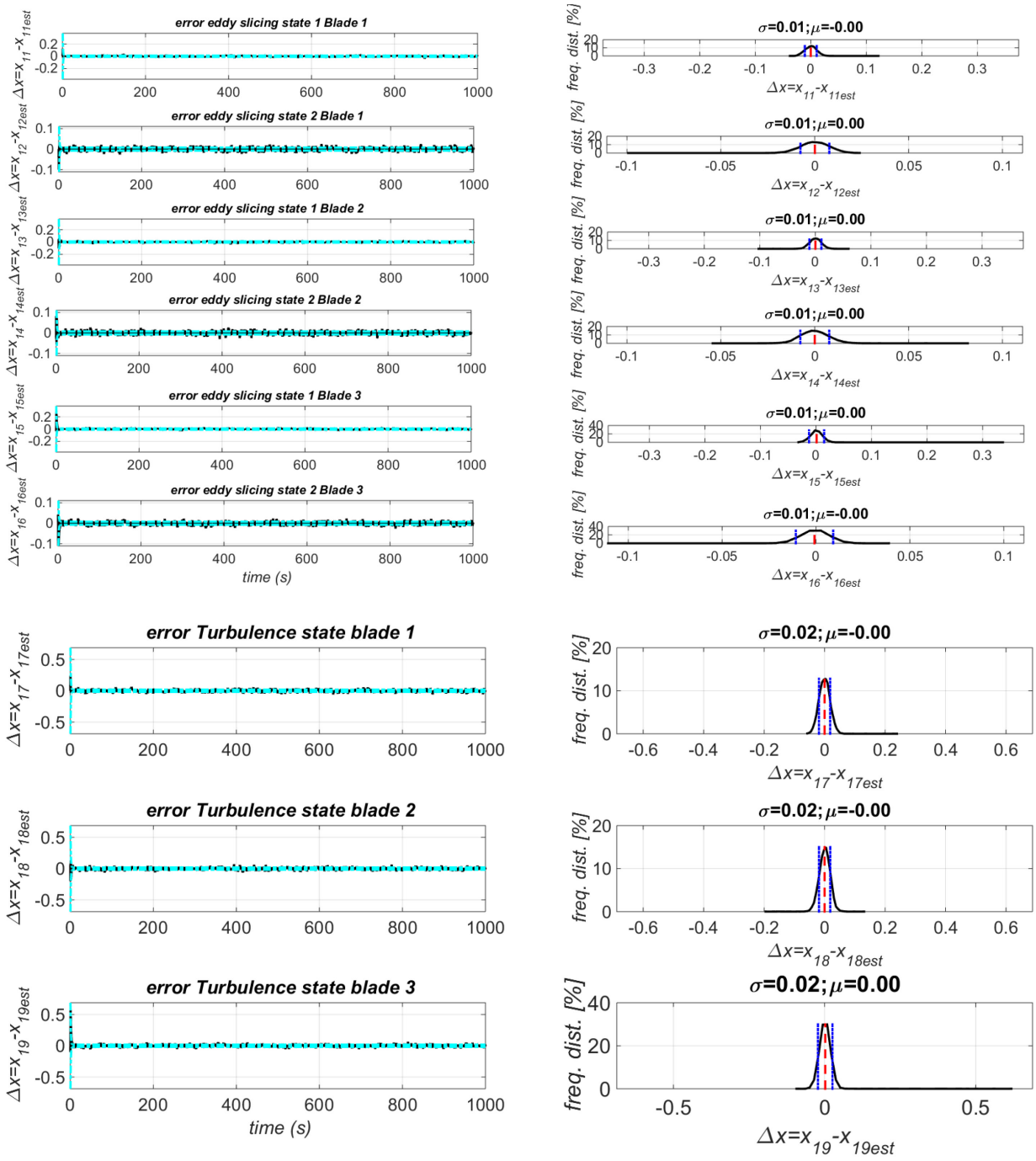

Figure A-1: Time series and frequency distribution of the error in the estimation for the wind turbine states and the disturbance states.

Figure A-2 shows the time series and frequency distribution of the error in the estimation for the following measured outputs:

1- Angular speed of the HSS and generator (GenSpeed)
2- Blade 1 edgewise moment (RootMxb1)
3- Blade 2 edgewise moment (RootMxb2)
4- Blade 3 edgewise moment (RootMxb3)
5- Blade 1 flapwise moment (RootMyb1)
6- Blade 2 flapwise moment (RootMyb2)
7- Blade 3 flapwise moment (RootMyb3)
8- Blade 1 pitching moment (RootMzb1)
9- Blade 2 pitching moment (RootMzb2)
10- Blade 3 pitching moment (RootMzb3)
11- Tower base roll (or side-to-side) moment (TwrBsMxt)
12- Tower base pitching (or fore-aft) moment (TwrBsMyt)
13- Tower base yaw (or torsional) moment (TwrBsMzt)

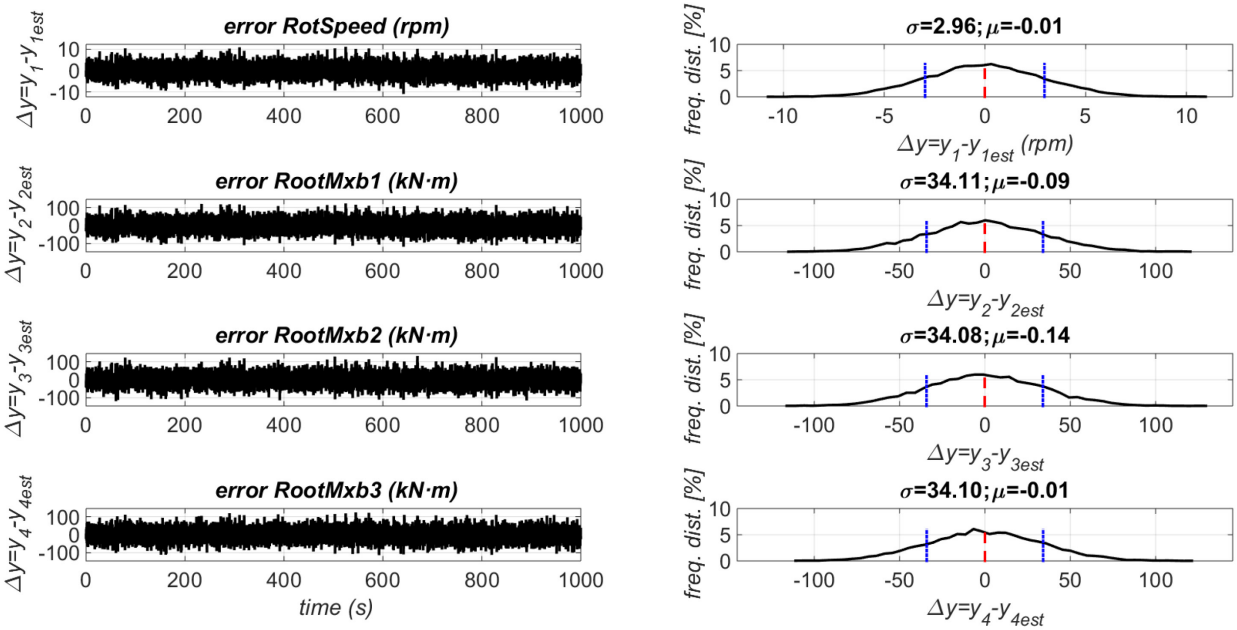

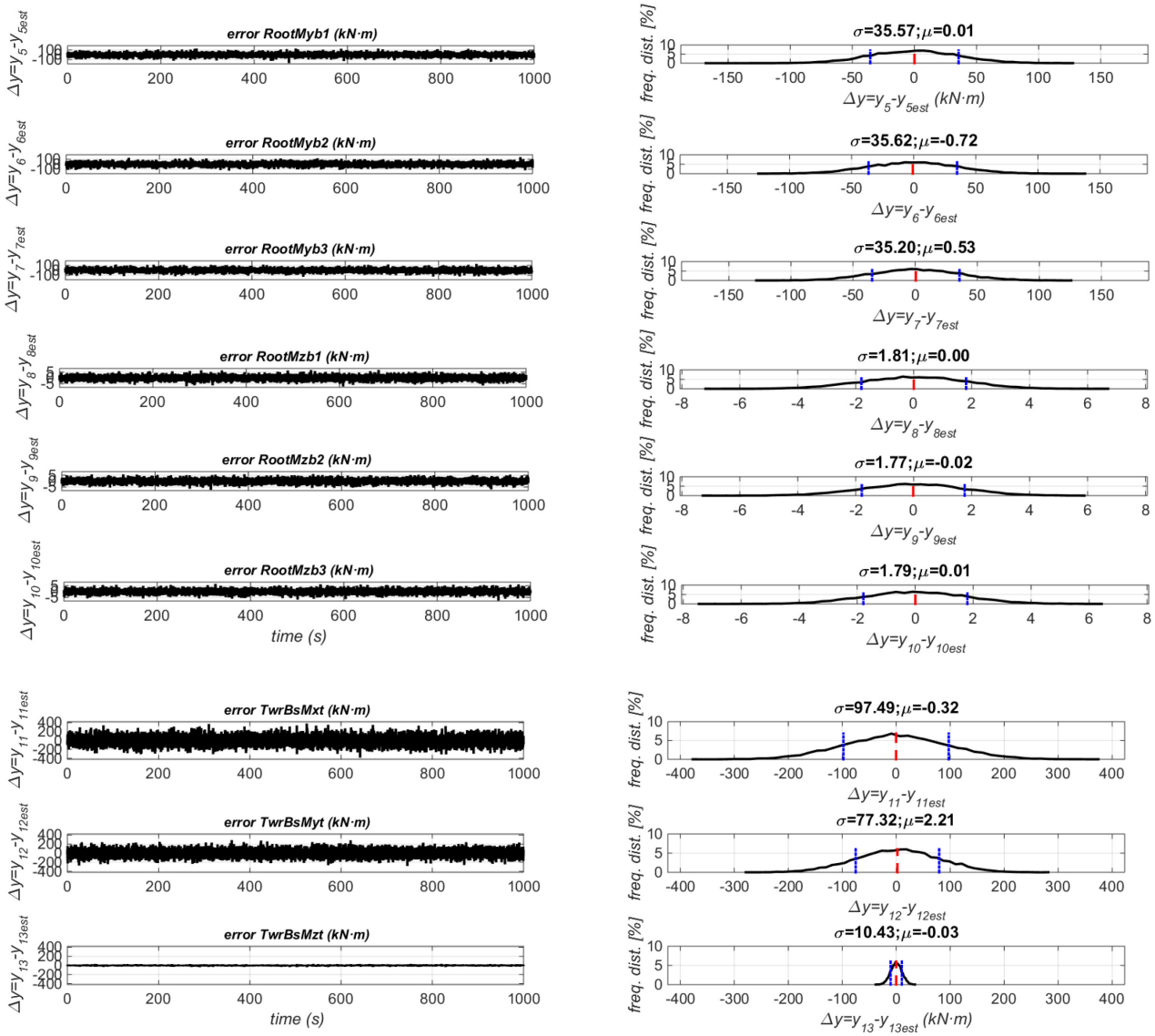

Figure A-2: Time series and frequency distribution of the error in the estimation for the measured outputs

A.2 The Controller Performance at 15 m/s wind speed conditions

Trim point: -

- 15 m/s steady horizontal wind speeds.
- 90 m as Reference height for horizontal wind speed.
- 10.45 degree as initial blade pitch angel for each blade.
- 12.1 rpm as initial rotor speed.

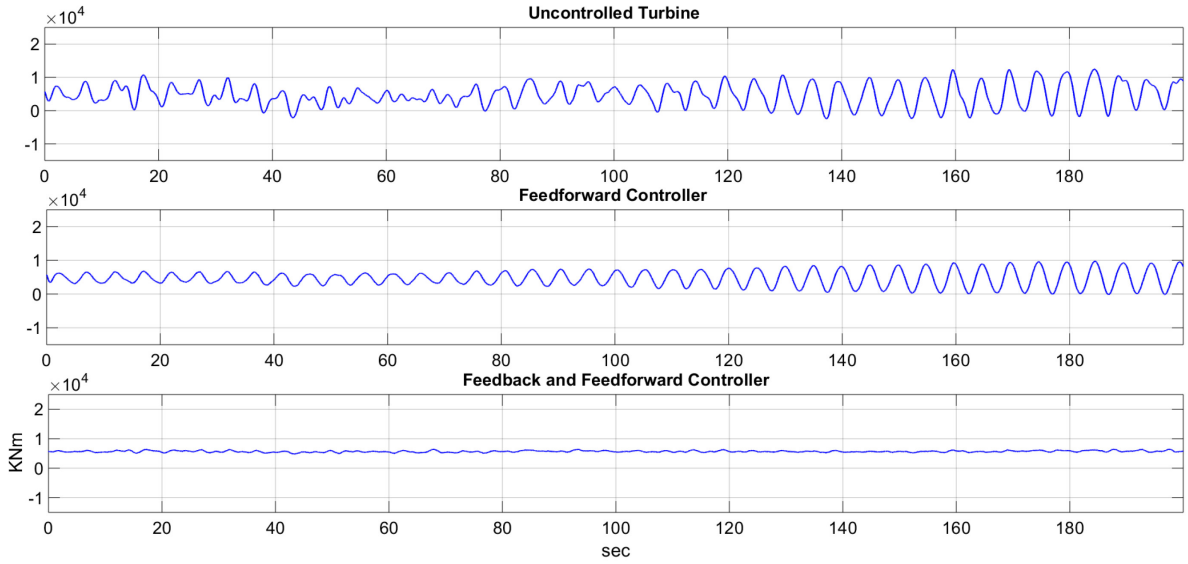

Figure A.3: Comparison of the uncontrolled turbine against the feedforward controlled turbine and the feedforward/feedback controlled turbine for the flap moment, 15 m/s wind speed

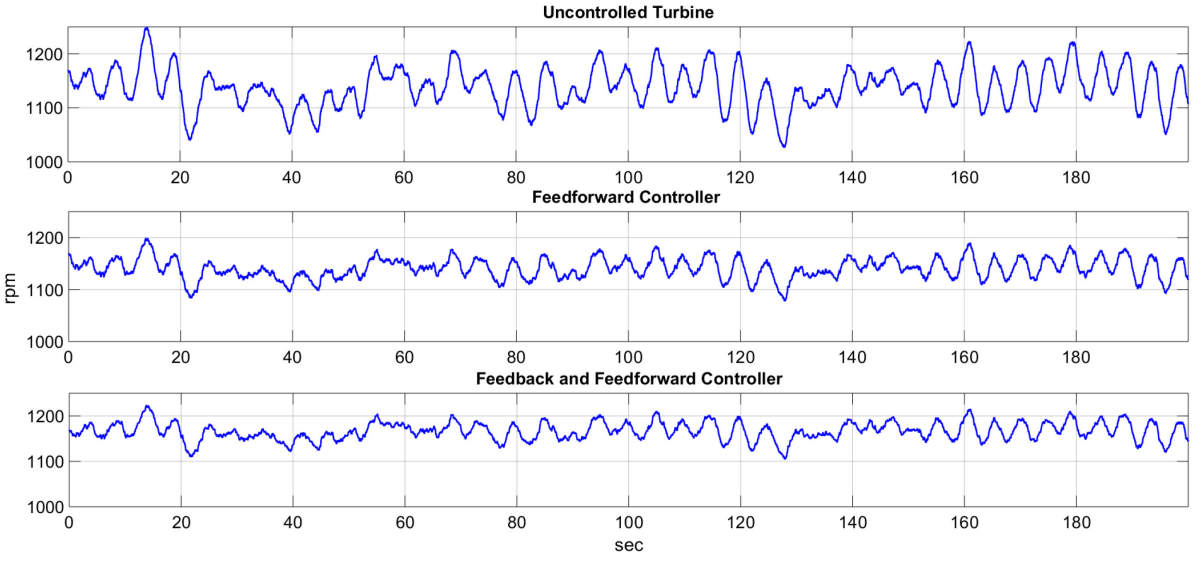

Figure A.4: Comparison of the uncontrolled turbine against the feedforward controlled turbine and the feedforward/feedback controlled turbine for the generator speed, 15 m/s wind speed

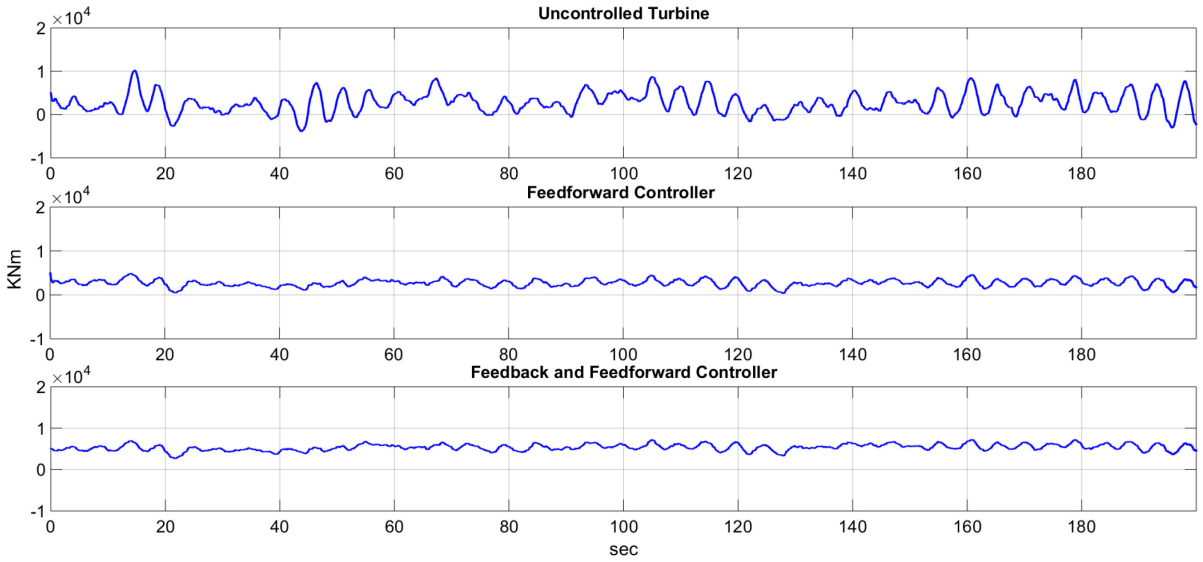

Figure A.5: Comparison of the uncontrolled turbine against the feedforward controlled turbine and the feedforward/feedback controlled turbine for the tower fore-aft moment, 15 m/s wind speed, 15 m/s wind speed

A.2 The Controller Performance at 25 m/s wind speed trim conditions

Trim point: -

- 25 m/s steady horizontal wind speeds.
- 90 m as Reference height for horizontal wind speed.
- 23.47 degree as initial blade pitch angel for each blade.
- 12.1 rpm as initial rotor speed.

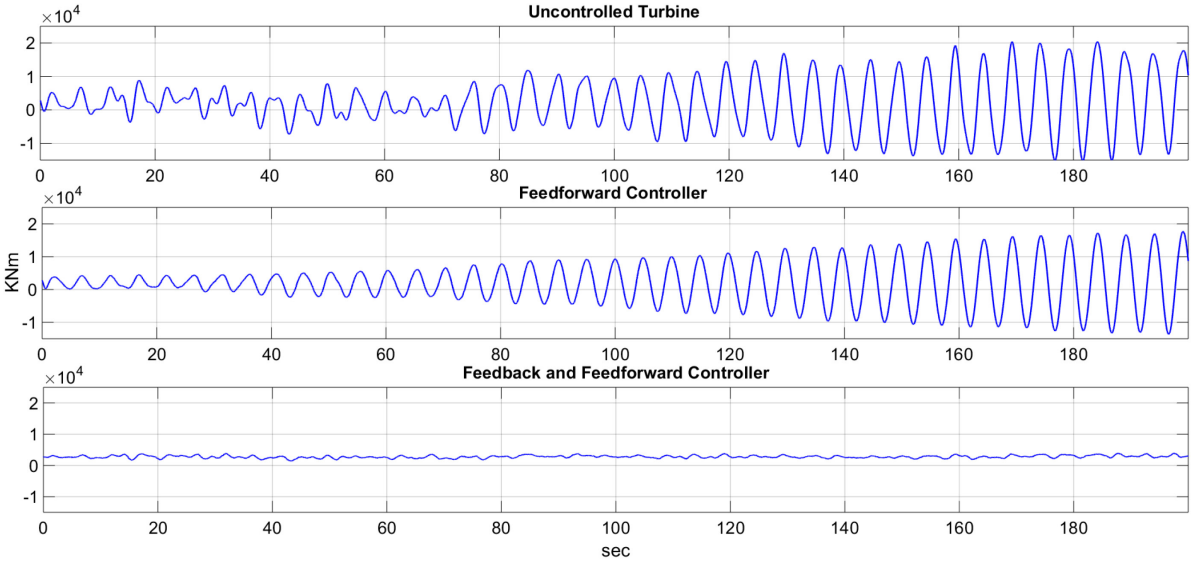

Figure A.6: Comparison of the uncontrolled turbine against the feedforward controlled turbine and the feedforward/feedback controlled turbine for the flap moment, 25 m/s wind speed

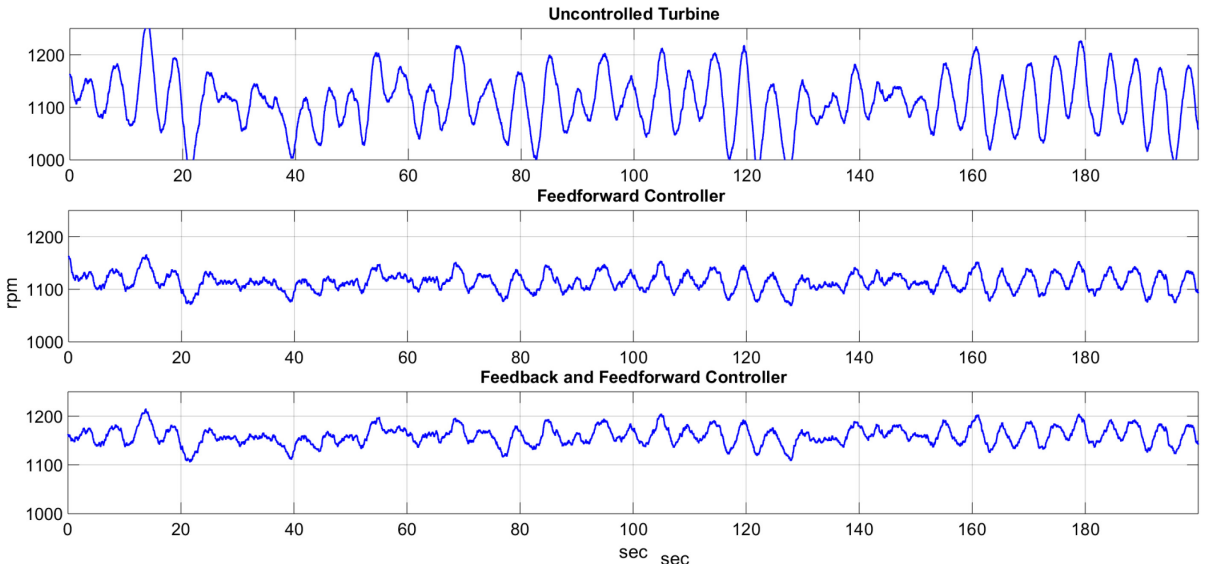

Figure A.7: Comparison of the uncontrolled turbine against the feedforward controlled turbine and the feedforward/feedback controlled turbine for the generator speed, 25 m/s wind speed

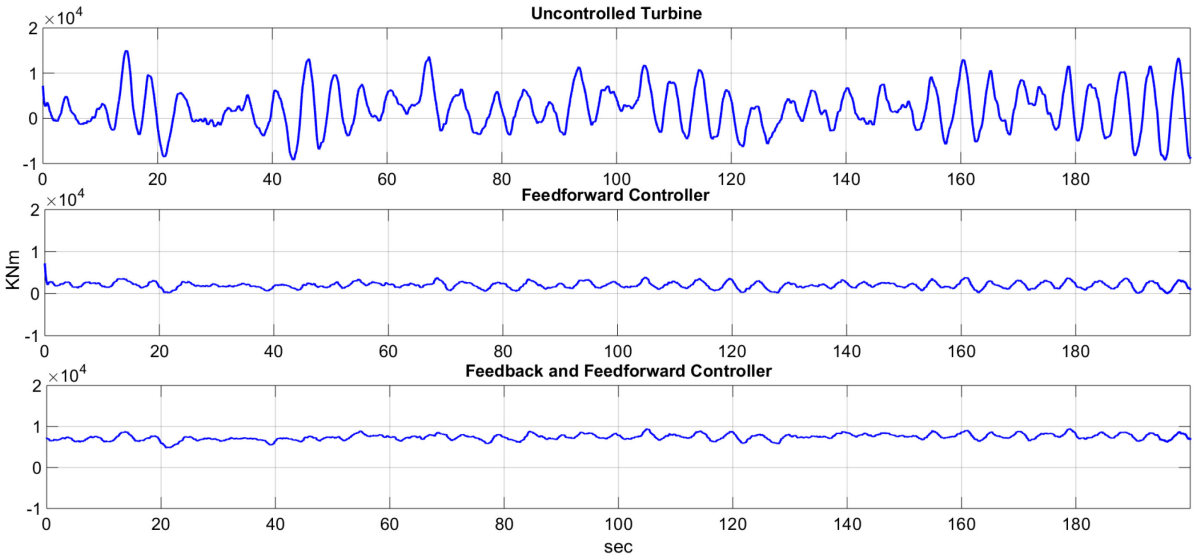

Figure A.8: Comparison of the uncontrolled turbine against the feedforward controlled turbine and the feedforward/feedback controlled turbine for the tower fore-aft moment, 25 m/s wind speed,

Figure A-7 shows a comparison between the uncontrolled turbine, feedforward controlled turbine and feedforward/feedback controlled turbine for the wind turbine states, the disturbance state and the measured outputs mentioned in the previous section.

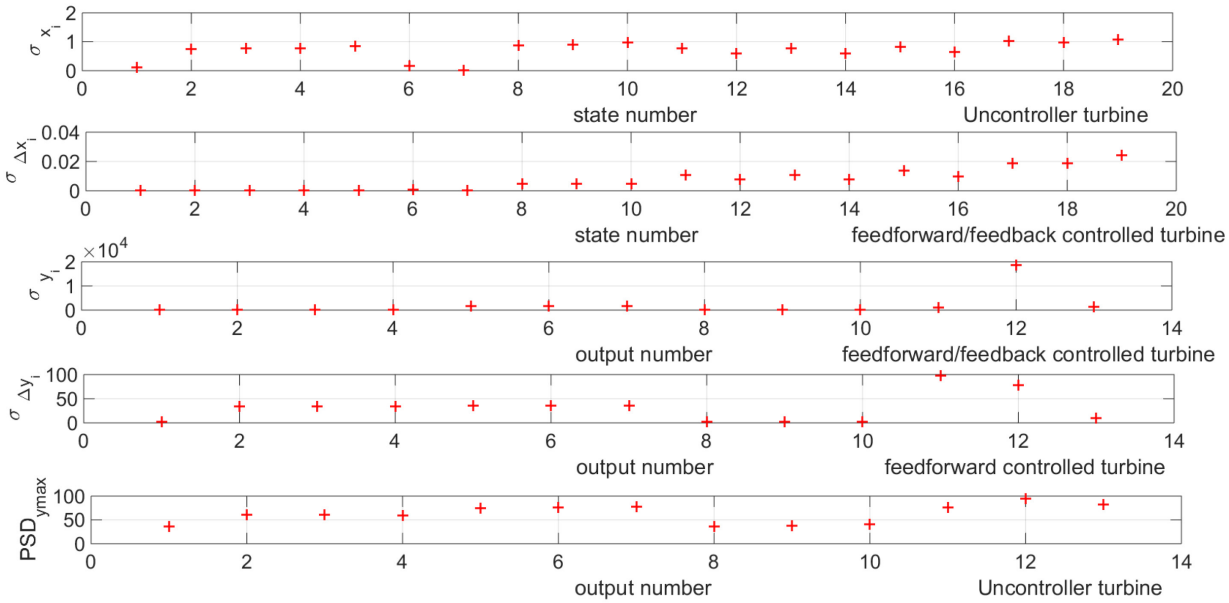

Figure A.9: A comparison between the uncontrolled turbine, feedforward controlled turbine and feedforward/feedback controlled turbine, 18 m/s wind speed

DLR Institutsbericht

DLR-IB-FT-BS-2017-248

Reduction of the rotor blade root bending moment and increase of the rotational-speed strength of a 5 MW IPC wind turbine based on a stochastic disturbance observer

Taha Fouda

Institut für Flugsystemtechnik

Braunschweig

56 Seiten
28 Abbildungen
5 Tabellen
21 Referenzen

Deutsches Zentrum für Luft- und Raumfahrt e.V.
in der Helmholtz Gemeinschaft
Institut für Flugsystemtechnik
Lilienthalplatz 7, 38108 Braunschweig

Stufe der Zugänglichkeit: II, intern unbeschränkt und extern beschränkt zugänglich
Availability/Distribution: Internally unlimited and externally limited distribution

Braunschweig, 16. März 2018

Unterschriften:

Institutsdirektor:	Prof. Dr.-Ing. Stefan Levedag
Abteilungsleiter:	Dr.-Ing. Christoph Keßler
Betreuer:	Dr.-Ing. Arndt Hoffmann
Verfasser:	BSc. Taha Fouda

Verfasser:

Taha Fouda

Titel:

Reduction of the rotor blade root bending moment and increase of the rotational-speed strength of a 5 MW IPC wind turbine based on a stochastic disturbance observer

Deutsches Zentrums für Luft- und Raumfahrt e.V. (DLR)

Institut für Flugsystemtechnik, Abteilung Hubschrauber

Institutsbericht

Acknowledgement

After I have finished this thesis, I would like to thank my supervisor Dr.-Ing. Arndt Hoffmann for his great help and advices. He had the idea behind this work. Recently, he investigated it and applied it for the aircraft wing. He guided me through all the steps from the beginning till the end.

I would also like to thank my family for their sincere encouragement throughout my studies.

Finally, I would like to thank all the colleagues working at DLR institute of flight systems specially M.Sc. Felix Weiß for his support in different technical issues.

Contents

List of Abbreviations

AeroDyn	Aerodynamics
ADAMS	Automatic Dynamic Analysis of Mechanical Systems
DAC	Disturbance Accommodation Control
DLL	Dynamic - Link – Library
DLR	Deutsches Zentrum für Luft- und Raumfahrt
DOF	Degree of Freedom
DOWEC	Dutch Offshore Wind Energy Converter project
Dry	Dryden spectrum
DUWECS	Delft University Wind Energy Converter Simulation Program
E	Expected value
CAE	Computer-Aided Engineering
ElastoDyn	Elasto Dynamics
FAST	Fatigue, Aerodynamics, Structures, and Turbulence
HAWT	Horizontal Axis Wind Turbine
IPC	Individual Pitch Control
LQG	linear Quadratic Gaussian
LQR	Linear Quadratic Regulator
MIMO	Multi Input Multi Output
NREL	National Renewable Energy Laboratory
OP	Operating point
PSD	Power Spectrum Density
RECOFF	Recommendations for Design of Offshore Wind Turbines project
ServoDyn	Servo Dynamics
VAR	Variance
WindPACT	Wind Partnerships for Advanced Component Technology project
WT	Wind Turbine

List of Symbols

$\underline{\underline{A}}$	State matrix	[...]
$\underline{\underline{B}}$	input matrix	[...]
$\underline{\underline{C}}$	output matrix	[...]
$\underline{\underline{D}}$	input-transmission matrix	[...]
D_i	Damage	[1]
$\underline{\underline{\underline{DspC}}}$	displacement output matrix	[...]
d	damping factor of the inverted notch	[1]
$\underline{\underline{E}}$	wind input disturbance matrix	[...]
$\underline{e_k}$	Posteriori estimate error	[...]
e_k^-	Priori estimate error	[...]
$\underline{\underline{F}}$	wind input disturbance transmission	[...]
f	nonlinear forcing function	-
$f_X(x)$	the probability density function	-
$\underline{\underline{G}}$	stiffness matrix	[...]
I	Turbulence intensity	[1]
J	cost function	[1]
$\underline{\underline{\underline{K_k}}}$	Kalman gain	[...]
$\underline{\underline{K}}^*$	observer gain	[...]
$\underline{\underline{K}}_{LQR}$	Feedback gain	[...]
$\underline{\underline{L}}$	control input matrix	[...]
L_u	length scale	[m]
$\underline{\underline{M}}$	mass matrix	[...]
m	number of the system	[1]
N	feedforward gain	[...]
N_i	Number of load cycles	[...]
n	number of the system states	[1]
$\underline{\underline{P}}_K$	error covariance matrix	[...]
P_i	Probability of x_i	-
p	number of the system outputs	[1]
$\underline{\underline{Q}}_{LQR}$	State weighting matrix for LQR	[...]
$\underline{\underline{Q}}_{var}$	Process noise covariance matrix	[...]

$\underline{q}$	Displacement DOF	[...]
$\underline{\dot{q}}$	Velocity DOF	[...]
$\underline{\ddot{q}}$	Acceleration DOF	[...]
$\underline{\underline{R}}_{LQR}$	Control effort weighting matrix for LQR	[...]
$\underline{\underline{R}}_{var}$	Measurement error covariance matrix	[...]
$\underline{\underline{R}}^*$	closed loop gain	[...]
s	Laplace variable	[1/s]
t	Time	[s]
T	time constant	[s]
$\underline{u}$	the vector of control inputs	[...]
V	wind speed	[m/s]
V_m	steady mean wind speed	[m/s]
$\underline{\underline{VelC}}$	velocity output matrix	[...]
v	atmospheric turbulence	[...]
$\underline{v_k}$	measurement noise	[...]
$\underline{w_k}$	system uncertainties	[...]
$\underline{x}$	the vector of system states	[...]
$\underline{x_d}$	the vector of disturbance states	[...]
$\underline{\hat{x}}$	Posteriori estimated state	[...]
$\underline{\hat{x}_k^-}$	Prior state estimate	[...]
$\underline{y}$	the vector of system outputs	[...]
$\underline{\hat{y}}$	Estimated output	[...]
$\underline{z}$	the vector of wind input "disturbances"	[...]
Ω	Rotational speed	rpm
θ	Pitch angel	°
σ	standard deviation	[...]
μ	Expected value or Mean	[...]
σ^2	Variance	[...]
σ_i	Stress	N/m

List of Figures

List of Table

Abstract

The control- and operation-system of a wind turbine must primarily ensure the fully automatic operation of wind turbines in a constantly changing environment (gusts, turbulence). In addition, economic efficiency charges the control-system to ensure that the highest possible efficiency is achieved, and the mechanical loads caused by disturbances are minimized. The reduction of loads in wind turbines becomes more important.

According to the "internal model principle", the control quality or the potential for disturbance rejection is increased; the more information there is available on the character of the disturbance (turbulence). This principle is directly taken up by the observer-based Disturbance Accommodation Control (DAC).

The ability of an observer to estimate non-measurable states from a set of measurements using a model of the plant suggests the idea of extending the model of the plant by a model of the disturbance. The states of the disturbance can thus also be reconstructed, and an easy-to-determine feedforward control can be implemented to counteract the disturbance. In this thesis DAC has to adjusted to suppress stochastic disturbances in wind turbines (NREL 5 MW).

1 Introduction

Wind energy is one of the most growing renewable energy technologies in the world. The total worldwide installed capacity increased from 8 MW at 1980 till 18039 MW at 2000. In 2016 the installed capacity reached 500 GW. At the same year, the total worldwide electricity generated by wind energy was 900 TWh which means more than 4% of the global electricity demand. It is expected that the worldwide installed capacity will reach 800 GW by the end of 2020 [1]. To cover the demand, the size and the rotor diameter increased over the last decades as you can see in figure 1.1. On the other hand, the increment in the size and the rotor diameter develops new challenges that need to be faced. One of those challenges is the increase in the blade mass and therefore the weight. Another one is the reduction in the natural frequencies.

These loads can be reduced by implementing a control system that must primarily ensure the fully automatic operation of wind turbines in a constantly changing environment (gusts, turbulence). In addition, economic efficiency charges the control-system to ensure that the highest possible efficiency is achieved.

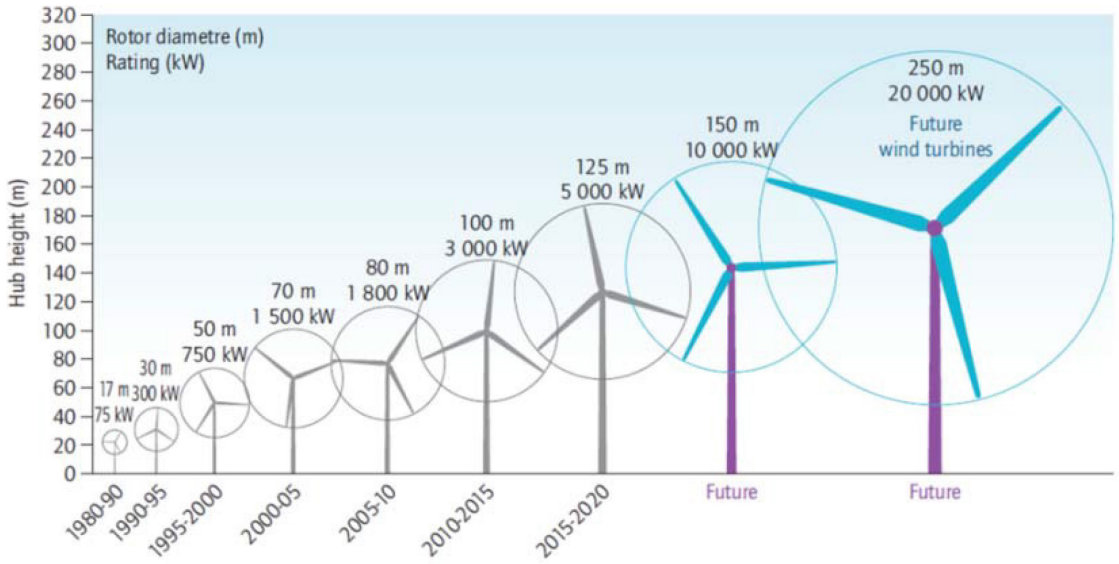

Figure 1.1: Trend towards increasingly larger wind turbines [2]

According to the "internal model principle", the control quality or the potential for disturbance rejection is increased; the more information about the disturbance is known. This principle is directly taken up by the observer-based Disturbance Accommodation Control. Disturbance Accommodation Control (DAC) is a new branch of modern control

theory that address the problems of dynamic modelling of uncertain disturbances which act on systems and designing feedback/feedforward controllers which achieve and maintain system performance specifications in the face of the disturbances [3]. It was developed by Johnson (1976) [3]. The theory was extended to wind turbine control by Balas (1998) [4]. He was the first who used it for the rejection of deterministic disturbances on the wind turbine [4]. He further elaborated and investigated the method in [5].

The turbulence is a stochastic disturbance that cannot be easily measured, However the disturbance states can be estimated. The ability of an observer to estimate non-measurable states from a set of measurements using a model of the plant suggests the idea of extending the model of the plant by a model of the disturbance. The states of the disturbance can thus also be reconstructed, and an easy-to-determine a feedforward controller that can be implemented to close the control loop, cf. [3]. This method was adapted for stochastic disturbances on a motor glider [6] and will be adjusted to suppress stochastic disturbances in wind turbines (NREL 5 MW reference turbine) in this thesis.

The thesis is organized as follows: Chapter two discusses the modelling of wind turbine for controller design, the definition of NREL 5 MW baseline turbine and the development of a linear representation of the nonlinear wind turbine using the aeroelastic FAST tool. Chapter three illustrates the modelling of wind disturbance based on the Dryden wind turbulence model. Chapter four explains the state estimation based on the Discrete Kalman Filter and the design of the controller based on the disturbance accommodation control theory. In chapter five, the controller structure is implemented in a linear and nonlinear simulation environment. Chapter six shows a comparative study with a given classical load controller. Finally, Chapter seven contains a summary of this thesis.

2 Modelling of wind turbines for controller design

A mathematical model of wind turbine gives the ability to understand the behavior of the wind turbine over its region of operation. A horizontal axis onshore wind turbine model can consist of a rotor model, a drive train model, a electrical generator model and a tower model.

Nowadays, all described models can be implemented in various analytical tools such as FAST, SymDyn and DUWECS. All these tools can Linearize and simulate. The aero-elastic simulation tool FAST has been used in this study for modelling of NREL 5 MW Baseline turbine. The baseline turbine is modelled nonlinear in FAST but can be linearized for analysis or controller design purposes. The definition of NREL 5 MW Baseline turbine will be discussed in the following section.

2.1 NREL 5 MW baseline wind turbine

This study is based on NREL 5 MW baseline onshore Individual Pitch Control (IPC) wind turbine as a reference turbine. NREL 5 MW baseline wind turbine has been developed by New and Renewable Energy Laboratory (NREL) to act as a reference model used for wind energy related studies and by wind turbine researches, however it has not been built. It has been designed based on the largest wind turbine prototypes in the world at that time; Multibrid M5000 and the REpower 5MW -each had a 5-MW rating. Because of unavailable detailed information about these machines at that time, available properties from other models used in WindPACT, RECOFF, and DOWEC projects have been gathered with Multibird M5000 and REpower 5 MW properties to extract the best available and most representative specifications [8].

NREL 5MW baseline turbine is a three-bladed upwind turbine with a variable-speed, active-pitch control system. Table 2.1 shows the baseline properties.

Rated Power	5 MW
Rotor Orientation, Configuration	Upwind, 3 Blades
Control	Variable Speed, Individual Pitch
Drivetrain	High Speed, Multiple-Stage Gearbox
Rotor, Hub Diameter	126 m, 3 m

Hub Height	90 m
Cut-In, Rated, Cut-Out Wind Speed	3 m/s, 11.4 m/s, 25 m/s
Cut-In, Rated Rotor Speed	6.9 rpm, 12.1 rpm
Rated Tip Speed	80 m/s
Rotor Mass	110,000 kg
Nacelle Mass	240,000 kg
Tower Mass	347,460 kg

Table 2.1: NREL 5MW baseline wind Turbine properties [8]

The relationships of the generator speed, rotor power, generator power, rotor thrust, and rotor torque are represented as a function of wind speed in figure 2.1.

Figure 2.1 is divided into four different regions. Region 1½ is the startup region where the wind speed is a little bit higher than the cut in speed. In this region, the generator speed is set to the lower limits which is defined to be in between 670 rpm and 30% above this value (or 871 rpm). Region 2 is a maximum power tracking control region where the generator torque is proportional to the square of the generator speed to maintain a constant (optimal) tip speed ratio. Region 2½ is a linear transition between region 2 and region 3 with a torque slope corresponding to the slope of an induction machine. The generator-slip percentage in this region is taken to be 10%, according to the value used in the DOWEC study. In region 3, the wind speed is above the rated speed. The generator speed is kept constant in this region so that the generator torque is inversely proportional to the generator speed [8].

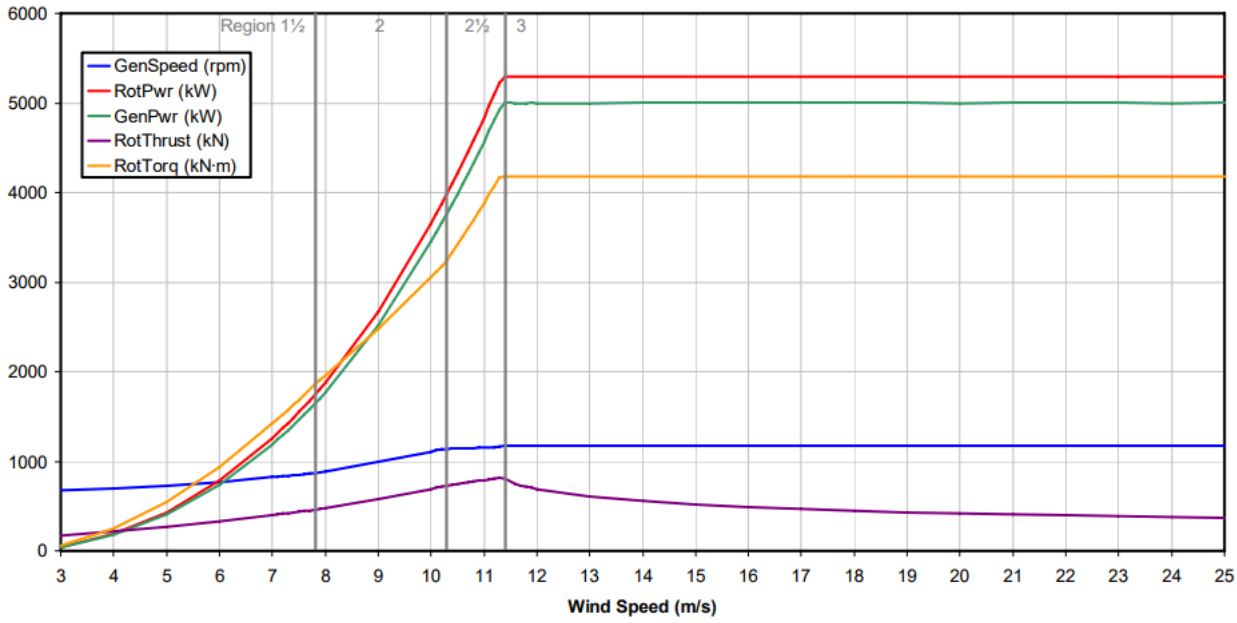

Figure 2.1: wind speed relationships of 5 MW baseline turbine [8]

2.2 FAST

FAST (Fatigue, Aerodynamics, Structures, and Turbulence) is an aeroelastic Computer-Aided Engineering (CAE) tool for onshore and offshore horizontal axes wind turbines developed by New and Renewable Energy Laboratory (NREL) to simulate the nonlinear coupled dynamic response of wind turbines in the time domain. Wind turbines with two or three blades, up wind or downwind rotor, pitch or stall regulation, rigid or teetering hub, and lattice or tabular tower can be analyzed using FAST [9].

The FAST Code is the result of combination of three distinct codes; the FAST2 Code for two-bladed HAWTs; the FAST3 Code for three-bladed HAWTs; and the AeroDyn subroutines for HAWTs with additional modification. The FAST Code have been modified since 2003 till now and additional features have been added. The ability of FAST to develop a linearized state space model used for control design was added in 2003. An interface between FAST and MATLAB Simulink has also been developed in 2004 which allows the user to implement a advanced turbine controls in Simulink environment. In 2005, FAST got Germanischer Lloyd certificate [9].

Three-bladed horizontal axes wind turbine with 24 degree of freedoms (DOFs) and two-bladed HAWT with 22 DOFs can be modelled using FAST. The three-bladed HAWT DOFs counts for 6 DOF for the platform translational (surge, sway, and heave) and rotational

(roll, pitch, and yaw) motions, 4 DOF for the tower flexibility; two are longitudinal modes, and two are lateral modes, 1 DOF for the Yaw motion of the nacelle, 2 DOF for the variations in generator speed and the drivetrain flexibility, 9 DOF for the blade flexibility; 3 for the first flapwise bending mode of each blade, 3 for the second flapwise bending modes of each blade and 3 for the edgewise motion of each blade. 1 DOF for the rotor-furl, and 1 DOF for the tail-furl. The two- bladed HAWT has the same DOFs as for the three-bladed but with the addition of 1 DOF for the blade teetering and only 6 DOF for the blade flexibility; 2 for the first flapwise bending mode of each blade, 2 for the second flapwise bending modes of each blade and 2 for the edgewise motion of each blade [9]. Here in this thesis, 10 DOFs are chosen to be modelled as shown in table 2.2.

There are two different modes of operation supported by FAST, Simulation mode and Linearization mode. The simulation mode is used for the load analyses where the linearization mode is used to develop a linear model from the aeroelastic nonlinear wind turbine model.

2.3 Linearization process using FAST

The nonlinear description of the wind turbine can be linearized by FAST through two main steps, determination of an operating point and derivation about the selected operating point.

2.3.1 Determination of an Operating point (OP)

A trim point or an operating point is the point at which the system is in steady state where the system's state derivatives equal zero. Selecting this point is one of the most important steps in the linearization process as the linear representation of the nonlinear system is only valid for small perturbations from an operating point. It can be steady state operating point for operating turbine as in our case or static-equilibrium operating point for idling turbine. It is defined by selecting the system DOFs that need to be modelled and setting the initial conditions for control inputs and wind inputs.

Trim conditions are defined as:

- 18 m/s steady horizontal wind speed.
- 5 MW rated power.
- Region III

- 12,1 rpm as initial rotor speed.

The result pitch angel is $\theta_{trim} = 14.92°$

The selected DOFs of the linear model are listed in table 2.2.

System DOFs: -

x_1	1st tower fore-aft bending mode
x_2	Variable speed generator
x_3	1st flapwise bending-mode of blade 1
x_4	1st flapwise bending-mode of blade 2
x_5	1st flapwise bending-mode of blade 3
x_6	First time derivative of 1st tower fore-aft bending mode
x_7	First time derivative of Variable speed generator
x_8	First time derivative of 1st flapwise bending-mode of blade 1
x_9	First time derivative of 1st flapwise bending-mode of blade 2
x_{10}	First time derivative of 1st flapwise bending-mode of blade 3

Table 2.2: Linearized model DOFs

System inputs: -

u_1	Blade 1 pitch command
u_2	Blade 2pitch command
u_3	Blade 3 pitch command

Table 2.3: Control inputs

3.3.2 linearization

Suppose that the system nonlinear differential equation can be written in the following form

$$\dot{\underline{x}} = \frac{d\underline{x}}{dt} = f(\underline{x}, \underline{u}) \quad , \qquad \underline{y} = g(\underline{x}, \underline{u}) \tag{2-1}$$

where $\underline{x}$ is the vector of the system states, $\underline{u}$ is the vector of the control inputs, and $\underline{y}$ is the vector of the system outputs.

By applying the Taylor expansion on the nonlinear equation (2-1) and neglecting the higher order terms, we get

$$\underline{\dot{x}} = f(\underline{x},\underline{u}) \approx f(\underline{x}|_{op},\underline{u}|_{op}) + \frac{\partial \underline{f}}{\partial \underline{x}}|_{op}\,\delta\underline{x} + \frac{\partial \underline{y}}{\partial \underline{u}}|_{op}\,\delta\underline{u} \tag{2-2}$$

$$\underline{y} = g(\underline{x},\underline{u}) \approx g(\underline{x}|_{op},\underline{u}|_{op}) + \frac{\partial \underline{g}}{\partial \underline{x}}|_{op}\,\delta\underline{x} + \frac{\partial g}{\partial u}|_{op}\,\delta\underline{u} \tag{2-3}$$

At steady state conditions

$$\underline{f}(\underline{x}|op,\underline{u}|op) = 0, \qquad \underline{g}(\underline{x}|op,\underline{u}|op) = 0$$

The description of the trim point is as following

$$\delta\underline{\dot{x}} \approx \frac{\partial \underline{f}}{\partial \underline{x}}|_{op}\,\delta\underline{x} + \frac{\partial \underline{y}}{\partial \underline{u}}|_{op}\,\delta\underline{u} \tag{2-4}$$

$$\delta\underline{y} \approx \frac{\partial \underline{g}}{\partial \underline{x}}\,\delta\underline{x} + \frac{\partial g}{\partial \underline{u}}\,|_{op}\delta\underline{u} \tag{2-5}$$

These two equations can be written in other two forms as

$$\delta\underline{\dot{x}} = \underline{\underline{A}}\delta\underline{x} + \underline{\underline{B}}\,\delta\underline{u} \tag{2-6}$$

$$\delta\underline{y} = \underline{\underline{C}}\,\delta\underline{x} + \underline{\underline{D}}\,\delta\underline{u} \tag{2-7}$$

The matrices $\underline{\underline{A}}$, $\underline{\underline{B}}$, $\underline{\underline{C}}$, $\underline{\underline{D}}$ in the last two equations are defined as

$$\underline{\underline{A}} = \frac{\partial \underline{f}}{\partial \underline{x}}|_{op}, \quad \underline{\underline{B}} = \frac{\partial \underline{y}}{\partial \underline{u}}|_{op}, \; \underline{\underline{C}} = \frac{\partial \underline{g}}{\partial \underline{x}}|_{op}, \; \underline{\underline{D}} = \frac{\partial \underline{g}}{\partial \underline{u}}|_{op}\,.$$

where $\underline{\underline{A}}$ is the state matrix, $\underline{\underline{B}}$ is the input matrix, $\underline{\underline{C}}$ is the output matrix and $\underline{\underline{D}}$is the input-transmission matrix.

FAST applies the same principle for the following nonlinear equation of motion to get the linear representation from the nonlinear wind turbine model.

$$\underline{\underline{M}}(\underline{q},\underline{u},t)\underline{\ddot{q}} + f\left(\underline{q},\underline{\dot{q}},\underline{u},\underline{z},t\right) = 0 \tag{2-8}$$

where $\underline{\underline{M}}$ is the mass matrix. $\underline{f}$ is the vector of the nonlinear forcing function, $\underline{q}$, $\underline{\dot{q}}$, $\underline{\ddot{q}}$ are the vectors of the displacements, velocities and accelerations DOFs. $\underline{\mathrm{u}}$ is the vector of control inputs, $\underline{z}$ is the vector of the wind disturbances input and t is the time [9].

The operating points are defined as

$$\underline{q} = \underline{q}|_{op} + \delta\underline{q}\,, \quad \dot{\underline{q}} = \dot{\underline{q}}|_{op} + \delta\dot{\underline{q}}, \quad \ddot{\underline{q}} = \ddot{\underline{q}}|_{op} + \delta\ddot{\underline{q}}, \quad \underline{u} = \underline{u}|_{op} + \delta\underline{u},$$
$$\underline{z} = \underline{z}|_{op} + \delta\underline{z}$$

by substituting these expressions into the equation of motion and applying Taylor expansion as it's mentioned before, we get the following linear equation

$$\dot{\underline{x}} = \underline{\underline{A}}\,\underline{x} + \underline{\underline{B}}\,\underline{u} + \underline{\underline{E}}\,\underline{z} \tag{2-9}$$
$$\underline{y} = \underline{\underline{C}}\,\underline{x} + \underline{\underline{D}}\,\underline{u} + \underline{\underline{F}}\,\underline{z} \tag{2-10}$$

The matrices $\underline{\underline{A}}$, $\underline{\underline{B}}$, $\underline{\underline{C}}$, $\underline{\underline{D}}$ into equations (2-9) and (2-10) are defined as

$$\underline{\underline{A}} = \begin{bmatrix} 0 & I \\ -\underline{\underline{M}}^{-1}\underline{\underline{G}} & -\underline{\underline{M}}^{-1}\underline{\underline{C}} \end{bmatrix}, \quad \underline{\underline{B}} = \begin{bmatrix} 0 \\ \underline{\underline{M}}^{-1}\underline{L} \end{bmatrix}, \quad \underline{\underline{E}} = \begin{bmatrix} 0 \\ \underline{\underline{M}}^{-1}\underline{\underline{F_d}} \end{bmatrix}, \quad \underline{\underline{C}} = \begin{bmatrix} \underline{\underline{DspC}} & \underline{\underline{VelC}} \end{bmatrix},$$
$$\underline{L} = \left[\frac{\partial \underline{\underline{M}}}{\partial \underline{u}}\ddot{\underline{q}} + \frac{\partial \underline{f}}{\partial \underline{u}}\right]|_{op}\,.$$

where

$\underline{\underline{M}}$: mass matrix; $\underline{\underline{M}} = M|_{op}$,

$\underline{\underline{C}}$: damping / gyroscopic matrix; $\underline{\underline{C}} = \frac{\partial f}{\partial \dot{q}}|_{op}$,

$\underline{\underline{G}}$: stiffness matrix; $\underline{\underline{G}} = \left[\frac{\partial \underline{f}}{\partial \underline{u}}\ddot{\underline{q}} + \frac{\partial \underline{f}}{\partial \underline{u}}\right]|_{op}$,

$\underline{\underline{E}}$: wind input disturbance matrix,

$\underline{\underline{F}}$: wind input disturbance transmission matrix,

$\underline{\underline{DspC}}$: the displacement output matrix wind input disturbance transmission matrix,

$\underline{\underline{VelC}}$: the velocity output matrix.

Figure 2.2 shows the state space representation of the Linearized model.

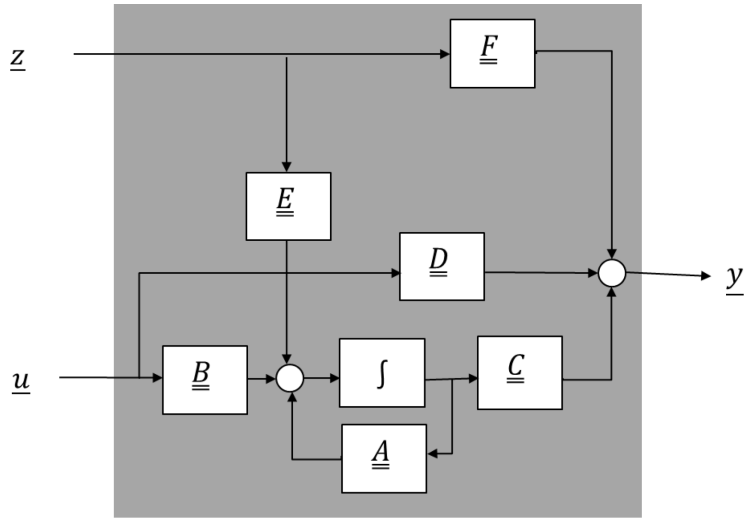

Figure2.2: FAST linearized state space model

As the wind turbine rotor is spinning by 12.1 rpm, the operating point is periodic that leads to periodicity in the state space matrices $\underline{\underline{A}}, \underline{\underline{B}}, \underline{\underline{C}}, \mathrm{D}, \underline{\underline{E}}$ and $\underline{\underline{F}}$. To overcome this problem, the linearization process has been done 36 times, every 10-degree azimuth angle position and the linearized output model is taken as an average over the number of linearization processes per one revolution.

3 Modelling of Wind Disturbance

According to Disturbance Accommodation Control (DAC) theory, the first requirement in order to accommodate the disturbance is to modell it. Here in this chapter, we will discuss how to model the wind disturbance based on Dryden wind turbulence model.

The wind speed V can be divided in two components,

$$V = V_m + v \tag{3-1}$$

Where V_m represents the steady mean wind speed and v represents the atmospheric turbulence that covers the fluctuations of the wind speed. As the wind speed is experienced by a rotating wind turbine, the rotational sampling effect should be taken into consideration. Figure 3.1 shows the block diagram of the effective wind model where the rotational sampling effect is added to the turbulence model [7]. Each part of this model will be discussed in the following subsections.

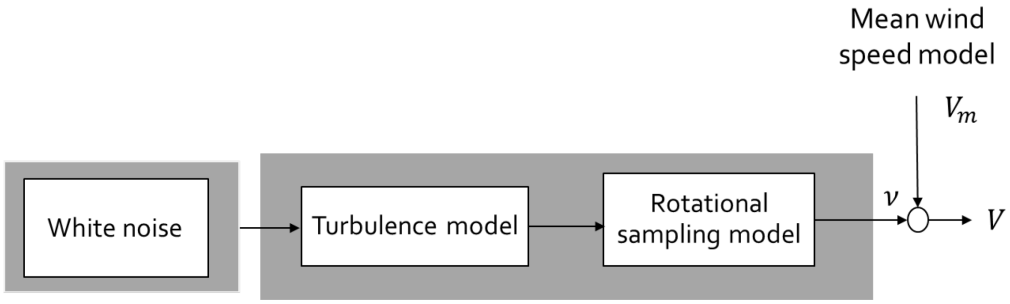

Figure 3.1: Effective wind model [7]

3.1 Mean wind speed

Mean wind speed describes the low frequency variations and is defined as the wind speed averaged over a specific time interval at a specific height. It is used to for the assessment of the expected energy yield. It is often modelled as a Weibull's distribution.

3.2 Turbulence

The high frequency random variations of the flow towards the wind turbine over a period typically 10 min is referred to Turbulence [10]. These variations can be caused by the friction of the flow with the earth surface or the thermal effects in the planetary boundary layer near the earth surface. The turbulence can't be avoided but it's effect can be reduced by implementing a good control system that can react to it.

3.2.1 Turbulence model

Turbulence is often considered as a stochastic process which is hard to be modelled in deterministic equations. Often, it is sufficient to modell just the characteristics via a Power Spectral Density (PSD).

The Dryden wind Turbulence model is of that kind and will be used here. because of its simpler form and its easy access to the time simulation, it's often used in the aerospace industry. The random functions associated with Dryden spectra can be generated by passing Gaussian white noise through appropriate form filter as shown in figure 3.2 [6]. The model consists of the power spectral density for the horizontal turbulence velocity u.

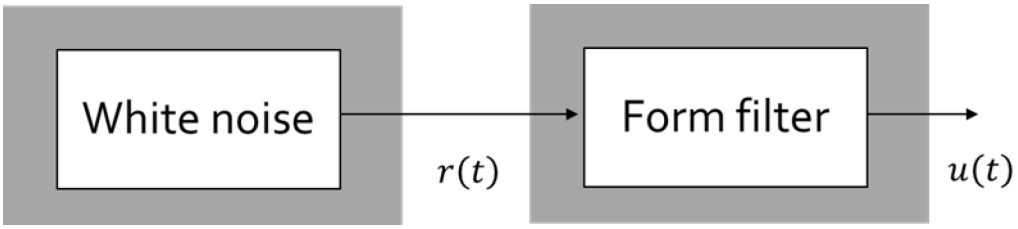

Figure 3.2: Dryden wind turbulence model [6]

The transfer function of the form filter generating a random signal having Dryden spectra from a white noise can be obtained by spectral factorization. it is given as the following equation for the horizontal turbulence.

$$\hat{F}_{u_w} = \frac{\underline{u}(s)}{\underline{r}(s)} = \sqrt{2{\sigma_u}^2 T_u} \cdot \frac{1}{1 + sT_u} \tag{3-2}$$

where

$$T_u = \frac{L_u}{V} = \frac{1}{\omega_u}$$

where L_u is the length scale, σ is the standard deviation and it is a measure of the turbulence intensity, T is the time constant, V is the steady mean wind speed, u is the index for the horizontal turbulence. L_u is modelled as described in [11] where $V = V_m =$ 18 m/s

Turbulence intensity I describes the level of the random variation from the mean wind speed as shown in figure 3.3. It is defined as the ratio of the standard deviation of wind speed variations to the mean wind speed V_m in a certain averaging time, usually defined over 10 min or 1 h.

$$I = \frac{\sigma}{V_m}$$

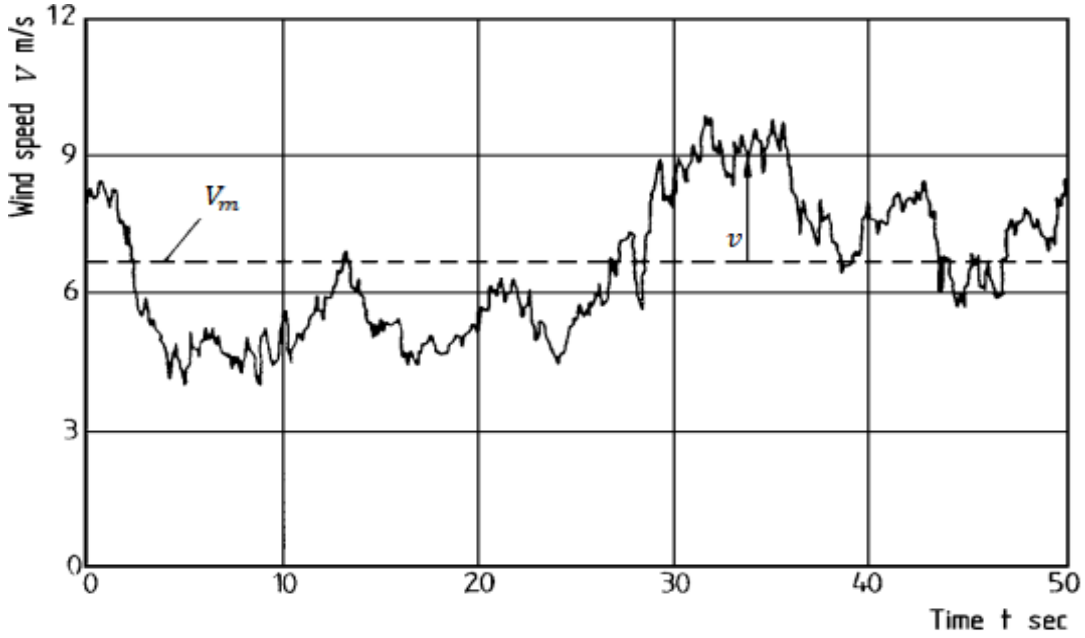

Figure 3.3: Measured time history of wind speed [12]

This equation can be represented in a state space form as

$$\underline{\dot{x}}_{Dry} = \underline{\underline{A}}_{Dry}\underline{x}_{Dry} + \underline{\underline{B}}_{Dry}\,\underline{r} \tag{3-4}$$

$$\underline{z} = \underline{\underline{C}}_{Dry}\underline{x}_{Dry} \tag{3-5}$$

where $\underline{\underline{A}}_{Dry} = \left[-\frac{V}{L_u}\right]$ $\underline{\underline{B}}_{Dry} = \left[\sigma\sqrt{2\frac{V}{L_u}}\right]$ $\underline{\underline{C}}_{Dry} = [1]$

Figure 3.4 shows the state space representation of Dryden model.

For a three-bladed wind turbine

$$\underline{\underline{A}}_{Dry} = \begin{bmatrix} \frac{-1}{T_u} & 0 & 0 \\ 0 & \frac{-1}{T_u} & 0 \\ 0 & 0 & \frac{-1}{T_u} \end{bmatrix}, \quad \underline{\underline{B}}_{Dry} = \begin{bmatrix} \sigma_u\sqrt{2\frac{V_k}{L_u}} & 0 & 0 \\ 0 & \sigma_u\sqrt{2\frac{V_k}{L_u}} & 0 \\ 0 & 0 & \sigma_u\sqrt{2\frac{V_k}{L_u}} \end{bmatrix}, \quad \underline{\underline{C}}_{Dry} = \begin{bmatrix} 1 & 0 & 0 \\ 0 & 1 & 0 \\ 0 & 0 & 1 \end{bmatrix}$$

To be sure that the turbulence acting on each blade is uncorrelated and the speed of the three white noise generators are different.

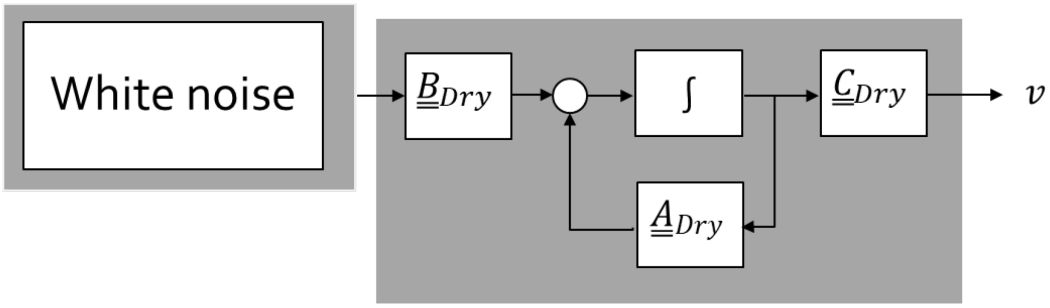

Figure 3.4: State space representation of Dryden model

3.3 Rotational Sampling Effect

The rotational sampling effect adds the effect of the rotating blades to the turbulence as shown in figure 3.5 where the PSD shows peaks at the rotational frequency f_{1b} and at higher harmonics ($f_{2b} = 2f_{1b}, f_{3b} = 3f_{1b}$).

For well understanding this effect, we need to discuss the following two cases. The first case, when the size of the eddy is much bigger than the rotor swept area. In this case there is no consideration for the rotational sampling effect and the observed wind speed will be the same for a rotating blade as for a fixed position. The second case, when the size of the eddy is smaller than the rotor swept area as we assume in our study. In this case, the turbine rotor samples the eddy periodically with each rotation until the eddy passes the rotor [13]. The sampling rate is dependent on the rotational speed and the loads acting on the blades in this case will be dependent on where the blade is.

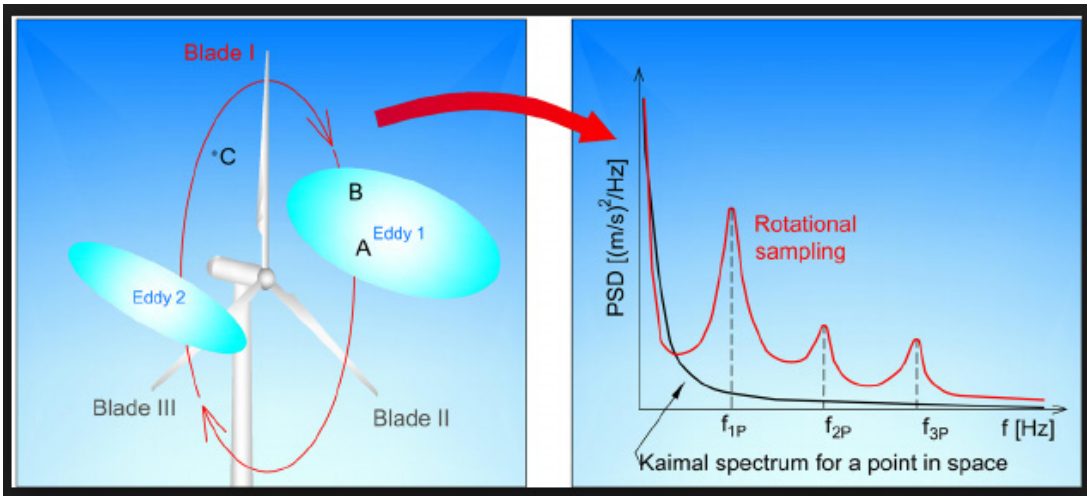

Figure 3.5: Schematic representation of the power spectral density (PSD) of rotational sampling [14]

This effect can be described by the meaning of the inverse notch filter. The inverse notch filter is a narrow band pass filter and it has an infinite impulse response. It rejects all frequencies expect of a stop frequency band centered on a center frequency, which is the wind turbine rotational frequency in our case. figure 3.6 shows the frequency response of the inverted notch filter. The state space representation of the three inverted notch filters for the three blades is:

$$\dot{\underline{x}}_{wind} = \underline{\underline{A}}_{Wind}\underline{x}_{wind} + \underline{\underline{B}}_{Wind}\,\underline{u}_{wind} \tag{4-6}$$

$$\underline{y}_{wind} = \underline{\underline{C}}_{Wind}\underline{x}_{wind} + \underline{\underline{D}}_{Wind}\underline{u}_{wind} \tag{4-7}$$

The matrices $\underline{\underline{A}}_{Wind}$, $\underline{\underline{B}}_{Wind}$, $\underline{\underline{C}}_{Wind}$, $\underline{\underline{D}}_{Wind}$ are represented as

$$\underline{\underline{A}}_{Wind} = \begin{bmatrix} 0 & 1 & 0 & 0 & 0 & 0 \\ -\Omega^2 & -2d\Omega^2 & 0 & 0 & 0 & 0 \\ 0 & 0 & 0 & 1 & 0 & 0 \\ 0 & 0 & -\Omega^2 & -2d\Omega^2 & 0 & 0 \\ 0 & 0 & 0 & 0 & 0 & 1 \\ 0 & 0 & 0 & 0 & -\Omega^2 & -2d\Omega^2 \end{bmatrix}, \underline{\underline{B}}_{Wind} = \begin{bmatrix} 0 & 0 & 0 \\ 1 & 0 & 0 \\ 0 & 0 & 0 \\ 0 & 1 & 0 \\ 0 & 0 & 0 \\ 0 & 0 & 1 \end{bmatrix}$$

$$\underline{\underline{C}}_{Wind} = \begin{bmatrix} 0 & 2\Omega & 0 & 0 & 0 & 0 \\ 0 & 0 & 0 & 2\Omega & 0 & 0 \\ 0 & 0 & 0 & 0 & 0 & 2\Omega \end{bmatrix}, \qquad \underline{\underline{D}}_{Wind} = \begin{bmatrix} 1 & 0 & 0 \\ 0 & 1 & 0 \\ 0 & 0 & 1 \end{bmatrix}$$

where d represents the damping factor and Ω the rotational speed.

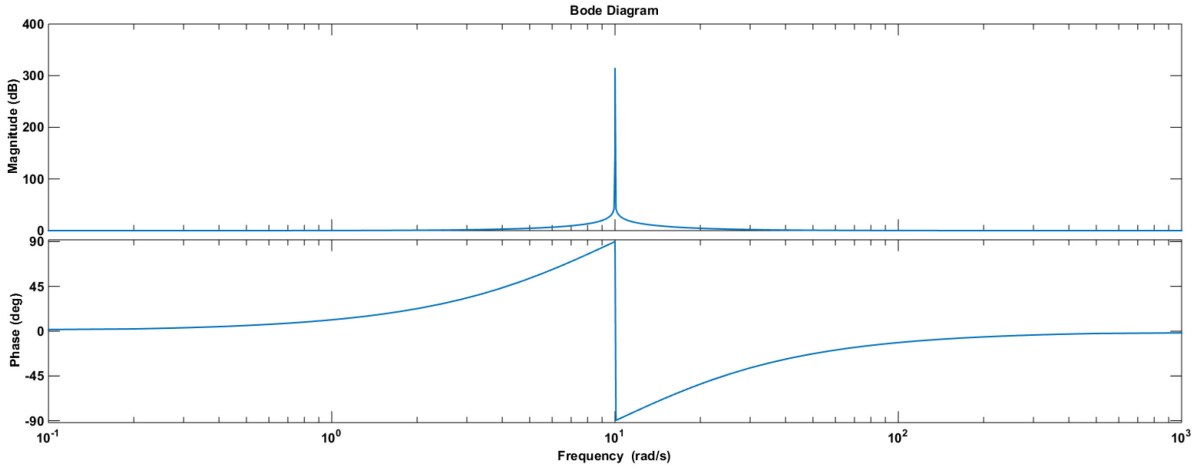

Figure 3.6: Inverted notch filter response.

4 Derivation of a controller structure based on a stochastic disturbance observer

4.1 Setting up design criteria

The high frequency variations in wind speed (turbulence) are the primary reasons for the fatigue of the different wind turbine components. Designing a control system to mitigate the loads caused by the turbulence will directly translate into a reduction in the fatigue damage. This directly leads to increase in the life time of the wind turbine as it will be illustrated in chapter 6.

Another impact of the turbulence on wind turbine is the fluctuations in the rotational speed. In order to increase the rotational speed strength, the turbulence effect should be reduced. Chapter 5 shows how much the reduction in the standard deviation of the rotational speed before and after applying the controller.

Briefly, the specific criteria for designing the control system are: -

1- Decreasing the fatigue damage.

2- Increasing the rotational speed strength.

4.2 State Estimation using Kalman Filter

The ability of an observer to estimate unmeasurable states from a set of measurements with the help of a model of the control path suggests the idea of extending the model of the control path by a model of the disturbance and reconstructing the states of the disturbance as well. State estimation is the process of determining an estimate of the internal system states depending on a set of measurements of system inputs and outputs. The estimated states are a combination of the wind turbine estimated states and the augmented wind disturbance estimated states. In this thesis, the Discrete Kalman Filter will be used as an observer for the estimation process. It is an optimal recursive data processing algorithm that gives the optimal estimates of the system states for a linear system with additive Gaussian white noise in the process and the measurements which is correct in our case [15]. Kalman filter is optimal by minimizing the mean squared error between the estimated state and the real state. The recursive operation mode of the Kalman filter comes from its ability to depend only the previous estimate to get the current estimate rather than depending on the history of all previous estimates. Figure 4.1 shows how is the Kalman filter estimates the system states with the help of the measurement of system's output.

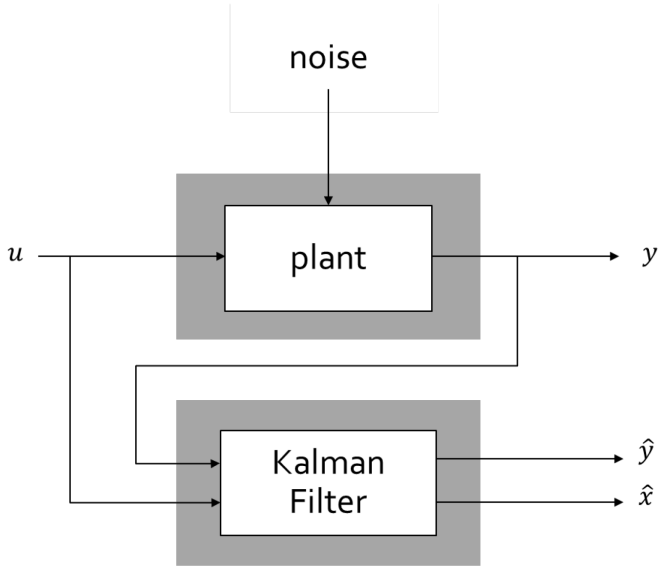

Figure 4.1: State estimation based on Kalman filter [16]

For nonlinear systems, different Kalman filters such as the extended Kalman filter and the unscented Kalman filter can be used. Nowadays, Kalman filter is used in many different applications such as tracking systems, navigation and many computer vision applications.

Before starting the discussion about the operation of the Kalman filter algorithm, we need to understand the definitions of what's called mean or expected value, variance and standard deviation.

Expected value or Mean (μ):-

For a random variable X, Expected value of X is

$$E[X] = \sum_{i}^{n} P_i x_i \tag{4-1}$$

where $x_1, x_2 \ldots\ldots\ldots x_n$ are the possible realization of X and $P_1, P_2 \ldots\ldots\ldots P_n$ are the corresponding probabilities. If X is a continuous random variable, the Expected value will be

$$E[X] = \int_{-\infty}^{\infty} x f_X(x)\, dx \tag{4-2}$$

where $f_X(x)$ is the probability density function.

Variance: -

$$VAR(X) = E\left[\left(X - E(X)\right)^2\right] \tag{4-3}$$
$$= E[X^2] - \mu^2$$

It is a measure of the spread of X around mean.

Standard deviation: -

It is the square root of variance.

$$\sigma(X) = \sqrt{VAR(X)} \tag{4-4}$$

4.2.1 The Discrete Kalman Filter derivation

For the derivation of the Discrete Kalman filter, suppose that the linear system is represented in a state space representation as following:

$$\underline{x}_{k+1} = \underline{\underline{A}}\underline{x}_k + \underline{\underline{B}}\underline{u}_{k+1} + \underline{w}_k \tag{4-5}$$

$$\underline{y}_k = \underline{\underline{C}}\underline{x}_k + \underline{\underline{D}}\underline{u}_k + \underline{v}_k \tag{4-6}$$

Where

$\underline{x}_k$: $(n \text{ x } 1)$ system state at time t_k

$\underline{y}_k$: $(p \text{ x } 1)$ measured output at time t_k

$\underline{u}_k$: $(m \text{ x } 1)$ control input at time t_k

$\underline{\underline{A}}$: $(n \text{ x } n)$ state matrix

$\underline{\underline{B}}$: $(n \text{ x } m)$ input matrix

$\underline{\underline{C}}$: $(p \text{ x } n)$ output matrix

$\underline{\underline{D}}$: $(p \text{ x } m)$ state matrix

$\underline{w}_k$: $(n \text{ x } 1)$ process noise

$\underline{v}_k$: $(p \text{ x } 1)$ measurement noise

n: number of the system states

p: number of the system outputs

m:number of the system

It is assumed that the process noise $\underline{w}_k$ and the measurement noise $\underline{v}_k$ are normally gaussian distributed and uncorrelated.

The covariance matrices for $\underline{w}_k$ and $\underline{v}_k$are given by

$$E\left[\underline{w}_k \underline{w}_i{}^T\right] = \underline{\underline{Q}}_{var}$$
$$E\left[\underline{v}_k \underline{v}_i{}^T\right] = \underline{\underline{R}}_{var}$$

Assume that the prior (or a priori) error in estimation is $\underline{e}_k^-$ where

$$\underline{e}_k^- = \underline{x}_k - \underline{\hat{x}}_k^- \tag{4-7}$$

where $\underline{\hat{x}}_k^-$ is the prior estimate.

A Priori means the estimation is done before the measurement and a posteriori means the estimation is done after the measurement.

The associated error covariance matrix $\underline{\underline{P}}_k^-$ is

$$\underline{\underline{P}}_k^- = E\left[\underline{e}_k^- \underline{e}_k^{-T}\right] = E\left[\left(\underline{x}_k - \underline{\hat{x}}_k^-\right)\left(\underline{x}_k - \underline{\hat{x}}_k^-\right)^T\right] \tag{4-8}$$

where $\underline{\hat{x}}_k^-$ is the prior state estimate.

With the new noisy measurement $\underline{y}_k$, the predicted state $\underline{\hat{x}}_k$ is corrected by a feedback of the difference between the measured output vector and the estimated output vector $\left(\underline{y}_k - \underline{\underline{C}}\,\underline{\hat{x}}_k^-\right)$ via a weighting factor $\underline{\underline{K}}_k$ as shown in the following equation

$$\underline{\hat{x}}_k = \underline{\hat{x}}_k^- + \underline{\underline{K}}_k\left(\underline{y}_k - \underline{\underline{C}}\,\underline{\hat{x}}_k^-\right) \tag{4-9}$$

This weighting factor is called Kalman gain and it will be determined later.

The updated error in the estimate or posteriori estimate error is

$$\underline{e}_k = \underline{x}_k - \underline{\hat{x}}_k \tag{4-10}$$

and the corresponding updated error covariance matrix is

$$\underline{\underline{P}}_k = E\left[\underline{e}_k\, \underline{e}_k^T\right] = E\left[\left(\underline{x}_k - \underline{\hat{x}}_k\right)\left(\underline{x}_k - \underline{\hat{x}}_k\right)^T\right]. \tag{4-11}$$

by substituting equation (4-9) into equation (4-11), we get

$$\begin{gathered} P_k = E\left[\underline{e}_k\, \underline{e}_k^T\right] = \\ E\left[\left(\underline{x}_k - \left[\underline{\hat{x}}_k^- + \underline{\underline{K}}_k(\underline{y}_k - \underline{\underline{C}}\,\underline{\hat{x}}_k^-)\right]\right)\left(\underline{x}_k - \left[\underline{\hat{x}}_k^- + \underline{\underline{K}}_k(\underline{y}_k - \underline{\underline{C}}\,\underline{\hat{x}}_k^-)\right]\right)^T\right] \end{gathered} \tag{4-12}$$

If equation (4-5) is substituted into equation (4-12), the updated error covariance matrix can be written as

$$\begin{aligned} \underline{\underline{P}}_k = E[&\left(\underline{x}_k - \left[\underline{\hat{x}}_k^- + \underline{\underline{K}}_k(\underline{\underline{C}}\,x_k + \underline{\underline{D}}\,\underline{u}_k + \underline{v}_k - \underline{\underline{C}}\,\underline{\hat{x}}_k^-)\right]\right) \\ &\left(\underline{x}_k - \left[\underline{\hat{x}}_k^- + \underline{\underline{K}}_k(\underline{\underline{C}}\,x_k + \underline{\underline{D}}\,\underline{u}_k + \underline{v}_k - \underline{\underline{C}}\,\underline{\hat{x}}_k^-)\right]\right)^T] \end{aligned} \tag{4-13}$$

$$\begin{aligned} \underline{\underline{P}}_k = E\{&\left(\underline{x}_k - \underline{\hat{x}}_k^-\right) - \underline{\underline{K}}_k(\underline{\underline{C}}\,x_k + \underline{\underline{D}}\,\underline{u}_k + \underline{v}_k - \underline{\underline{C}}\,\underline{\hat{x}}_k^-)]\big] \\ &\left[\left(\underline{x}_k - \underline{\hat{x}}_k^-\right) - \underline{\underline{K}}_k(\underline{\underline{C}}\,x_k + \underline{\underline{D}}\,\underline{u}_k + \underline{v}_k - \underline{\underline{C}}\,\underline{\hat{x}}_k^-)\right]^T\} \end{aligned} \tag{4-14}$$

performing this expectation, we get

$$\underline{\underline{P}}_k = \underline{\underline{P}}_k^- - \underline{\underline{K}}_k\underline{\underline{C}}\,\underline{\underline{P}}_k^- - \underline{\underline{P}}_k^-\,\underline{\underline{C}}^T\underline{\underline{K}}_k^T + \underline{\underline{K}}_k\left(\underline{\underline{C}}\,\underline{\underline{P}}_k^-\,\underline{\underline{C}}^T + \underline{\underline{R}}_{var}\right)\underline{\underline{K}}_k^T\ . \tag{4-15}$$

Now, the Kalman gain $\underline{\underline{K}}_k$ needs to be determined such that $\underline{\underline{P}}_k$ is minimized. This can be done using the straightforward differential calculus approach [17]. This approach can be

applied by differentiating the trace of $\underline{\underline{P}}_k$ which represents the sum of the mean square errors in the estimate with respect to $\underline{\underline{K}}_k$ and setting this derivative equal to zero

$$\frac{d(trace\ \underline{\underline{P}}_k)}{d\underline{\underline{K}}_k} = -2\left(\underline{\underline{C}}\,\underline{\underline{P}}_k^-\right)^T + 2\,\underline{\underline{K}}_k\left(\underline{\underline{C}}\,\underline{\underline{P}}_k^-\,\underline{\underline{C}}^T + \underline{\underline{R}}_{var}\right)\underline{\underline{K}}_k{}^T \tag{4-16}$$

$$-2\left(\underline{\underline{C}}\,\underline{\underline{P}}_k^-\right)^T + 2\,\underline{\underline{K}}_k\left(\underline{\underline{C}}\,\underline{\underline{P}}_k^-\,\underline{\underline{C}}^T + \underline{\underline{R}}_{var}\right)\underline{\underline{K}}_k{}^T = 0 \tag{4-17}$$

$$\underline{\underline{K}}_k = \underline{\underline{P}}_k^-\,\underline{\underline{C}}^T\left(\underline{\underline{C}}\,\underline{\underline{P}}_k^-\,\underline{\underline{C}}^T + \underline{\underline{R}}_{var}\right)^{-1} \tag{4-18}$$

Substituting the Kalman gain $\underline{\underline{K}}_k$ into equation (4-15), we get

$$\underline{\underline{P}}_k = \underline{\underline{P}}_k^- - \underline{\underline{P}}_k^-\,\underline{\underline{C}}^T\left(\underline{\underline{C}}\,\underline{\underline{P}}_k^-\,\underline{\underline{C}}^T + \underline{\underline{R}}_{var}\right)^{-1}\underline{\underline{C}}\,\underline{\underline{P}}_k^- \tag{4-19}$$

or

$$\underline{\underline{P}}_k = \underline{\underline{P}}_k^- - \underline{\underline{K}}_k\,\underline{\underline{C}}\,\underline{\underline{P}}_k^- \tag{4-20}$$

$$\underline{\underline{P}}_k = \left(I - \underline{\underline{K}}_k\,\underline{\underline{C}}\right)\underline{\underline{P}}_k^- \tag{4-21}$$

The next estimation can be obtained using equation (4-4) with ignoring w_k because it has zero mean and it is not correlated with any of the previous values

$$\underline{\hat{x}}_{k*1}^- = \underline{\underline{A}}\,\underline{\hat{x}}_k + \underline{\underline{B}}\,\underline{u}_{k+1}\ . \tag{4-22}$$

The associated error is

$$\begin{aligned} \underline{e}_{k*1}^- &= x_{k+1} - \underline{\hat{x}}_{k*1}^- \\ \underline{e}_{k*1}^- &= \underline{\underline{A}}\,\underline{x}_k + \underline{\underline{B}}\,\underline{u}_{k+1} + \underline{\underline{D}}\,\underline{u}_{k+1} + \underline{w}_k - \underline{\underline{A}}\,\underline{\hat{x}}_k - \underline{\underline{B}}\,\underline{u}_{k+1} - \underline{\underline{D}}\,\underline{u}_{k+1} \\ \underline{e}_{k*1}^- &= \underline{\underline{A}}\,\underline{e}_k + \underline{w}_k \end{aligned} \tag{4-23}$$

and the associated error covariance matrix in this case is

$$\underline{\underline{P}}_{k*1}^- = E\left[\underline{e}_{k*1}^-\,\underline{e}_{k*1}^{-\,T}\right]$$

$$\underline{\underline{P}}_{k*1}^- = E\left[\left(\underline{\underline{A}}\,\underline{e}_k + \underline{w}_k\right)\left(\underline{\underline{A}}\,\underline{e}_k + \underline{w}_k\right)^T\right] \tag{4-24}$$

$$\underline{\underline{P}}_{k*1}^- = \underline{\underline{A}}\,\underline{\underline{P}}_k\underline{\underline{A}}^T + \underline{\underline{Q}}_{var}\ .$$

Figure 4.2 shows the operation of the Kalman filter algorithm

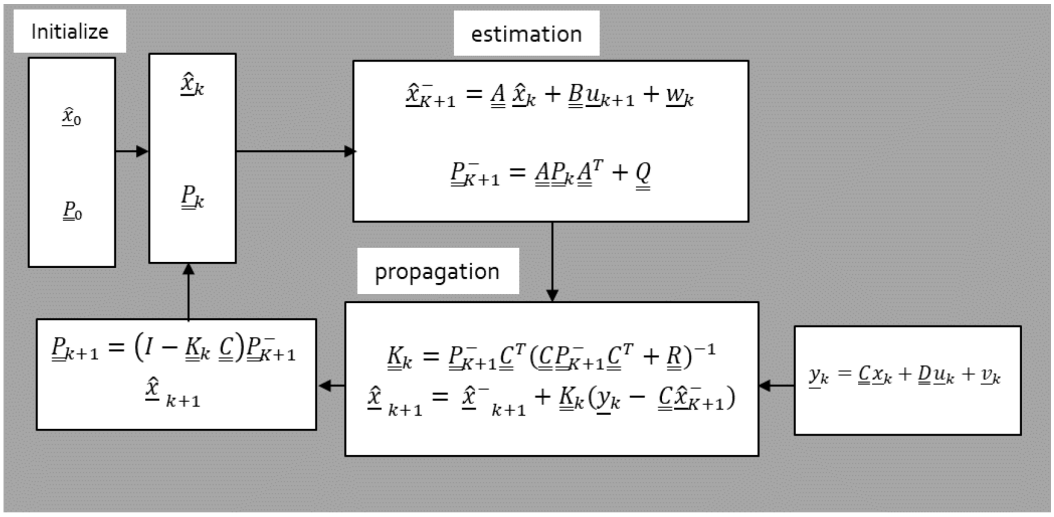

Figure 4.2: Kalman filter algorithm

4.2.2 Disturbance Observation

The model required for a disturbance observation using the Discrete Kalman filter consists of the combination of the linearized wind turbine model and the disturbance model as shown in figure 4.3. where $\underline{w}_k$ and $\underline{w}_{k_{Dry}}$ represent the process noise and the turbulence noise respectively. WT is an index for Wind Turbine and Dis is an index for Disturbance.

$$\begin{bmatrix} \dot{\underline{x}}_{WT} \\ \dot{\underline{x}}_{Dis} \end{bmatrix} = \begin{bmatrix} \underline{\underline{A}} & \underline{\underline{E}}\,\underline{\underline{C}}_{Dis} \\ 0 & \underline{\underline{A}}_{Dis} \end{bmatrix} \begin{bmatrix} \underline{x}_{WT} \\ \underline{x}_{Dis} \end{bmatrix} + \begin{bmatrix} \underline{\underline{B}} \\ 0 \end{bmatrix} \underline{u} + \begin{bmatrix} 0 \\ \underline{\underline{B}}_{Dis} \end{bmatrix} \underline{r} + \begin{bmatrix} \underline{w}_k \\ \underline{w}_{k_{Dis}} \end{bmatrix} \tag{4-25}$$

$$\underline{y}_{WT} = [\underline{\underline{C}} \quad \underline{\underline{F}}\,\underline{\underline{C}}_{Dis}] \begin{bmatrix} \underline{x}_{WT} \\ \underline{x}_{Dis} \end{bmatrix} + \underline{\underline{D}}\,\underline{u} + \underline{v}_k \tag{4-26}$$

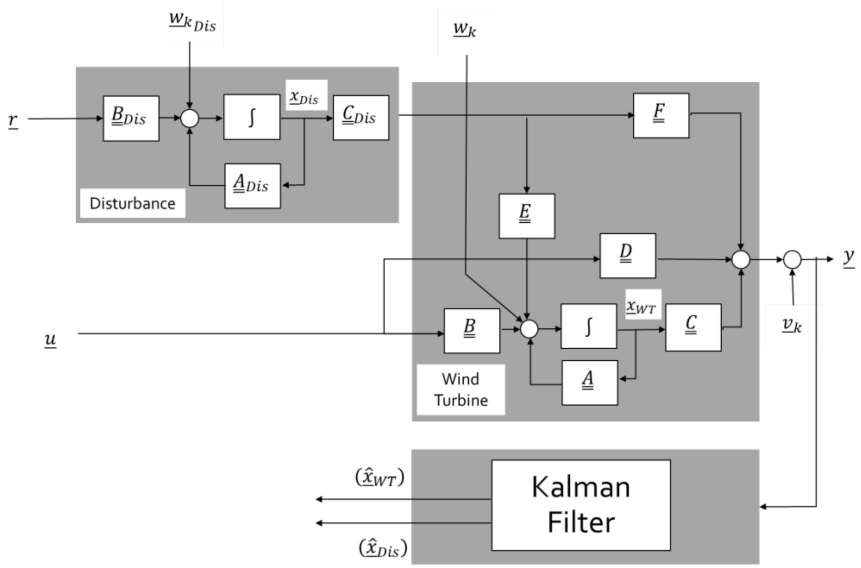

Figure 4.3: The required model for state estimation using Kalman filter

4.2.3 Kalman Filter Tuning

The tuning of the Kalman filter is done via determination of the process noise covariance matrix $\underline{\underline{Q}}_{var}$ and the measurement noise covariance matrix $\underline{\underline{R}}_{var}$.

For the tuning process, often just the main diagonal elements $\underline{\underline{Q}}_{var}$ and $\underline{\underline{R}}_{var}$ are engaged where the other elements are neglected.

The measurement noise covariance matrix is determined through the error in the measurement. This error can be obtained from the sensors datasheet. The approximated measured noise is modelled by the following values

$\underline{\underline{R}}_{var}(1,1) = 6{,}25 * 10^{-6}$

$\underline{\underline{R}}_{var}(2,2) = 0{,}0001$

$\underline{\underline{R}}_{var}(3,3) = 0{,}0001$

$\underline{\underline{R}}_{var}(4,4) = 0{,}0001$

$\underline{\underline{R}}_{var}(5,5) = 0{,}0001$

$\underline{\underline{R}}_{var}(6,6) = 0{,}0001$

$\underline{\underline{R}}_{var}(7,7) = 0{,}0001$

$\underline{\underline{R}}_{var}(8,8) = 0{,}0001$

$\underline{\underline{R}}_{var}(9,9) = 0{,}0001$

$\underline{\underline{R}}_{var}(10,10) = 0{,}0001$

The process noise covariance matrix is not so easy to be determined because there is no specific way to get it. Often this noise is selected via trial and error. One of these trials, which has been used here uses the model uncertainties caused by the preciosity of the un models. This can be shown in figure 4.4 where a66, a77, a88, a99 and a 1010 represents the average model uncertainties over the azimuth for $\underline{\underline{A}}(6,6)$, $\underline{\underline{A}}(7,7)$, $\underline{\underline{A}}(8,8)$, $\underline{\underline{A}}(9,9)$, $\underline{\underline{A}}(10,10)$ respectively.

These are the values of the diagonal elements of the process noise covariance matrix where the first ten elements are for the wind turbine states and the other 9 elements are for the disturbance states.

$\underline{\underline{Q}}_{var}(1,1) = 6 * 10^{-9}$

$\underline{\underline{Q}}_{var}(6,6) = 6 * 10^{-9}$

$\underline{\underline{Q}}_{var}(2,2) = 3 * 10^{-8}$

$\underline{\underline{Q}}_{var}(7,7) = 3 * 10^{-8}$

$\underline{\underline{Q}}_{var}(3,3) = 9 * 10^{-6}$

$\underline{\underline{Q}}_{var}(8,8) = 9 * 10^{-6}$

$\underline{\underline{Q}}_{var}(4,4) = 9 * 10^{-6}$

$\underline{\underline{Q}}_{var}(5,5) = 9 * 10^{-6}$

$\underline{\underline{Q}}_{var}(9,9) = 9 * 10^{-6}$

$\underline{\underline{Q}}_{var}(10,10) = 3 * 10^{-7}$

$\underline{\underline{Q}}_{var}(11,11) = 3 * 10^{-7}$

$\underline{\underline{Q}}_{var}(12,12) = 3 * 10^{-7}$

$\underline{\underline{Q}}_{var}(13,13) = 3 * 10^{-7}$

$\underline{\underline{Q}}_{var}(13,13) = 3 * 10^{-7}$

$\underline{\underline{Q}}_{var}(14,14) = 3 * 10^{-7}$

$\underline{\underline{Q}}_{var}(14,14) = 3 * 10^{-7}$

$\underline{\underline{Q}}_{var}(15,15) = 3 * 10^{-7}$

$\underline{\underline{Q}}_{var}(16,16) = 3 * 10^{-7}$

$\underline{\underline{Q}}_{var}(17,17)$ =0.0006666

$\underline{\underline{Q}}_{var}(18,18)$ =0.00066667

$\underline{\underline{Q}}_{var}(19,19)$ =0.00066667

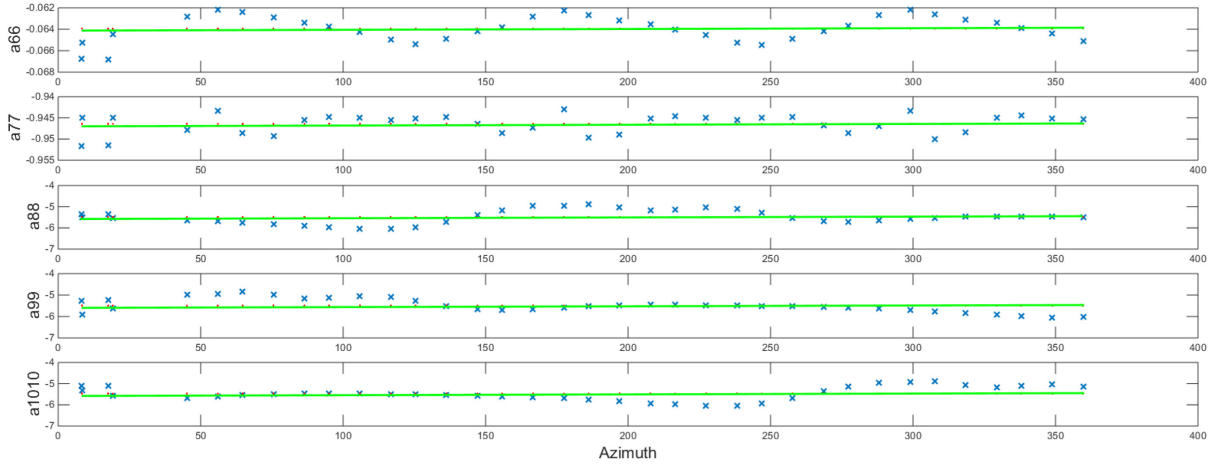

Figure 4.4: Determination of the process noise covariance matrix

4.3 Controller structure based on stochastic Disturbance accommodation control

As it is discussed before, the second requirement in the disturbance accommodation control theory is to design a feedback/feedforward controller in order to stabilize the system and accommodate the disturbance. In our case, the Linear Quadratic Regulator (LQR) will be used as a full state feedback controller for tuning the wind turbine plant and a feedforward controller to accommodate the wind disturbances.

4.3.1 linear quadratic regulator

The linear quadratic regulator design is as an important design technique for linear systems since the sixties. There are two main objectives of LQR design, the first objective is to find a full state feedback controller to stabilize the wind turbine based on the turbine estimated states, which have been obtained from the Kalman filter, as we discussed in the previous section, where the second objective is to minimize the cost function J that has been given in equation (4-27). This combination of an optimal estimator and an optimal regulator is called linear Quadratic Gaussian (LQG).

Due to the separation principle, the estimation process via an observer e.g. Kalman Filter can be done separately to the controller tuning.

According to Kalman, a linear time - invariant system is optimal if the following quadratic cost function is minimized

$$J = \int_0^\infty (\underline{x}^T \underline{\underline{Q}}_{LQR}\, \underline{x} + \underline{u}^T \underline{\underline{R}}_{LQR}\, \underline{u}) dt \ . \qquad (4\text{-}27)$$

where $\underline{\underline{Q}}_{LQR}$ and $\underline{\underline{R}}_{LQR}$ are constant weighting matrices and must meet the following conditions:

- $\underline{\underline{R}}_{LQR}$ must be positive definite (regular and symmetrical)
- $\underline{\underline{Q}}_{LQR}$ must be positive semidefinite (all principal determinants ≥ 0)

Therefore, no negative cost components will occur. By appropriate selection of the weighting matrices, it can be a more meaningful compromise between the system states and the control effort [18].

The solution of the above variational problem (minimization of the cost function under the constraint of the state equations) leads to Hamiltonian canonical equations, which are solved by linear approach. From this, the cost function is minimized for the control law

$$\underline{u} = -\underline{\underline{K}}_{LQR}\ \underline{x} \tag{4-29}$$

The $\underline{\underline{K}}_{LQR}$ is defined as

$$\underline{\underline{K}}_{LQR} = \underline{\underline{R}}_{LQR}{}^{-1}\underline{\underline{B}}^{T}\underline{\underline{P}} \tag{4-30}$$

where $\underline{\underline{P}}$ is an (nxn) matrix and equal to the solution of the following non-linear Riccati differential equation

$$\dot{\underline{\underline{P}}} = \underline{\underline{P}}\,\underline{\underline{A}} + \underline{\underline{A}}^{T}\underline{\underline{P}} - \underline{\underline{P}}\,\underline{\underline{B}}\,\bar{\bar{R}}^{-1}\underline{\underline{B}}^{T}\underline{\underline{P}} + \underline{\underline{Q}}_{LQR} = 0\ . \tag{4-31}$$

If the process is fully controllable and $\underline{\underline{A}}, \underline{\underline{B}}, \underline{\underline{C}}, \underline{\underline{Q}}_{LQR}$ and $\underline{\underline{R}}_{LQR}$ are constants, $\underline{\underline{P}}$ is a constant, real, symmetric, positive-definite nxn matrix [18].

The advantages of this approach are: -

- It provides an optimal controller structure including its parameters.
- It always leads to a stable control system.
- Relatively fast calculation algorithms are available to solve the nonlinear algebraic Riccati equation for $\underline{\underline{P}}$.
- It is also optimal in the sense of minimizing the variance of the state variables in stochastic disorders.

But it has the following disadvantages: -

- The structure of the quality function and the selection of the weighting matrices are formally restricted.
- The cost function converges only when $\underline{x}$ and $\underline{u}$ are close to zero for $t \to \infty$.
- It is only applicable to a complete state vector feedback, so the state variables must be measured or estimated, the controller structure is specified fixed.

4.3.1.1 LQR Tuning

LQR Tuning means choosing values for the weighting matrices $\underline{\underline{Q}}_{LQR}$ and $\underline{\underline{R}}_{LQR}$ to penalize the state variables and the control effort. In case of choosing a large value for $\underline{\underline{R}}_{LQR}$, the control effort will be highly penalized. Similarly, for $\underline{\underline{Q}}_{LQR}$, if the $\underline{\underline{Q}}_{LQR}$ value is large, this means that the system is stabilized with less changes in the states. The values of the main diagonal elements in the $\underline{\underline{Q}}_{LQR}$ are calculated according to this rule of thumb

$$\underline{x}^T \underline{\underline{Q}}_{LQR} \underline{x} = q_{11}\underline{x}_1^2 + \cdots + q_{1010}\underline{x}_{1010}^2 \quad (4\text{-}31)$$

where q_{11} is inversely proportional to maximum allowed value of $\underline{x}_1$(similar withq_{22}). Those are the calculated values of the main diagonal elements of $\underline{\underline{Q}}_{LQR}$ and $\underline{\underline{R}}_{LQR}$.

$\underline{\underline{R}}_{LQR}(1,1) = 1$

$\underline{\underline{R}}_{LQR}(2,2) = 1$

$\underline{\underline{R}}_{LQR}(3,3) = 1$

$\underline{\underline{Q}}_{LQR}(1,1) = 1$

$\underline{\underline{Q}}_{LQR}(2,2) = 0{,}1$

$\underline{\underline{Q}}_{LQR}(3,3) = 10$

$\underline{\underline{Q}}_{LQR}(4,4) = 10$

$\underline{\underline{Q}}_{LQR}(5,5) = 10$

$\underline{\underline{Q}}_{LQR}(6,6) = 1$

$\underline{\underline{Q}}_{LQR}(7,7) = 0{,}1$

$\underline{\underline{Q}}_{LQR}(8,8) = 10$

$\underline{\underline{Q}}_{LQR}(9,9) = 10$

$\underline{\underline{Q}}_{LQR}(10,10) = 10$

4.3.2 Feedforward Control

In this subsection, we will discuss how a feedforward controller can be used to accommodate the wind disturbances.

If the disturbance can be modelled as

$$\dot{\underline{x}_d} = \underline{\underline{A}}_d \underline{x}_d \tag{4-32}$$

$$\underline{z} = \underline{\underline{C}}_d \underline{x}_d \tag{4-33}$$

The disturbance model can be combined with the model of wind turbine and giving the following state space model

$$\dot{\underline{x}} = \underline{\underline{A}}\underline{x} + \underline{\underline{B}}\,\underline{u} + \underline{\underline{E}}\underline{\underline{C}}_d \underline{x}_d \tag{4-34}$$

$$\underline{y} = \underline{\underline{C}}\,\underline{x} + \underline{\underline{D}}\,\underline{u} + \underline{\underline{F}}\underline{\underline{C}}_d \underline{x}_d \ . \tag{4-35}$$

This can be written in matrix form as

$$\begin{bmatrix} \dot{\underline{x}} \\ \dot{\underline{x}}_d \end{bmatrix} = \begin{bmatrix} \underline{\underline{A}} & \underline{\underline{E}}\underline{\underline{C}}_d \\ 0 & \underline{\underline{A}}_d \end{bmatrix} \begin{bmatrix} \underline{x} \\ \underline{x}_d \end{bmatrix} + \begin{bmatrix} \underline{\underline{B}} \\ 0 \end{bmatrix} \underline{u} \tag{4-36}$$

$$\underline{y} = \begin{bmatrix} \underline{\underline{C}} & \underline{\underline{F}}\underline{\underline{C}}_d \end{bmatrix} \begin{bmatrix} \underline{x} \\ \underline{x}_d \end{bmatrix} \tag{4-37}$$

Or in a short form as

$$\dot{\underline{x}}^* = \underline{\underline{A}}^*\,\underline{x}^* + \underline{\underline{B}}^*\,\underline{u} \tag{4-38}$$

$$\underline{y} = \underline{\underline{C}}^*\,\underline{x}^* \tag{4-39}$$

Where

$$\underline{\underline{A}}^* = \begin{bmatrix} \underline{\underline{A}} & \underline{\underline{E}}\underline{\underline{C}}_d \\ 0 & \underline{\underline{A}}_d \end{bmatrix}, \qquad \underline{\underline{B}}^* = \begin{bmatrix} \underline{\underline{B}} \\ 0 \end{bmatrix}, \qquad \underline{\underline{C}}^* = \begin{bmatrix} \underline{\underline{C}} & \underline{\underline{F}}\underline{\underline{C}}_d \end{bmatrix}$$

The previous state equations (4-38) and (4-39) combines the turbine states and the wind disturbance states. Those states can be estimated using the Luenberger full state observer as shown in figure 4.5.

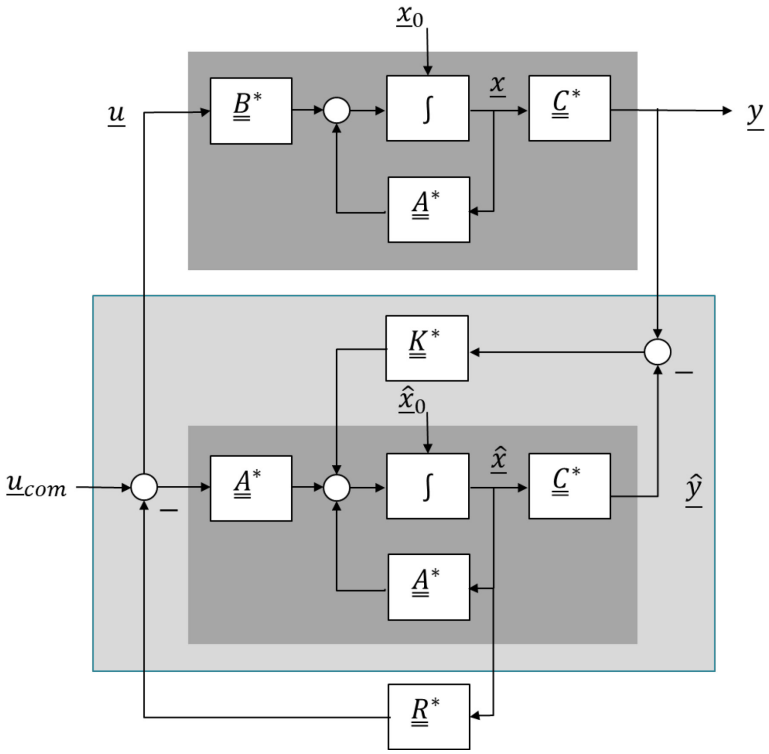

Figure 4.5: State estimation and state feedback based on Luenberger full state observer

The control input $\underline{u}$ can be written as

$$\underline{u} = -\underline{\underline{R}}^* \hat{\underline{x}}^* + \underline{u}_{com} \tag{4-40}$$

where $\underline{\underline{R}}^*$ is the closed loop gain; $\underline{\underline{R}}^* = [\underline{\underline{K}}_{LQR} \quad \underline{\underline{N}}]$, $\underline{\underline{K}}_{LQR}$ is the feedback gain, $\underline{\underline{N}}$ is the feedforward gain.

The observed state equation can be written as

$$\dot{\hat{\underline{x}}}^* = \underline{\underline{A}}^* \hat{\underline{x}}^* + \underline{\underline{B}}^* \underline{u} + \underline{\underline{K}}^* \underline{\underline{C}}^* \left(\underline{x}^* - \hat{\underline{x}}^*\right) \tag{4-41}$$

where $\underline{\underline{K}}^*$ is the observer gain; $\underline{\underline{K}}^* = [\underline{\underline{K}}_x \quad \underline{\underline{K}}_{xd}]^T$.

Equation (4-42) expresses the error in estimation which is the difference between the real state and the estimated state.

$$\underline{e}^* = \underline{x}^* - \underline{\hat{x}}^* = \begin{bmatrix} \underline{e}^* x \\ \underline{e}^* xd \end{bmatrix} = \begin{bmatrix} \underline{x} \\ \underline{x}_d \end{bmatrix} - \begin{bmatrix} \underline{\hat{x}} \\ \underline{\hat{x}}_d \end{bmatrix} \tag{4-42}$$

The first-time derivative in the estimation error is

$$\underline{\dot{e}}^* = \begin{bmatrix} \underline{\dot{e}}_x \\ \underline{\dot{e}}_{xd} \end{bmatrix} = \dot{x}^* - \underline{\hat{\dot{x}}}^* = \left[\underline{\underline{A}}^* - \underline{\underline{K}}^* \underline{\underline{C}}^*\right] \begin{bmatrix} \underline{e}_x \\ \underline{e}_{xd} \end{bmatrix} \tag{5-43}$$

The state equation of the total system can be obtained by substituting the control input u into the state equation (4-38). it can be written as

$$\begin{bmatrix} \underline{\dot{x}}^* \\ \underline{\dot{e}}^* \end{bmatrix} = \begin{bmatrix} \underline{\underline{A}}^* - \underline{\underline{B}}^* \underline{\underline{R}}^* & \underline{\underline{B}}^* \underline{\underline{R}}^* \\ 0 & \underline{\underline{A}}^* - \underline{\underline{K}}^* \underline{\underline{C}}^* \end{bmatrix} \begin{bmatrix} \underline{x}^* \\ \underline{e}^* \end{bmatrix} + \begin{bmatrix} \underline{\underline{B}}^* \\ 0 \end{bmatrix} \underline{u}_{com} \tag{4-44}$$

If A^*,$\underline{\underline{B}}^*$,$C^*$,$K^*$,$R^*$ are replaced into equation (4-44) by their definitions, the total system state equation will be written in the following detailed form

$$\begin{bmatrix} \underline{\dot{x}} \\ \underline{\dot{x}}_d \\ \underline{\dot{e}}_x \\ \underline{\dot{e}}_{xd} \end{bmatrix} = \begin{bmatrix} \underline{\underline{A}} - \underline{\underline{B}} \underline{\underline{K}}_{LQR} & \underline{\underline{E}}\, \underline{\underline{C}}_d - \underline{\underline{B}} \underline{\underline{N}} & \underline{\underline{B}} \underline{\underline{K}}_{LQR} & \underline{\underline{B}} \underline{\underline{N}} \\ 0 & \underline{\underline{A}}_d & 0 & 0 \\ 0 & 0 & \underline{\underline{A}} - \underline{\underline{K}}_x \underline{\underline{C}} & \underline{\underline{E}} \underline{\underline{C}}_d - \underline{\underline{K}}_x \underline{\underline{F}} \underline{\underline{C}}_d \\ 0 & 0 & -\underline{\underline{K}}_{xd} \underline{\underline{C}} & \underline{\underline{A}}_d - \underline{\underline{K}}_{xd} \underline{\underline{F}} \underline{\underline{C}}_d \end{bmatrix} \begin{bmatrix} \underline{x} \\ \underline{x}_d \\ \underline{e}_x \\ \underline{e}_{xd} \end{bmatrix} + \begin{bmatrix} \underline{\underline{B}} \\ 0 \\ 0 \\ 0 \end{bmatrix} \underline{u}_{com} \,. \tag{4-45}$$

From the previous equation, it is shown that the disturbance states $\underline{x}_d$ influences the first-time derivative of the system state $\underline{\dot{x}}$ through the term $\underline{\underline{E}} \underline{\underline{C}}_d - \underline{\underline{B}} \underline{\underline{N}}$.
This influence can be neglected if

$$\underline{\underline{N}} = \underline{\underline{B}}^{-1} \underline{\underline{E}} \underline{\underline{C}}_d \,. \tag{4-46}$$

In case of matrix $\underline{\underline{B}}$ is not invertible, an optimal disturbance variable response is possible in the sense of the smallest error squared using the pseudo inverse $\underline{\underline{B}}^* = (\underline{\underline{B}}^T \underline{\underline{B}})^{-1} \underline{\underline{B}}^T$.
It can be seen from equation (4-44) that the error in the estimation of the disturbance e_{xd} has an effect on the state vector of the control loop via matrix $\underline{\underline{E}} \underline{\underline{C}}_d - \underline{\underline{K}}_x \underline{\underline{F}} \underline{\underline{C}}_d$. A 100% compensation of this error is only possible for the theoretical case of an infinitely rapid estimation error dynamics. Due to the stochastic character of the turbulence but the variance in the estimation error $\sigma^2 = E\left(\underline{x}_i - \underline{\hat{x}}_i\right)$ can be minimized by using an optimal estimator such as Kalman filter as we discussed before.

5. Results

All the results shown in this chapter are done with the linear model at the trim point mentioned in chapter 2. The linearization has also been done for the following trim points and the results are shown in the appendix.

Trim point A: -

- 15 m/s steady horizontal wind speeds.
- 90 m as Reference height for horizontal wind speed.
- 10.45 degree as initial blade pitch angel for each blade.
- 12.1 rpm as initial rotor speed.

Trim point B: -

- 25 m/s steady horizontal wind speeds.
- 90 m as Reference height for horizontal wind speed.
- 23.47 degree as initial blade pitch angel for each blade.
- 12.1 rpm as initial rotor speed.

The system states after the combination between the wind turbine model and the disturbance model are the wind turbine states that were mentioned in chapter 2 with the addition of the following disturbance states: -

- Turbulence state for blade 1
- Turbulence state for blade 2
- Turbulence state for blade 3
- eddy slicing state 1 for blade 1
- eddy slicing state 2 for blade 1
- eddy slicing state 1 for blade 2
- eddy slicing state 2 for blade 2
- eddy slicing state 1 for blade 3
- eddy slicing state 2 for blade 3

where the measured outputs are: -

- Angular generator speed
- Blade 1 edgewise moment

- Blade 2 edgewise moment
- Blade 3 edgewise moment
- Blade 1 flapwise moment
- Blade 2 flapwise moment
- Blade 3 flapwise moment
- Tower side-to-side moment
- Tower fore-aft moment
- Tower torsional moment

The system stability has been checked and it shows that the system is unstable because of unstable pole. The reason behind this instability issue is a numerical problem with FAST caused from the generator azimuth state after applying Multi Blade Coordinate transformation (MBC). This unstable response can be shown in the first plot at figure 5.6. with applying the LQR as a full state feedback controller, the system becomes stable as shown in the third plot in the same figure. In case of neglecting this state, the wind turbine becomes stable as shown in the output response in figure 5.1 and 5.2.

The implementation of the linearized wind turbine model, Kalman filter and the controller structure is shown in MATLAB Simulink. The validations of the Discrete Kalman Filter and the feedback/feedforward controller are done first for the linear models then for the nonlinear model.

The advantage of the interface between FAST and Simulink with MATLAB gives the ability to use the FAST-nonlinear equations of motion through the FAST S-Function that has been incorporated in a Simulink model as shown in figure 6.4. This allows the validation of the results in the nonlinear simulation environment.

5.1 Validation of the Linear Model

Figure 5.1 and 5.2 show a good correspond between the linear model and the FAST-nonlinear model for the flapwise moment and the tower fore-aft.

The first 10 secs in those figures show the open loop response for the linear and nonlinear models without command pitch input. The next 50 secs show the open loop response for both models with pitch command input of one-degree pitch angle.

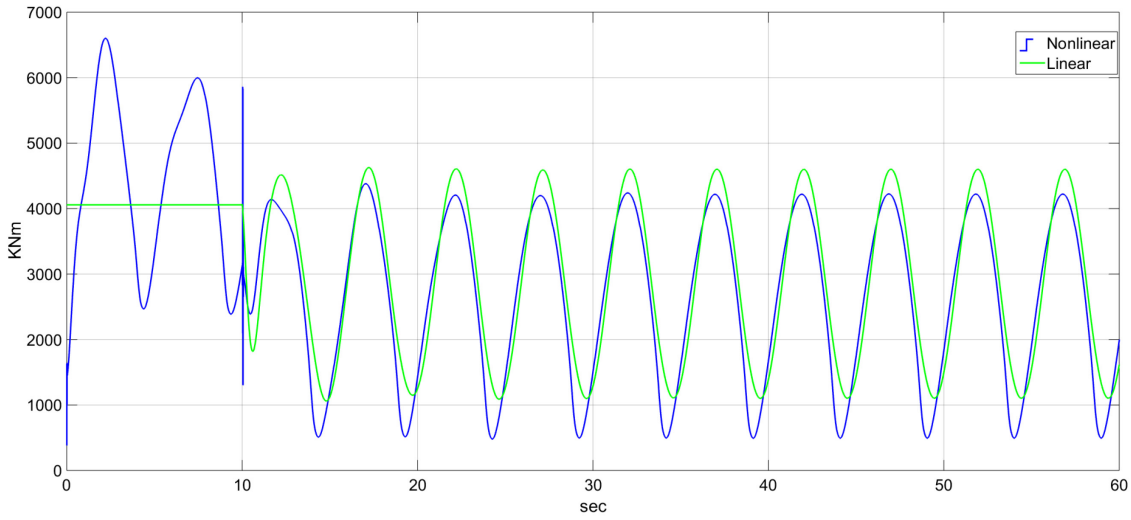

Figure 5.1: Validation of the linear model for the flapwise moment

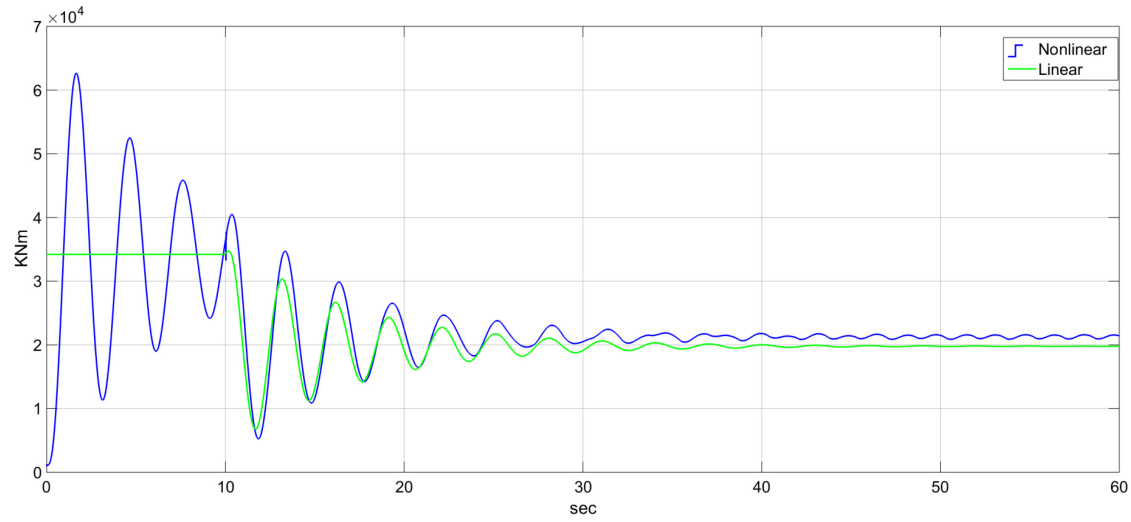

Figure 5.2: Validation of the linear model for the tower fore-aft moment

5.2 Validation of the Discrete Kalman Filter with the linear model

The Discrete Kalman Filter has been implemented in MATLAB Simulink and connected to the linearized model in combination with the disturbance model. The simulation has been run, the results shows a good and fast estimation for the wind turbine states as shown in figure 5.3 for the generator speed DoF and 1st flapwise bending mode DoF.

The prefect gaussian distribution with zero mean shows a correct implementation of the filter. The good quality of the estimation is shown by the low value of the standard deviation of the error.

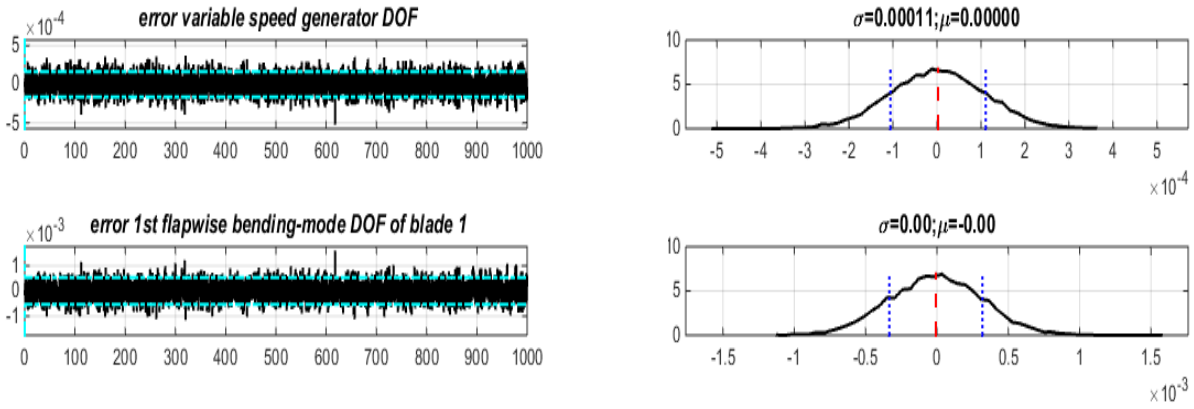

Figure 5.3: State estimation for generator speed DoF and 1st flapwise bending mode DoF based on Discrete Kalman Filter

The standard deviation of the error in estimation calculated from time series and plotted as a red dashed line in figure 5.3 shows a very fast and stable performance of the Kalman filter. It has a value of 0,00011 for the variable speed generator DOF where its value the first flapwise bending-mode DOF is zero. The cyan line shown in the same figure shows the standard deviation of the error in estimation calculated from the Kalman filter as shown in equation (4-10). it is shown that it has a smaller value less than 0,001 KNm for the first flapewise bending-mode DOF and less than 0,0005 rpm for the variable speed generator DOF. Results for other states and outputs are shown in figure A.1 and A.2 in the appendix.

The simulation also shows a good estimation of the disturbance states where the standard deviations of the errors between the real states and the estimated states are very small as shown in figure 5.4 for the turbulence states.

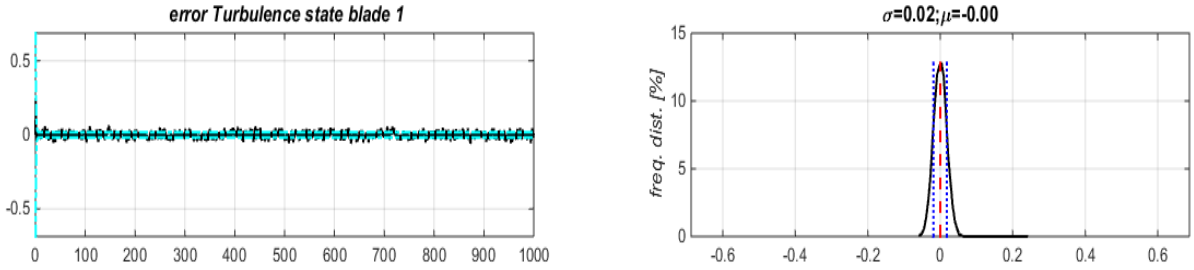

Figure 5.4: Turbulence state estimation for blade 1

5.3 Validation of the Discrete Kalman Filter with the nonlinear model

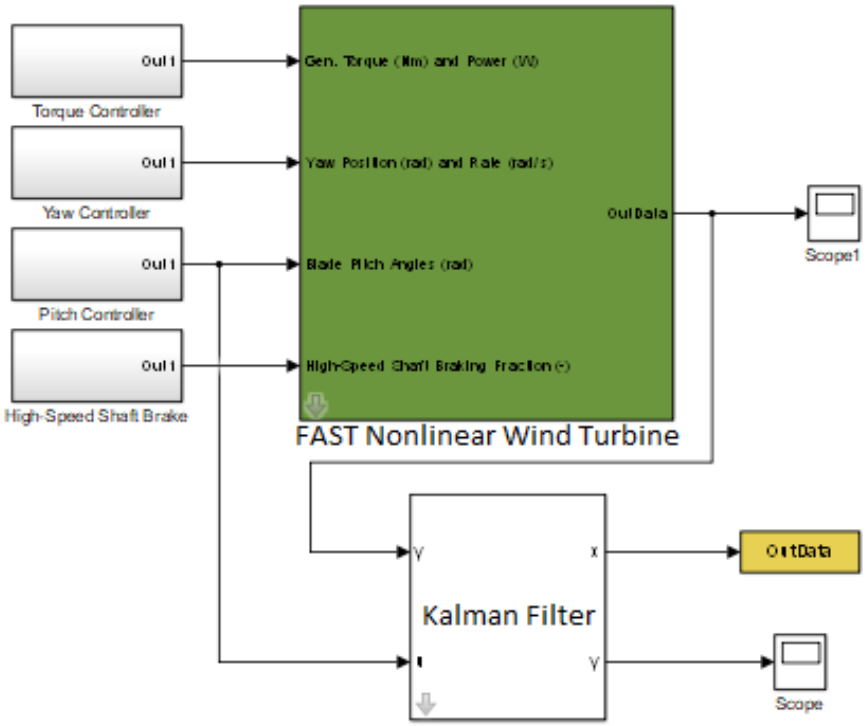

Figure 5.5: State estimation for FAST nonlinear wind turbine

The operation of the Kalman filter has been also validated with the nonlinear wind turbine supported by FAST as a S-Function in Simulink as shown in figure 5.5. Kalman Filter shows a good and fast estimation for the nonlinear wind turbine outputs as shown in Figure 5.6 for the flapwise moment.

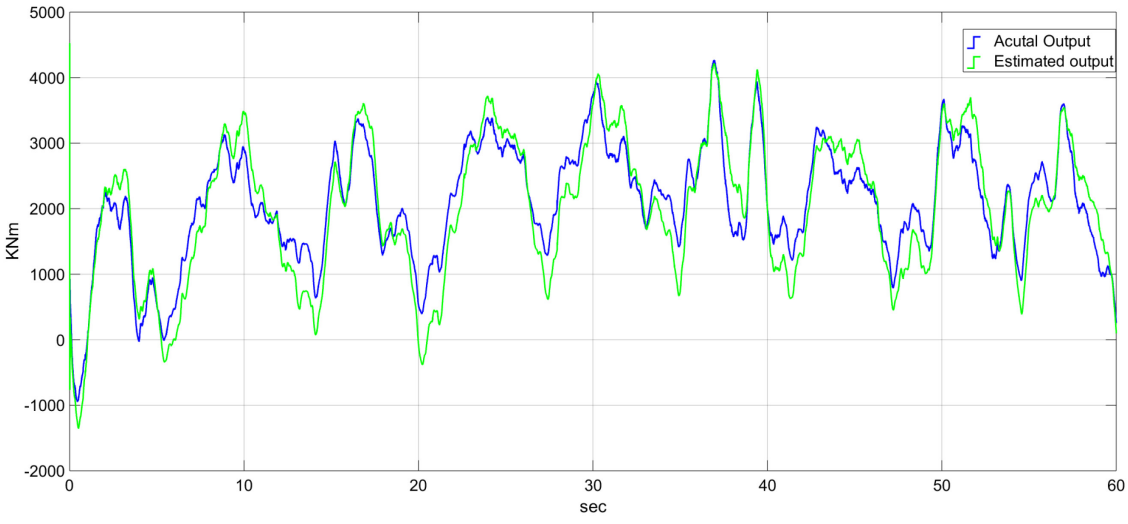

figure 5.6: Kalman filter state estimation for the flapwise moment in turbulent atmosphere.

5.4 The Controller Performance

The stochastic disturbance accommodation controller that is described in the previous chapter is implemented in this subsection. The controller structure consists of the feedback and the feedforward controller as shown in figure 5.7 where $\underline{\underline{K}}_{LQR}$ represents the feedback gain and $\underline{\underline{K}}_{FF}$ represents the feedforward gain.

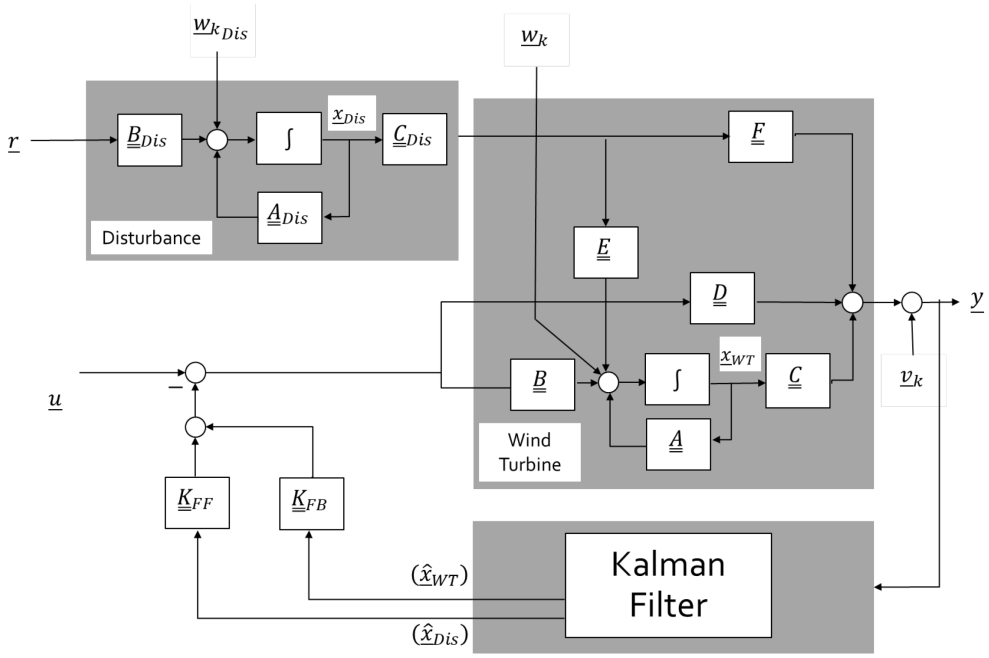

Figure 5.7: Controller structure in the linear simulation environment

The Controller shows a good behavior in the disturbance accommodation and wind turbine stabilization. Table 5.1 shows a comparison between uncontrolled turbine, feedforward controlled turbine and feedforward/feedback controlled turbine for the generator speed, blade flapwise moment and tower fore-aft moment where the standard deviation has a lower value for the feedforward/feedback controlled turbine and a higher value for the uncontrolled turbine. Other comparison for all the measured outputs including the blade torsion moment for each blade and the system stats are shown in figure A.9 the appendix.

	Uncontrolled turbine	Feedforward control	Feedforward/Feedback control
Generator speed	34.45 rpm	15.62 rpm	15.62 rpm
blade Flapwise	6272.9 KNm	5442.65 KNm	240.63 KNm

moment			
Tower fore-aft moment	2503.39 KNm	647.23 KNm	633.66 KNm

Table 5.1: A comparison between the uncontrolled turbine, feedforward controlled turbine and feedforward/feedback controlled turbine

It is noticed that the standard deviation has the same value with the feedforward/feedback control and the feedforward control alone for the generator speed but the difference between the two controllers in this case is shown in figure 5.9 where the generator speed has a higher value near the rated speed with the feedforward/feedback control that its value for the feedforward alone.

Figure 5.8 shows the controller behavior on the flap moment where the disturbance accommodation is achieved by the feedforward controller and the reduction in the flap moment is achieved by the LQR. The instability caused by unstable pole in the output response shown in the first two graphs in the same figure and not shown in the third graph clarifies that the Kalman Filter and the feedforward gain have no influence on the system eigenvalues, only the feedback via $\underline{\underline{K}}_{LQR}$ has an influence on the eigen values.

Figure 5.9 and figure 5.10 show also the controller behavior on the generator speed and the tower fore-aft moment respectively.

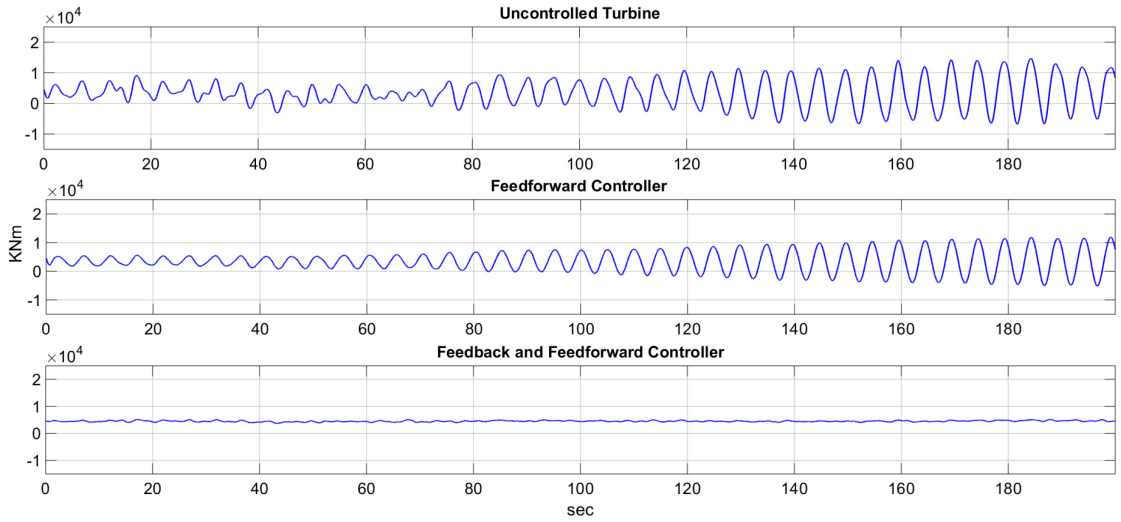

Figure 5.8: Comparison of the uncontrolled turbine against the feedforward controlled turbine and the feedforward/feedback controlled turbine for The flap moment

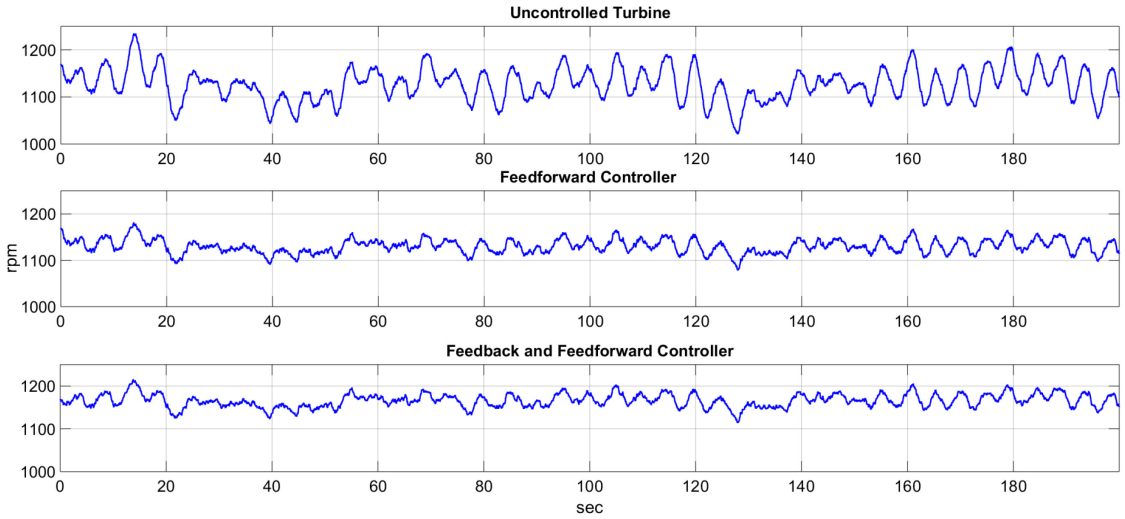

Figure 5.9: Comparison of the uncontrolled turbine against the feedforward controlled turbine and the feedforward/feedback controlled turbine for the generator speed

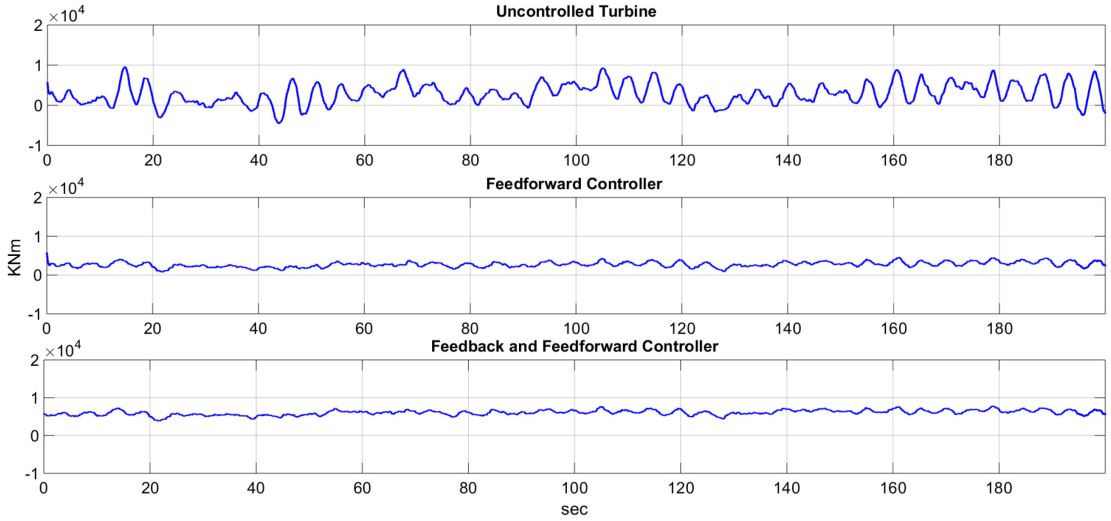

Figure 5.10: Comparison of the uncontrolled turbine against the feedforward controlled turbine and the feedforward/feedback controlled turbine The tower fore-aft moment

6. Comparative studies with a given "classical load controller"

The results of this study have to compared with the results of a classical load controller study [20]. The blade fatigue damage, the tower fatigue damage, and the rotational speed-strength are used as comparison criteria. The fatigue damage for the blade and the tower is calculated using rainflow counting that allows the application of Palmgren-Miner linear damage hypothesis or what's called Miner's rule. Miner's rule is one of the most widely models used to calculate the damage caused by cyclic loads. It had been proposed by A. Palmgren in 1924. It states that if a body that can stand certain amount of damage D experiences to damages D_i where $i = 1,2,3, \dots N$ from N loads, then it might be expected that the failure can occur if

$$\sum_{i=1}^{N} D_i = D \tag{6-1}$$

or

$$\sum_{i=1}^{N} \frac{D_i}{D} = 1 \tag{6-2}$$

This linear cumulative damage concept can be used in fatigue settings by considering the body is subjected to n_1 cycles at cyclic stress σ_1, n_2 cycles at cyclic stress $\sigma_2, \dots, n_n$ cycles at cyclic stress σ_n. the number of cycles to failure can be calculated from the $S - N$ curve for the body martialas shown in figure 6.1.

It can be clearly shown that the fractional fatigue damage at stress σ_i can be calculated as n_i/N_i and the fatigue failure occurs when the summtion of the fractional damages reaches the critical damage

$$\frac{n_1}{N_1} + \frac{n_2}{N_2} + \frac{n_3}{N_3} + \cdots = \sum_{i=1}^{N} \frac{n_i}{N_i} = 1 \tag{6-3}$$

Mathematically, the Miner´s rule is given by,

$$\sum_{i=1}^{N} \frac{n_i}{N_i} = 1 \tag{6-3}$$

In order to apply rainflow counting algorithm, the time series need to be first processed into peak-valley series to extrapolate the data from extrema, i.e., maxima and minima of a time series. Then this count is weighted and added using the Miner rule for damage accumulation.

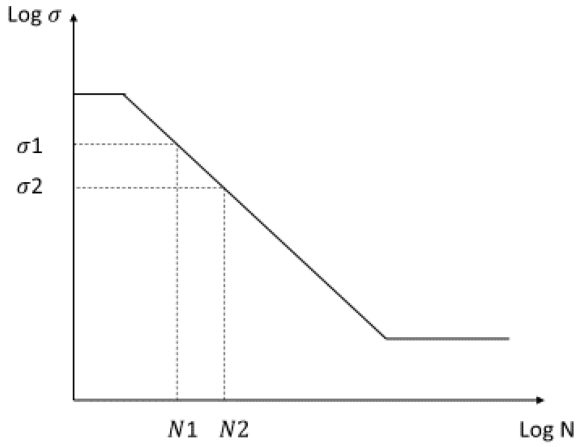

Figure 6.1: S-N material curve example

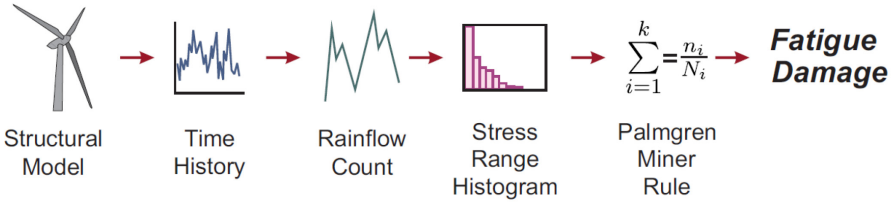

Figure 6.2: Rainflow counting damage estimation procedure [22]

The comparison shows a good behavior for the modern controller over the classical controller. The fatigue damage for the blade is reduced by a factor of 2.2 with appllying the feedforward controller alone and by a factor of 200 with the feedforward/feedback controller. The fatigue damage for the tower doesn't reduce so much with the feedforward controller but it reduced by a factor of 100 with the feedback/feedforward controller. Table 6.1 shows the comparison between the modern controller and the classical controller where the **where the standard deviation of the rotational speed is used as comparison criteria. The values in the table represent the division of the standard deviation before applying the controller to the standard deviation after applying the controller at 15 m/s and 25 m/s wind speeds.**

	Modern Control	**Classical control**
15 m/s	0,53	0,55
25 m/s	0,35	0,97

Table 6.1: A comparison between the modern controller and the classical controller where the standard deviation of the rotational speed is used as comparison criteria at 15 m/s and 25 m/s wind

7. Conclusion

In this thesis an observer based Disturbance Accomodation Controller was designed, implemented and tested with the linear and nonlinear models . The controller was benchmarked with a dreived set of critera for the well known NREL 5 MW wind turbine. The ability of an observer to estimate non-measurable states from a set of measurements using a model of the plant suggests the idea of extending the model of the plant by a model of the disturbance. The Discrete Kalman Filter has been used as an observer. The results show a good and fast estimation of the filter for the disturbance states. A feedforward/feedback controller has been used for counteracting the disturbance and stabilizing the wind turbine. The disturbance effect is reduced via a feedforward controller where the wind turbine is stabilized via a feedback controller. The LQR is used as a full state fedback controller. The results show that the better the estimation of the disturbance states, the better the disturbance rejection.

A comparative study has been done between this study; Modern load controller and a classical load controller. The modern controller shows a better performance than the classical controller.

8. References

[1] Sawyer, S., Teske, S., Dyrholm, M.: Global Wind Energy Outlook, Global Wind Energy Council ,2016

[2] N.N.: Technology Roadmap Wind Energy, 2013 Edition, International Energy Agency, 2013

[3] Johnsons, C.D.: Accommodating of external disturbances in linear regulator and servomecha-nism problems, IEEE Transaction on automatic control, Vol. AC-16, No. 6, 1972

[4] Balas, M., et. Al.: Disturbance Tracking Control Theory with Application of horizontal axis wind turbines, Proc. 17th ASME Wind Energy Symposium, Reno, Nv, 1998

[5] Wright, A.: Modern control design for flexible wind turbines, NREL/TP-500-35816, July 2004

[6] Hoffmann, A.: Regelungstechnische Beiträge zur Böenlastabminderung bei Flugzeugen, Dissertation, Technische Universität Berlin, 2016

[7] Bianchi, F., et. al.: Wind Turbine Control Systems, ISBN-10 978-1-84628-492-2, Springer Ver-lag, London, 2007

[8] Jonkman, J., Butterfield, S., Musial, W., and Scott, G. "Definition of a 5-MW Reference Wind Turbine for Offshore System Development," National Renewable Energy Laboratory: NREL/TP-500-38060, 2009

[9] Buhl, M.L., Jr., Jonkman, J.M., Wright, A.D., Wilson, R.E., Walker, S.N.; Heh, P.: FAST User's Guide. NREL/EL-500-29798. Golden, CO: NREL, 2005

[10] Burton,T., Sharpe,D., Jenkins,N., Bossanyi.E.: Wind Energy Handbook, ISBN 0-471-48997-2, John Wiley & Sons, Ltd , West Sussex, England, 2001

[11] Dryden, H.L.: A review of the statistical theory of turbulence. Turbulence-classical paper on statistical theory, New York: Interscience Publishers, Inc., 1961 (Nachdruck aus Quart. Appl. Math. I, S7-42, 1943).

[12] DEWI DeutschesWindenergie Institut: Offshore Potentialstudie für das Land Niedersachsen, Wilhelmshaven, 2000

[13] Halfpenny. A.: Dynamic Analysis of Both on and Oftshore Wind Turbines in the

Frequency Domain, Faculty of Engineering, University of London, 1998

[14] Bhattacharya, S., Arany, L., macdonald, J., Hogan, S.: Simplified critical mudline bending moment spectra of offshore wind turbine support structures, Wiley Online Library, 2014.

[15] Peter S. Maybeck.: Stochastic models, Estimation, and Control, ISBN 0-12-480701-1(v.1), Academic press, INC, New York, 1979

[16] Peter S. Maybeck.: The Kalman Filter: An Introduction to Concepts in Autonomous Robot Vehciles, I.J. Cox, G. T.Wilfong (eds), Springer-Verlag,1990

[17] Brown, R.,Hwang.,P.: Introduction to random signals and applied Kalman filtering: with MATLAB exercises —4th ed, ISBN 978-0-470-60969-9, John Wiley & Sons, Inc.

[18] Lunze, J.: Regelungstechnik 2, Mehrgrößensysteme, Digitale Regelung , 3. Auflage, Springer, ISBN 3-540-22177-8, Berlin

[19] Murry, R.: Lecture notes, CDS 110b, Control and Dynamical Systems, California Institute of Technology, 2006

[20] Voß,A.: Regelungstechnische Reduktion des Rotorblattwurzelbiegemoments und Erhöhung der Drehzahlfestigkeit einer 5 MW IPC-Windenergieanlage, DLR, Institut für Flugsystemtechnik, Braunschweig

[21] Barradas-Berglind, J.: Fatigue-Damage Estimation and Control for Wind Turbines, ISBN (online): 978-87-7112-398-2, Faculty of Engineering and Science, Aalborg University, Denmark, 2015

A Appendix

A.1 The Discrete Kalman Filter Performance

Figure A-1 shows the performance of the Discrete Kalman filter in the estimation of the wind turbine states and the disturbance states. The standard deviation for the error between the actual state and the estimated state is calculated through a MATLAB script and it's written upon each plot in the same figure.

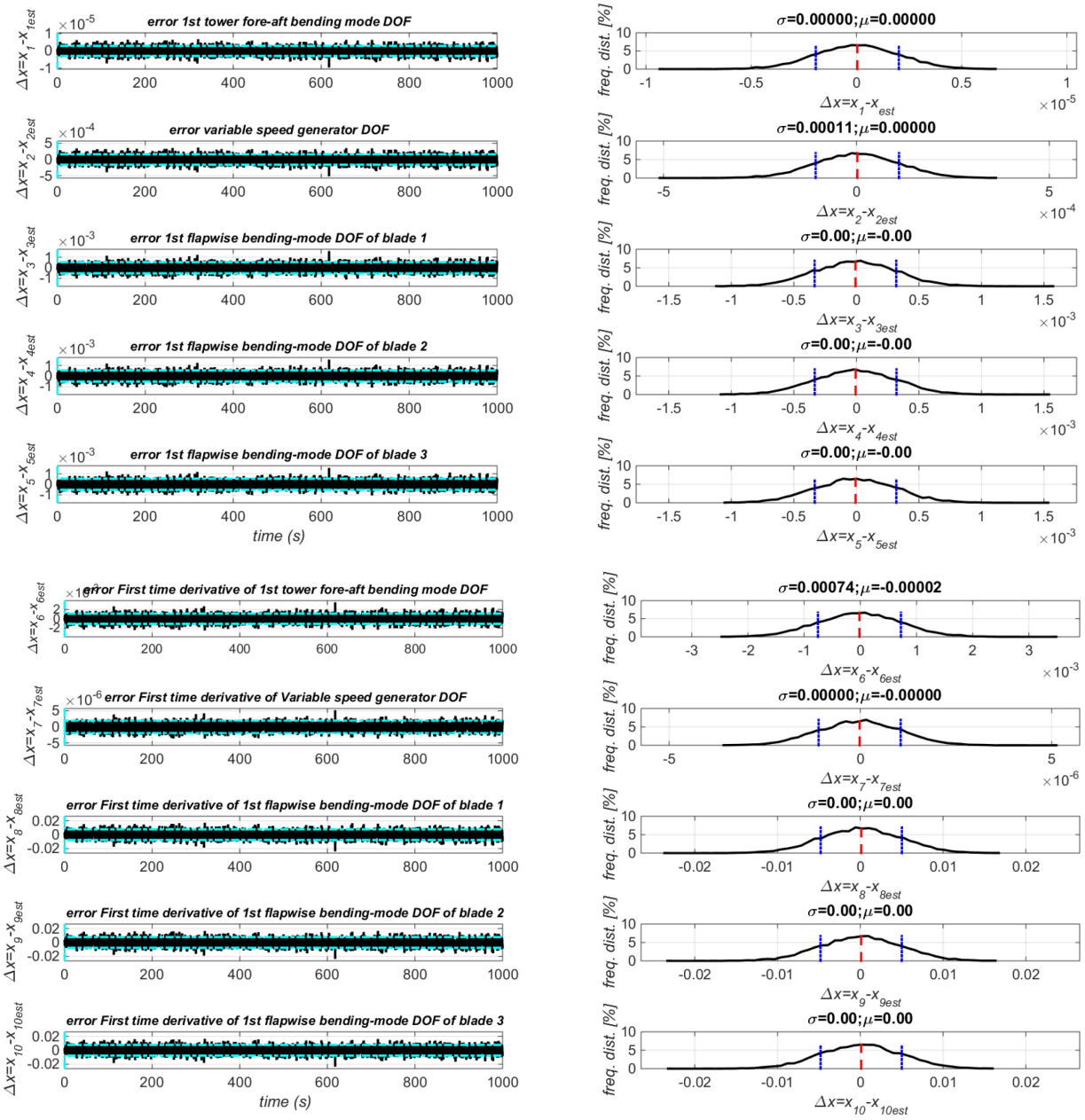

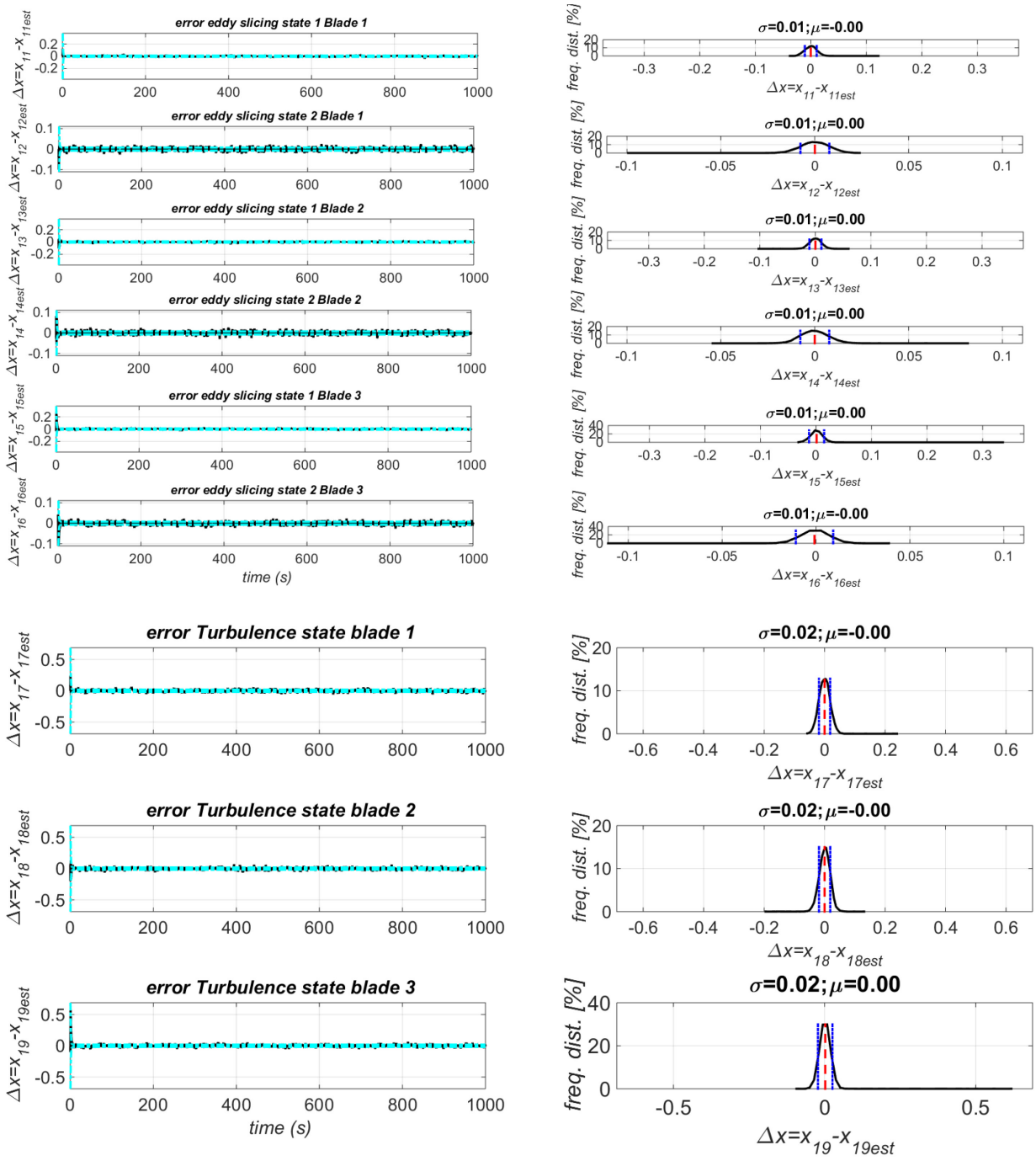

Figure A-1: Time series and frequency distribution of the error in the estimation for the wind turbine states and the disturbance states.

Figure A-2 shows the time series and frequency distribution of the error in the estimation for the following measured outputs:

1- Angular speed of the HSS and generator (GenSpeed)
2- Blade 1 edgewise moment (RootMxb1)
3- Blade 2 edgewise moment (RootMxb2)
4- Blade 3 edgewise moment (RootMxb3)
5- Blade 1 flapwise moment (RootMyb1)
6- Blade 2 flapwise moment (RootMyb2)
7- Blade 3 flapwise moment (RootMyb3)
8- Blade 1 pitching moment (RootMzb1)
9- Blade 2 pitching moment (RootMzb2)
10- Blade 3 pitching moment (RootMzb3)
11- Tower base roll (or side-to-side) moment (TwrBsMxt)
12- Tower base pitching (or fore-aft) moment (TwrBsMyt)
13- Tower base yaw (or torsional) moment (TwrBsMzt)

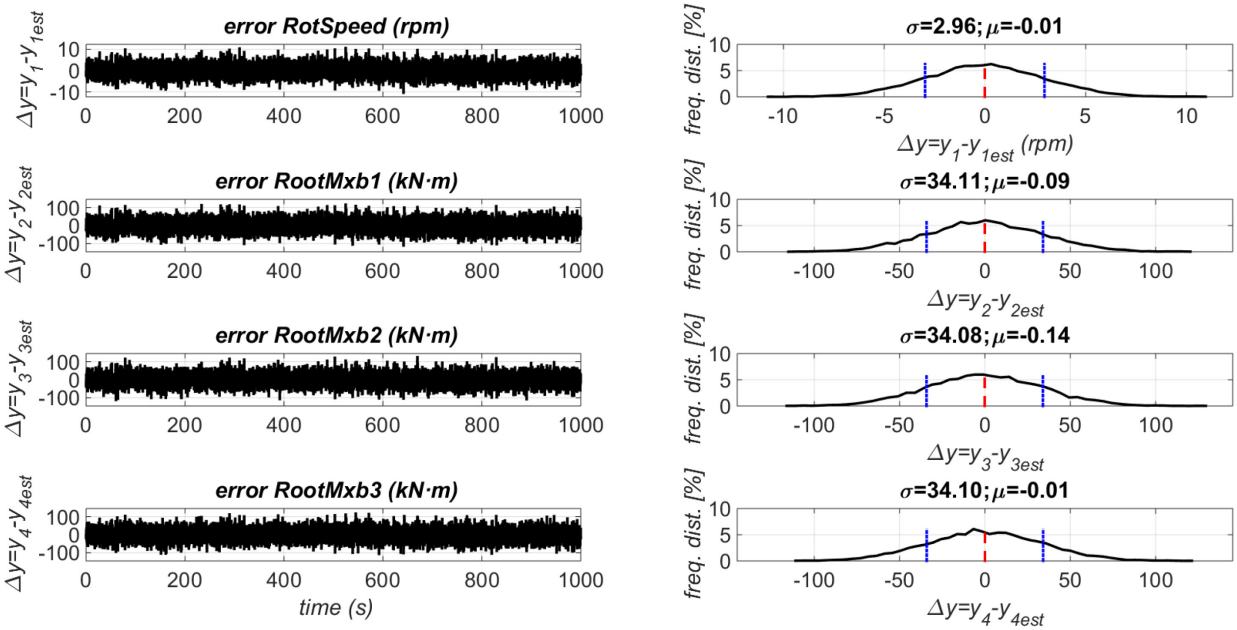

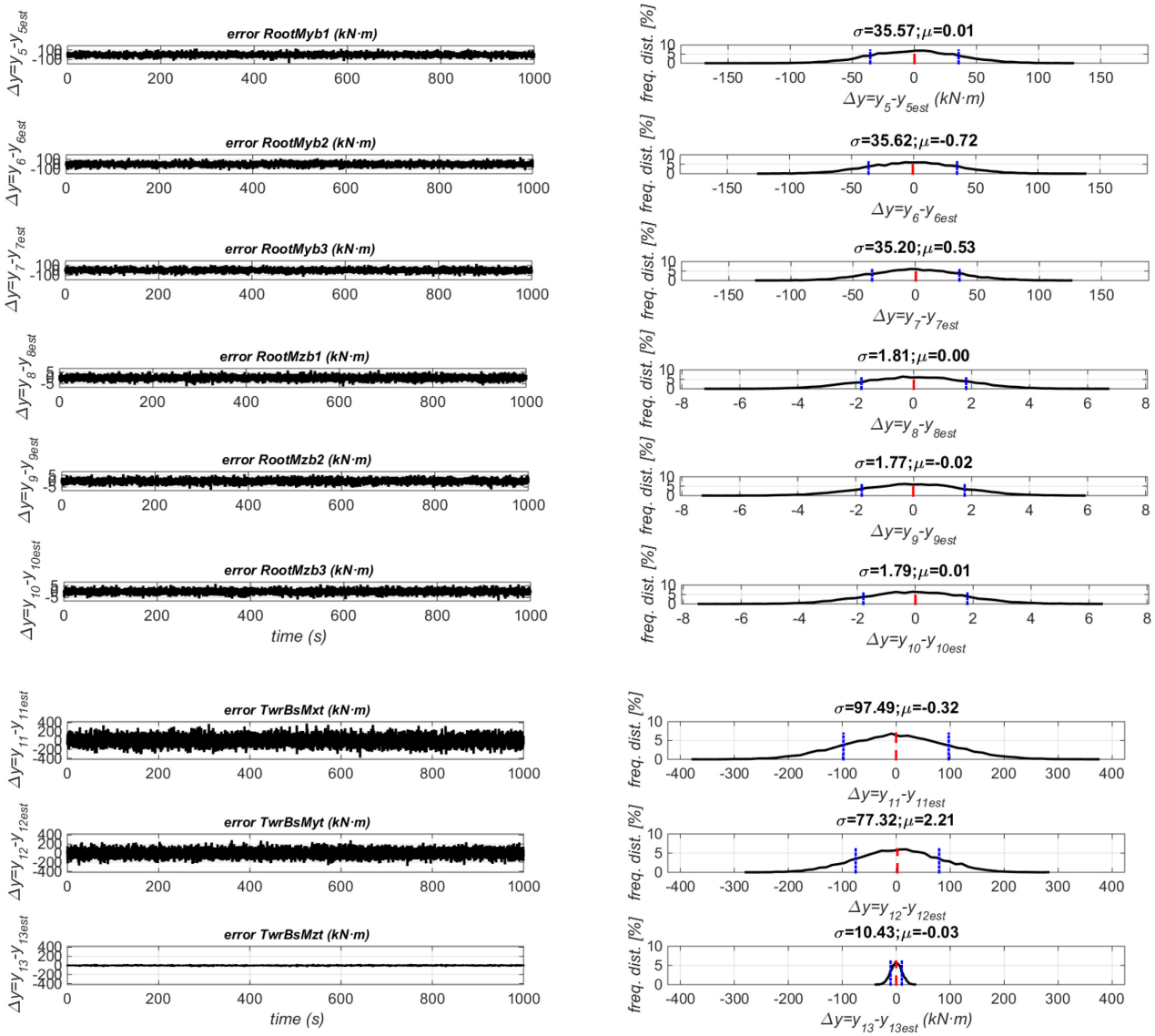

Figure A-2: Time series and frequency distribution of the error in the estimation for the measured outputs

A.2 The Controller Performance at 15 m/s wind speed conditions

Trim point: -

- 15 m/s steady horizontal wind speeds.
- 90 m as Reference height for horizontal wind speed.
- 10.45 degree as initial blade pitch angel for each blade.
- 12.1 rpm as initial rotor speed.

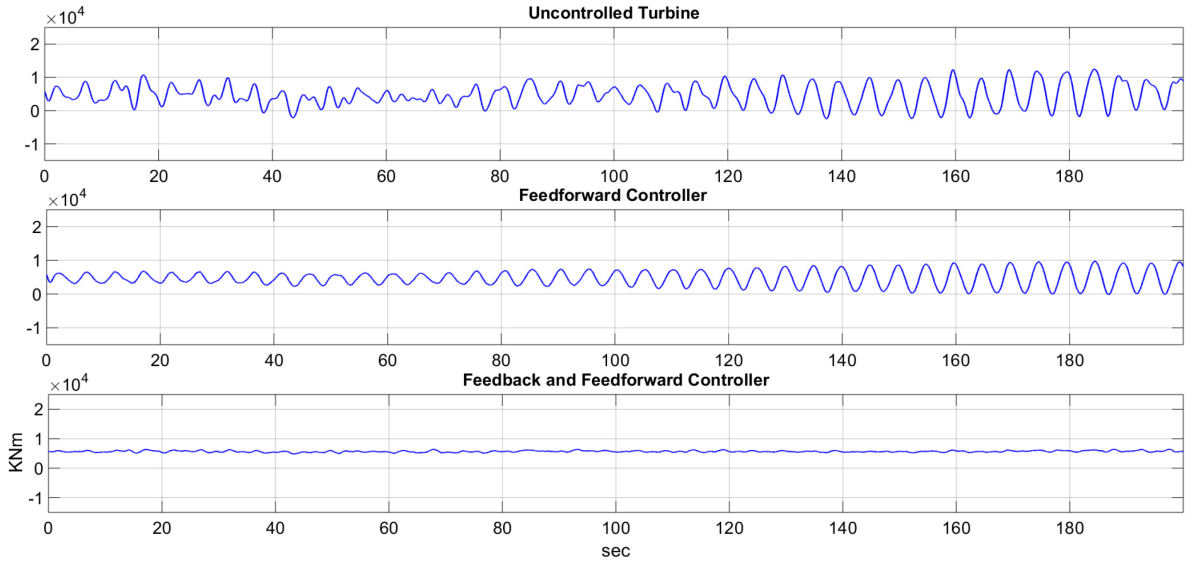

Figure A.3: Comparison of the uncontrolled turbine against the feedforward controlled turbine and the feedforward/feedback controlled turbine for the flap moment, 15 m/s wind speed

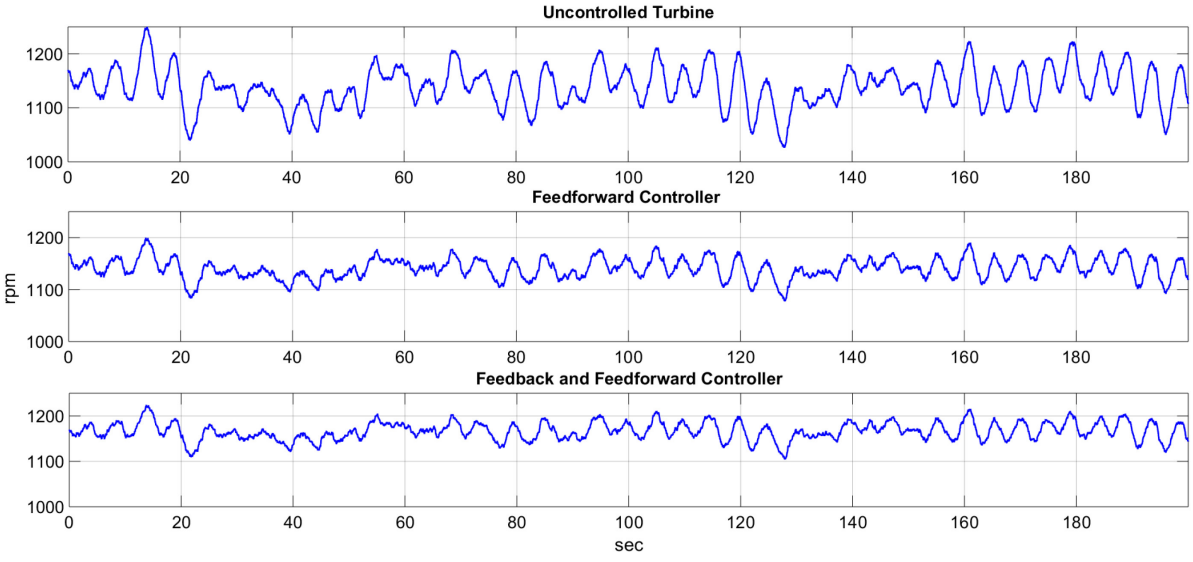

Figure A.4: Comparison of the uncontrolled turbine against the feedforward controlled turbine and the feedforward/feedback controlled turbine for the generator speed, 15 m/s wind speed

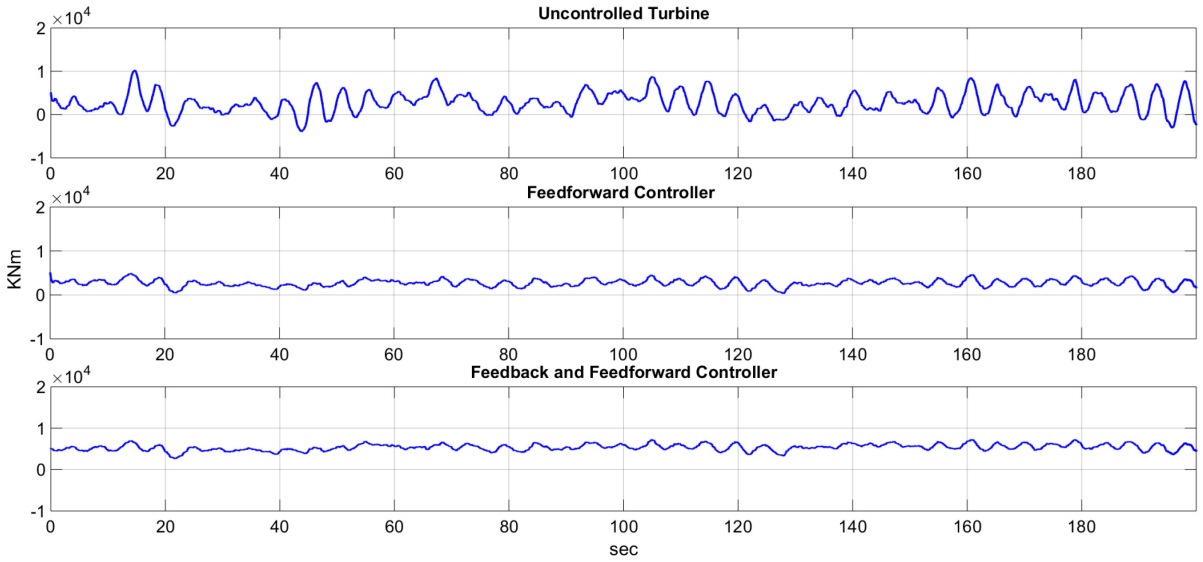

Figure A.5: Comparison of the uncontrolled turbine against the feedforward controlled turbine and the feedforward/feedback controlled turbine for the tower fore-aft moment, 15 m/s wind speed, 15 m/s wind speed

A.2 The Controller Performance at 25 m/s wind speed trim conditions

Trim point: -

- 25 m/s steady horizontal wind speeds.
- 90 m as Reference height for horizontal wind speed.
- 23.47 degree as initial blade pitch angel for each blade.
- 12.1 rpm as initial rotor speed.

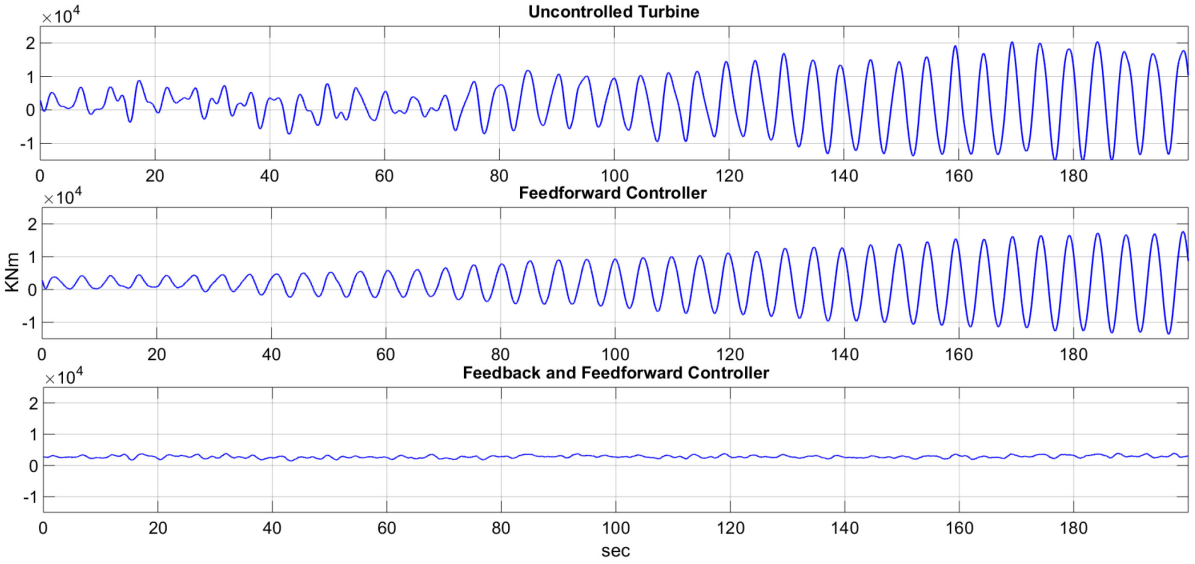

Figure A.6: Comparison of the uncontrolled turbine against the feedforward controlled turbine and the feedforward/feedback controlled turbine for the flap moment, 25 m/s wind speed

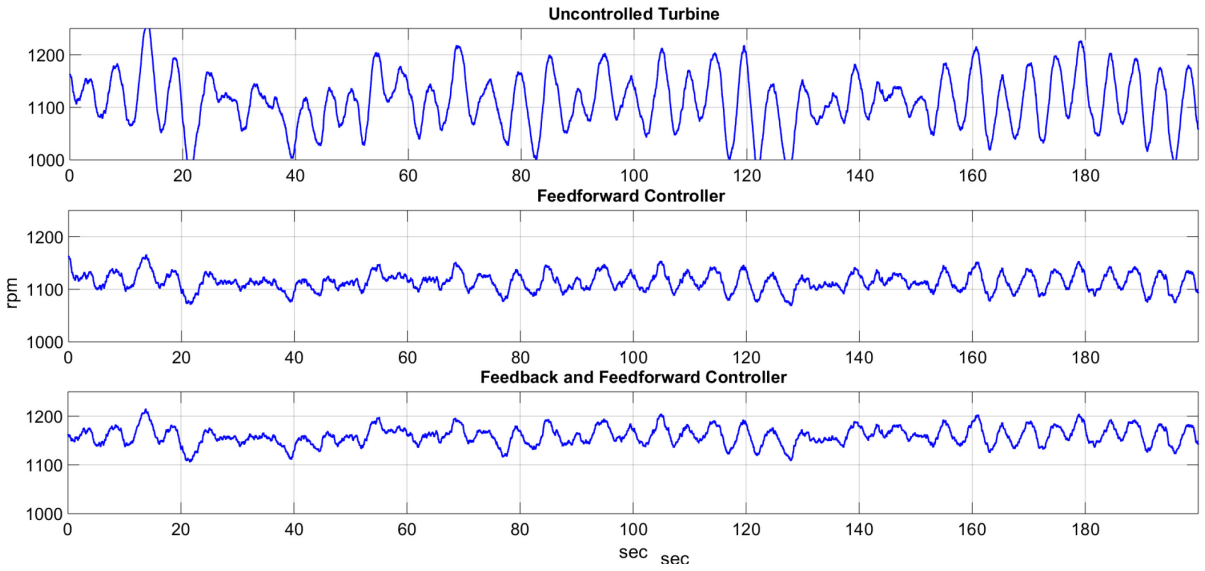

Figure A.7: Comparison of the uncontrolled turbine against the feedforward controlled turbine and the feedforward/feedback controlled turbine for the generator speed, 25 m/s wind speed

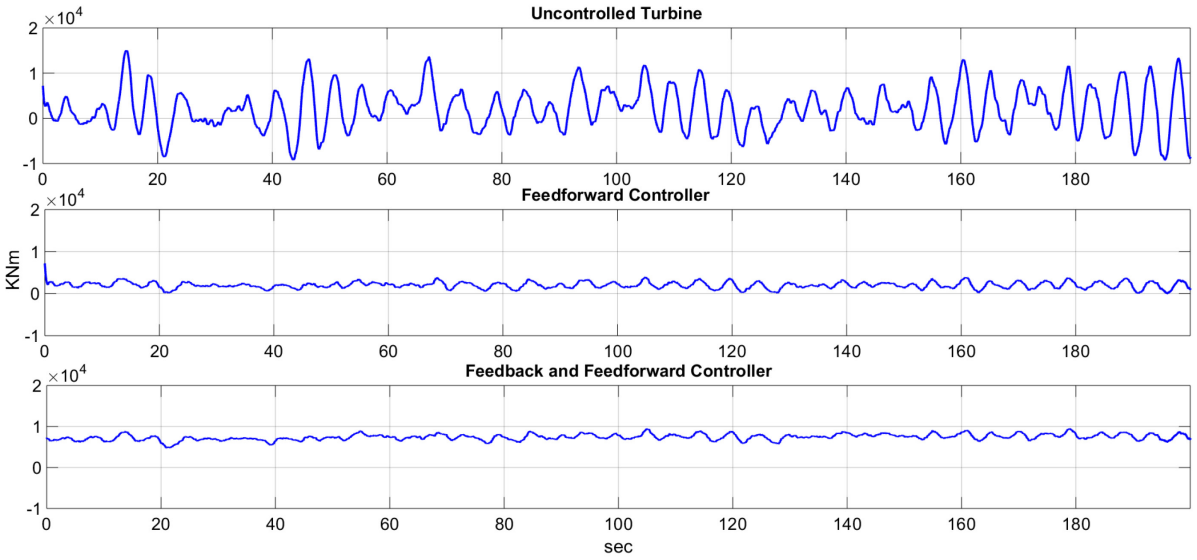

Figure A.8: Comparison of the uncontrolled turbine against the feedforward controlled turbine and the feedforward/feedback controlled turbine for the tower fore-aft moment, 25 m/s wind speed,

Figure A-7 shows a comparison between the uncontrolled turbine, feedforward controlled turbine and feedforward/feedback controlled turbine for the wind turbine states, the disturbance state and the measured outputs mentioned in the previous section.

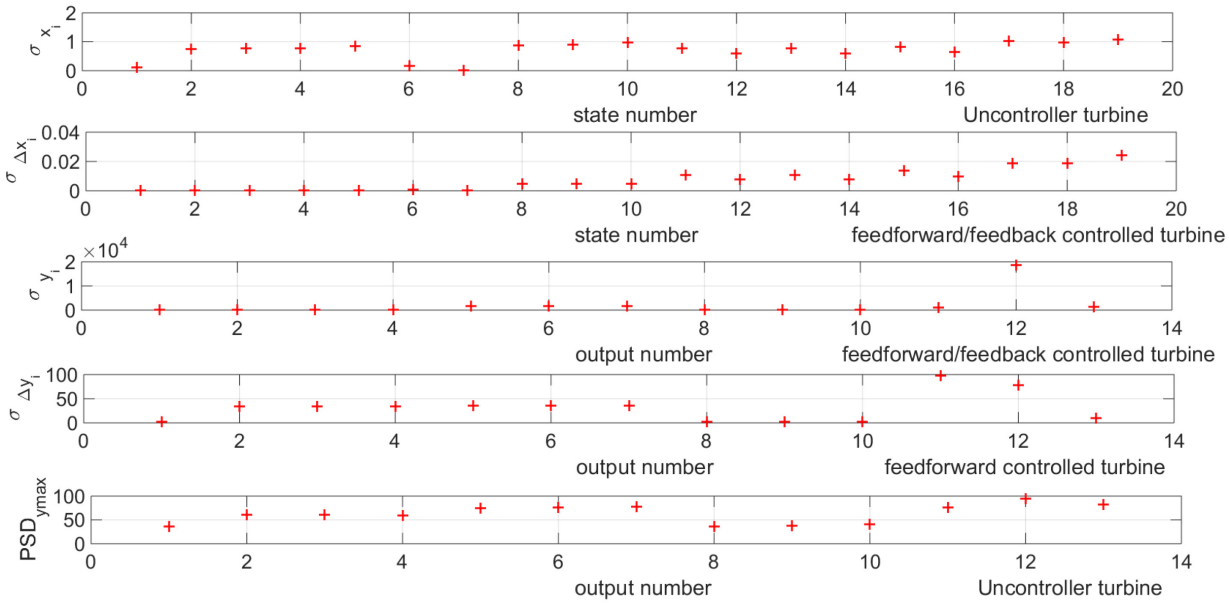

Figure A.9: A comparison between the uncontrolled turbine, feedforward controlled turbine and feedforward/feedback controlled turbine, 18 m/s wind speed